iScience

CellPress
OPEN ACCESS

Review

Progress in Bioinspired Dry and Wet Gradient Materials from Design Principles to Engineering Applications

Xiaoxiao Dong,[1] Hong Zhao,[1] Jiapeng Li,[1] Yu Tian,[2,*] Hongbo Zeng,[3] Melvin A. Ramos,[4] Travis Shihao Hu,[4] and Quan Xu[1,*]

SUMMARY

Nature does nothing in vain. Through millions of years of revolution, living organisms have evolved hierarchical and anisotropic structures to maximize their survival in complex and dynamic environments. Many of these structures are intrinsically heterogeneous and often with functional gradient distributions. Understanding the convergent and divergent gradient designs in the natural material systems may lead to a new paradigm shift in the development of next-generation high-performance bio-/nano-materials and devices that are critically needed in energy, environmental remediation, and biomedical fields. Herein, we review the basic design principles and highlight some of the prominent examples of gradient biological materials/structures discovered over the past few decades. Interestingly, despite the anisotropic features in one direction (i.e., in terms of gradient compositions and properties), these natural structures retain certain levels of symmetry, including point symmetry, axial symmetry, mirror symmetry, and 3D symmetry. We further demonstrate the state-of-the-art fabrication techniques and procedures in making the biomimetic counterparts. Some prototypes showcase optimized properties surpassing those seen in the biological model systems. Finally, we summarize the latest applications of these synthetic functional gradient materials and structures in robotics, biomedical, energy, and environmental fields, along with their future perspectives. This review may stimulate scientists, engineers, and inventors to explore this emerging and disruptive research methodology and endeavors.

INTRODUCTION

Nature gives birth to millions of wonderful living organisms on earth. Through 4 billion years of evolution, nature has developed nano-/micro-scale structures and systems with astonishing complexity and multifunctionality, adapting to the ever-changing and dynamic environments. For example, lotus leaf (Jiang et al., 2004; Karthick and Maheshwari, 2008; Feng et al., 2002; Liu et al., 2010) and pitcher plant (Bauer and Federle, 2009; Nishimoto and Bhushan, 2013; Wong et al., 2011) have evolved complex superhydrophobic surfaces. Tree fog (Barnes et al., 2011; Federle et al., 2006; Hanna et al., 1991) and gecko (Autumn et al., 2002; Murphy et al., 2009; Tian et al., 2006) have evolved reversible adhesive toe pad. Mussel thread (Ceylan et al., 2013) can withstand ten gale of winds in air and have strong adhesion and self-healing capability under seawater. Spider silk (Chen and Guo, 2019; Chen and Zheng, 2014; Zheng et al., 2010) and cactus (Guo and Tang, 2015; Heng et al., 2014; Kim et al., 2017; Ju et al., 2012) have effective water-collecting capabilities in arid conditions. One common observation is that they all have multifunctional and diverse material structures. Functional diversity is assumed to be a special requirement for organisms to adapt to and survive their local environments and habitats. Different from most artificial materials and structures that have simple shapes and homogeneous micro-/nano-constituents, living organism and biological materials normally have varying degrees of heterogeneity and responsive properties. One the most interesting phenomenon seen in nature is the utilization of functional gradients (i.e., geometrically, physically, and chemically) (Ries et al., 2014; Walsh et al., 2005). For instance, gradients in structures can lead to increased distribution of dissimilar mechanical components, reduced contact deformation and damage, elimination of stress singularities, and improved fracture toughness (Suresh, 2001).

[1]State Key Laboratory of Heavy Oil Processing, China University of Petroleum-Beijing, Beijing 102249, China

[2]State Key Laboratory of Tribology, Tsinghua University, Beijing 100084, China

[3]Department of Chemical and Materials Engineering, University of Alberta, Edmonton, AB T6G 1H9, Canada

[4]Department of Mechanical Engineering, California State University, Los Angeles, CA 90032, USA

*Correspondence: tianyu@mail.tsinghua.edu.cn (Y.T.), xuquan@cup.edu.cn (Q.X.)

https://doi.org/10.1016/j.isci.2020.101749

After millions of years of nature selection and optimization, gradient structures have evolved in various biological system. These systems include, but are not limited to, cells, bones, connective tissues, and plant stems. Through the gradient design they can maximize functionalities and minimize the material cost (Jiang et al., 2004; Wu et al., 2014). In nature, the gradient structure can arise from the size change of fibers, cells, and pores from interior to surface, which lead to the change of properties. Under quasi-static loading, gradient structures can achieve optimized strength and ductility. There are two possible reasons for this phenomenon. The first reason is nanostructured surface layer having mechanically driven grain growth, which is unstable. Another reason is that the strain gradient and the stress state change for the gradient structure would produce extra strain (Bian et al., 2017; Karthick and Maheshwari, 2008).

In-depth investigations of the gradient phenomena can help further understand the biological behaviors and ecology and bring more inspiration for biomimicry. Last decade witnessed some comprehensive review papers on biological materials and structural design elements (Arzt, 2006; Chen et al., 2012; Meyers et al., 2013; Naleway et al., 2015). The seven unique characteristics that distinguish biological materials from synthetic ones (the Arzt heptahedron) and eight most common biological structural design elements are listed in Table 1. The proposed biological structural design elements include the "Gradient." The biological materials and structural design elements play essential roles in the biological field. Despite a previous review on the gradient phenomena in nature exited (Liu et al., 2017b), a more up-to-date review is critically needed to capture this fast growing field.

In current review, the gradient phenomena and related functional biomimetics are compared and discussed on the basis of models, various experimental methods, design theories, functional classification, and applications. Attention is paid to the two forms of gradients, namely under dry or wet condition (Dry Gradient and Wet Gradient); the models conceptualize gradient phenomena (Simplified Models of Gradient Phenomenon), the design process of bioinspired gradient phenomenon, and classification according to different functionalities (Process Design and Function Classification). Finally, the applications of gradient biomimetics in medical, energy, environmental, and robotics are surveyed, which reveals the promises of combining gradient design with artificial intelligence in the future (Bioinspired Applications from Gradient Organisms).

DRY GRADIENT AND WET GRADIENT

Living organisms have adapted gradient designs compositionally, structurally, and geometrically. They are based off changing units in a limit region or a wide range of structures or even throughout the entire parts or components (Liu et al., 2017b). Some organisms are only limited on the surfaces or within a limit depth of the surface such as gecko seta (Tian et al., 2006; Yu et al., 2011) or lotus leaves (Jiang et al., 2004; Karthick and Maheshwari, 2008), whereas others should require the whole 3D gradient structures to unravel its functionality such as human teeth or abalone shell (Weiss et al., 2000; DeRocher et al., 2020; Autumn et al., 2002). In this section, we will review several organisms with gradient property in detail. These organisms are divided into two categories: (1) dry gradient (D-gradient) and (2) wet gradient (W-gradient). The D-gradient accounts for the composition, microstructure, and geometry of the materials, and the gradient-induced properties are manifested in a dry environment. Whereas, the W-gradient means that in addition to the gradient features mentioned above, the existence of liquid is essential to the underlying mechanisms and properties.

D-Gradient

Compositions

Herein, we focus on two organisms (i.e., geckos and ladybird beetles). One common characteristic is both require compositional changes in the axial direction of the setae or fibrils.

Geckos have exceptional toepad structures, which allow them to run on smooth vertical surfaces and ceiling upside down, while keeping their "sticky" foot clean from containments for as long as three months between molting cycles (Maderson, 1964). Autumn et al. first reported single gecko seta can generate a formidable 20 uN of adhesion force. With millions of setae on their toe pads, the whole gecko can generate adhesion as large as 200 N, which is equal to the weight of a child (Autumn et al., 2000). The adhesion of individual seta is mainly caused by van der Waals force, whereas humidity can also affect the adhesion forces (Wang, 2018). Recently Dong et al. discovered that the Young's modulus of each individual seta gradually decreases from the proximal to distal direction along the setal stalk. This effect is caused by the gradient distribution of β-keratin and the gradient distribution of the proteins evident by confocal laser microscope (CLSM) (Dong et al., 2020). Although single seta shows distinctive gradient properties in the

	Types	Characteristics
Biological materials	Self-assembly	The structures are assembled from the bottom up, rather than from the top down, due to the lack of a preexisting scaffold.
	Multifunctionality	Many components serve more than one purpose.
	Hierarchy	Different, organized scale levels; distinct and translatable properties from one level to the next.
	Hydration	The properties are highly dependent on the level of water in the structure. This rule applies to most biological materials and is of importance to mechanical properties.
	Mild synthesis conditions	The majority of biological materials are fabricated at ambient temperature and pressure as well as in an aqueous environment.
	Evolution and environmental constraints	The limited availability of useful elements dictates the morphology and resultant properties.
	Self-healing capability	Biological materials often have the capability to reverse the effects of damage by healing.
Biological structural design elements	Fibrous	Offering high tensile strength when aligned in a single direction, with limited to nil compressive strength.
	Helical	Common to fibrous or composite materials, offering toughness in multiple directions and in-plane isotropy.
	Gradient	Materials and interfaces that accommodate property mismatching through a gradual transition in order to avoid interfacial mismatch stress buildup.
	Layered	

Table 1. Summary of Biological Materials and Structural Design Elements

(Continued on next page)

	Types	Characteristics
		Complex composites that increase the toughness of brittle materials through the introduction of interfaces.
	Tubular	Organized porosity that allows for energy absorption and crack deflection.
	Cellular	Lightweight porous or foam architectures that provide directed stress distribution and energy absorption.
	Suture	Interfaces comprising wavy and interdigitating patterns that control strength and flexibility.
	Overlapping	Featuring multiple plates or scutes that overlap to form flexible and often armored surfaces.

Table 1. Continued

out-of-plane direction and are angled, the setae are distributed relatively evenly in-plane. With this special anisotropic design, gecko shows reversible adhesion and self-cleaning properties (Figure 1A) (Tian et al., 2006; Zhou et al., 2015). Beside geckos, the material composition and properties along the adhesive tarsal setae of the ladybird beetle *Coccinella septempunctata* also show gradient distribution (Peisker et al., 2013). The tarsal setae of ladybird shows a changing Young's modulus from 1.2 MPa at the tip to 6.8 GPa at the base. This effect is attributed to the higher concentration of the elastic protein resilin toward the tip of the tarsal setae by using CLSM (Figure 1B) (Peisker et al., 2013). Gorb et al. showed that gradient-bearing fibers with short soft tips and stiffer base (like the ladybird) have great advantage in maximizing adhesion while minimizing clustering of fibrils in multiple attachment-detachment cycles (Gorb and Filippov, 2014). Specifically, the base of the beetle seta is composed of relatively stiff chitinous materials, and the transition zones between the central part and the tip of the seta consists of a large proportion of soft and elastic protein resilin, forming a joint-like element. PVS and PMMA were adopted to fabricate biomimetic gradient mushroom-shaped adhesives. The results show that the joint-like element plays a critical role in achieving better stability and conformability on non-flat or non-parallel substrates. Heepe and et al. found an interesting phenomenon in subsequent research that the females produce significantly lower forces compared with males in all experiments on glass (Heepe et al., 2018). This is attributed to the need for males to hold on to the surfaces during long-terms of copulation, as well as mate guarding on the smooth elytra of females. However, adhesion on rough and porous surfaces did not show such variation. The results of these studies are similar to the results of some previous researches (Gorb et al., 2019; Vickers, 2017; Ballen et al., 2012; Magazù et al., 2005; Stork, 1980; Voigt et al., 2017). In addition, such gradient in the setal material composition have also been discovered in flies (Heepe et al., 2018; Petersen et al., 2018) and stink bugs (Rebora et al., 2018), suggesting a convergent evolution across different insect lineages (Gorb and Filippov, 2014). Nevertheless, the gradient distribution of Young's modulus of gecko seta and ladybird beetle are both formed by the gradient distribution of varied proteins.

Microstructure

In this section, two kinds of organisms, bamboo and shellfish, will be reviewed, which have D-gradient due to their microstructure changes.

Desirable mechanical properties can be achieved through excellent structural design, such as those seen in bamboo. Bamboo exhibits high specific strength, elastic stiffness, and fracture toughness. All of these

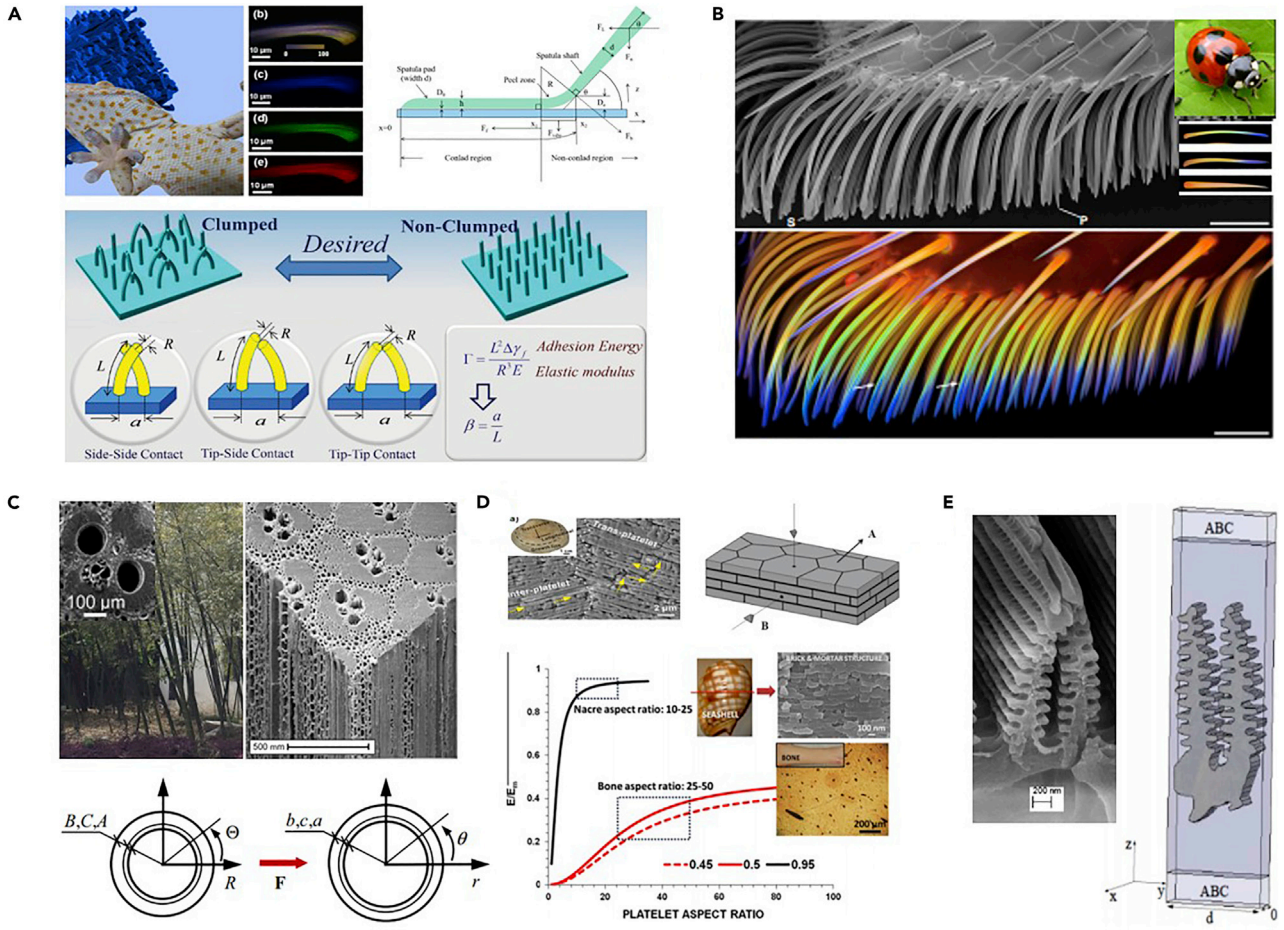

Figure 1. Several Representative Organisms of D-gradient

(A) An SEM images and the CLSM maximum intensity projection of a gecko seta. The CLSM image of a single gecko seta shows an overlay image of three different autofluorescences of blue, green, and red, which give off an excitation wavelength of 458, 561, and 633 nm, respectively. The results show that the protein in the seta presents a gradient distribution. The model was established by theoretically analyzing the geckos' friction and adhesion behavior and the schematic of an XY-plane bionic material preparation process (Tian et al., 2006; Zhou et al., 2015; Dong et al., 2020).

(B) An SEM image and the CLSM maximum intensity projection of a spatula-like adhesive tarsal setae of the second adhesive pad of a foreleg of a female *Coccinella septempunctata*. The CLSM images show the tips of beetle's material composition is mainly determined by resilin. The protein resilin decreases toward to the bottom of the beetle (Peisker et al., 2013).

(C) Bamboo stems and its SEM images. The cellulose fibers' gradient distribution decreases from the outside to the inside of the bamboo stems. At the bottom of the figure a cross-sectional mathematical model of bamboo culm before and after growth-induced deformation can be seen (Habibi et al., 2015; Silva et al., 2006; Wang et al., 2017b).

(D) SEM images of a shell and a sketch of the indentation part of the nacre structure, which present the "brick and mortar" state. The variation of the stiffness of shell-related biocomposites with the aspect ratio of ceramic bricks and volume fraction of ceramic as laid down (Gao et al., 2003; Jiao et al., 2016; Song et al., 2015).

(E) SEM images of butterfly wings in the shape of a "Christmas tree" and a 3D symmetrical model (Mejdoubi et al., 2013).

properties change with age, which is why young bamboos have better mechanical properties than older ones (Low et al., 2006a). Studies have shown that bamboo has excellent characteristics because of their hollow and functionally gradient structures (Suresh, 2001; Chand et al., 2006; Ray et al., 2005; Low et al., 2006b). Models have been used to prove the differences in properties because of the gradient distribution and anisotropy of bamboo (Wang et al., 2017b; Long et al., 2015; Tan et al., 2011; Habibi and Lu, 2014; Palombini et al., 2016; Cui et al., 2020; Zhang et al., 2020). Recently, Wang et al. found that the gradient distribution and variation of the cell size of the fibers embedded in the parenchyma cells arranged along the thickness of the bamboo stem are mainly responsible for the flexible bending gradient of the bamboo slivers. The shape and size of the vascular bundles are different from inner to outer layers and play a vital role in directional bending flexibility (Wei et al., 2019). For axisymmetric bamboos, the growth and deformation

resistance mechanisms operate in Z-axis and X-Y directions, respectively. A mathematical model can investigate the influence of stress on bamboo growth and can analyze the gradient and anisotropy of the bamboo. This can be used to establish a cross-section, namely in the X-Y directions (Figure 1C) (Habibi et al., 2015; Silva et al., 2006; Wang et al., 2017b). Ulrike G.K. Wegst confirms that bamboos and palms are both fiber-reinforced cellular materials. The fibers in bamboos and palms are parallel to the culm and stem, respectively (Wegst, 2011). The distribution of these fibers has density and modulus gradients across the cross-sections. The gradient characteristics of plants is beneficial to enhance the flexural rigidity of the plants per unit mass. However, the complex transverse behavior of bamboo in the direction transverse to the fiber does not seem to be like the classic fiber-reinforced composite material (Akinbade et al., 2019). The properties of the bamboo fibers are determined through the chemical composition, tensile test, and SEM test. These results show that the modulus and ultimate strength of bamboo fibrils are higher than that of bamboo fibers. This is due to the following main factors: bamboo age, bamboo species, and multilamella structures of the fibrils, etc. (Tan et al., 2020). Chen et al. used acoustic emission (AE) test to prove that the structure and water content of the gradient fibers have an important impact on the bending and fracture properties of natural bamboo (Chen et al., 2018a).

Next comes another organism, the shellfish. The tough mechanical properties of small shells have attracted the attention of scientists. A series of studies have shown that the mechanical properties of shells are related to their microstructure (Lin et al., 2009; Rousseau et al., 2005). The shells of various species of shellfishes have slightly different structures, but the whole structure is hierarchical and similar to gradient arrangement. The constituent aragonite units of *Saxidomus purpuratus* shells are stacked in a loosely packed porous form in the middle layer and a dense crossed-lamellar arrangement in the inner layer. The gradient mechanical properties along the thickness direction of shell are favorable for the protection of the mollusk (Jiao et al., 2016). The *Hyriopsis cumingii* is a typical limnetic shell made up of a prismatic "pillar" structure and a nacreous "brick and mortar" structure. However, the microstructure in each layer is still the hierarchical feature (Song et al., 2015). Zhang and co-worker provided evidence that the morphology and thickness of the platelets in green mussel shells exhibit a gradient arrangement. They also hypothesized that the gradient phenomenon was due to the various growth rates between the edge and the center of the shell and the closure of the outer shell by the adductor muscle or removal of the periosteum by the mantle (Xu and Zhang, 2015). With respect to the research on the toughness and strength of shell structure, compared with transverse study, the axial study is more conducive to the analysis of driving stress and resistance of different cracking modes from the perspective of basic mechanics, which is helpful to the deep understanding of the strong stiffness of shell microstructure. All of these lay a foundation for the design of new bioinspired synthetic materials (Figure 1D) (Song et al., 2015; Gao et al., 2003; Jiao et al., 2016). For example, Yin et al. prepared laminated glass, which draws inspiration from nacre. This glass has high strength, high rigidity, and two to three times stronger impact resistance than ordinary laminated glass or tempered glass (Yin et al., 2019). To summarize, bamboo and shellfish exhibit superior mechanical properties due to their internal microstructure, and the display of these biological functional characteristics does not require an external liquid state. This section boils them down to D-gradient microstructure.

Geometry

A typical example of gradient phenomenon caused by geometry is the butterfly. Scientists' attention is focused on the beautiful and colorful butterfly wings. Research into butterfly wings has inspired different fields such as the research into antireflective surfaces (Han et al., 2016), photonic crystals (Lu et al., 2016; Poncelet et al., 2016; Pouya et al., 2016) etc.. The microstructure and formation of butterfly wings are also being researched. Increasingly realistic optical models are proposed as butterflies are investigated (Iwata and Otaki, 2016; Mejdoubi et al., 2013; Monteiro et al., 2001; Otaki, 2011a, 2011b; Saranathan et al., 2010; Stavenga et al., 2004; Sekimura et al., 2015; Márk et al., 2019). In the process of building the model the wings of butterfly can be considered a 3D symmetrical structure presenting a gradient state in the Z-axis direction. This is conducive to the establishment and analysis of the model. Kinoshita et al. found that the microstructure of butterfly wings presented a gradient distribution through SEM test in the early studies (Figure 1E) (Mejdoubi et al., 2013). Peter Vukusic and J. Roy Sambles researched photonic structures in biology. The SEM image of a broken scale of *Morpho rhetenor* showed that the morphology of a butterfly shows a Christmas-tree-like cross-section of the ridges. This result also confirmed the gradient phenomenon of the microstructures of butterfly wings (Chen et al., 2004). Potyrailo et al. found that the biological pattern of surface functionality exists in a butterfly's photonic structures. The pattern is a gradient of

surface polarity of the ridge structures, which run from their polar tops to their less-polar bottoms (Potyrailo et al., 2013). Recently, Lu et al. proved that guided cells orient concurrently with the cell density gradient on butterfly wings (Lu et al., 2019). This gradient phenomenon caused by the geometry of butterfly wings is the main reason for the physical and optical phenomenon, which gives colors to the butterfly wing scales.

W-Gradient

Compositions

Squid beaks are one of the hardest and stiffest organic materials deeply embedded within the soft buccal envelope. The way that the impact forces are transmitted between beaks and envelope is of considerable scientific interest. Squid beaks provide an inspiration for designing robust organic composites (Miserez et al., 2007, 2010). Previous scientific studies have shown that the connection parts have a gradient distribution. The hydrated beak exhibits a large stiffness gradient, which spans two orders of magnitude from the tip to the base. The beak tip has a modulus of stiffness of 5 GPa, whereas the base section has a stiffness of 0.05 GPa. In addition, the research shows that the squid beaks have water-enhanced mechanical gradient characteristics (Miserez et al., 2008; Suresh, 2001). Further research suggests this is because the content of histidine-rich proteins decreases from the tip to the base. At the same time the hydration degree varies inversely, leading to a gradient in Young's modulus (Tan et al., 2015). Chitin binding beak proteins (DgCBPs) and histidine-rich beak proteins (DgHBPs) are two families of proteins in the squid beak. Due to the ability to coacervate under physiological conditions of DgHBP-2, its temperature was found to be the most suitable material for encapsulation and its PH response. Therefore, the exploration of DgHBP-2 is beneficial and can play an important role in drug delivery systems. These proteins are cross-linked to form a three-dimensional structure. This provides useful information on how they bind to other macromolecules and describe their unique function (Cherel et al., 2019; Heymann et al., 2020) (Figure 2A). Unlike the gecko seta the squid beaks cross-section is enlarged along the Z-axis, which appears more axially symmetric (Fox et al., 2013; Miserez et al., 2008; Tan et al., 2015).

The mussel is an organism with a gradient structure, whose chemical composites present a gradient distribution. Previous studies have shown that the mussel byssal plaques have a surprising degree of fine and hierarchical structure (Tamarin et al., 1976; Lappin-Scott and Costerton, 1989). The plaque of mussels exhibits around 40% porosity, and the diameter of the pores presents a gradient state. These pores are open, and near the substratum the diameter is only 200 nm. However, near the thread, where meets the plaque, the diameter is about 3 um. The pores are filled with fluid in their native state and are interconnected by channels with smooth walls (Figure 2B) (Waite et al., 2004). The expandable byssal threads of marine mussels are protected by a layer of outer cuticle, which is rich in high protein (mfp-1) and approximately five times harder than the thread core. The presence of the outer cuticle protects byssal threads of mussels from the wear and tear of the wave-swept habits. Harrington et al. reports that granular cuticles of the mussel thread contain a protein that is rich in the catecholic amino acid 3,4-dihydroxyphenylalanine (dopa) as well as inorganic ions, notably Fe^{3+}. The granulated cuticle shows a remarkable combination of high hardness and high ductility. They also demonstrate that the cuticle is a polymeric scaffold stabilized by catecholic iron chelate with an unusual cluster distribution (Harrington et al., 2010). In addition, Zeng et al. found that Fe^{3+} ions in the mussel foot can mediate unusually strong interactions between the positively charged proteins. It can also put forward the dopa-metal interaction and may provide an energetic new paradigm for engineering strong, self-healing interactions between polymers under water (Tramacere et al., 2015). Recently, Xu et al. reported that Fe^{2+} and Fe^{3+} present a gradient in the mussel thread, and its REDOX action between Fe^{2+} and Fe^{3+} enabled the mussel to have a self-healing ability in seawater. The reasons of self-healing ability of mussel are that one water molecule adsorbs on the iron in O_2 adsorbed (O_2-Fe^{2+})$DOPA_2$ complex to form (H_2O-Fe^{2+}-O_2)$DOPA_2$, and next a DOPA reacts with (H_2O-Fe^{3+}-O_2)$DOPA_2$ to form $Fe^{3+}DOPA_3$ by replacing the adsorbed O_2 and H_2O on the iron to achieve self-healing. Research has shown that the oxygen content has an important impact on the mechanical properties of mussel thread. Tests on the mechanical properties of a mussel thread in environments with different oxygen levels show that an increase of oxygen content leads to a downward trend of the strength and ductility (Xu et al., 2019; Lee et al., 2011; Zeng et al., 2010). Therefore, the biological functional characteristics of squid beaks and mussels need to be realized in seawater. As a result, mussels are classified in this chapter as a W-gradient because of their microstructure in a gradient state and gradient distribution of their chemical elements.

Structures

The gradient phenomenon caused by structures in W-gradient mainly include spider silk, cacti, water striders, pitcher plants, wheat awns, and pinecones. Although the gradient phenomenon of these

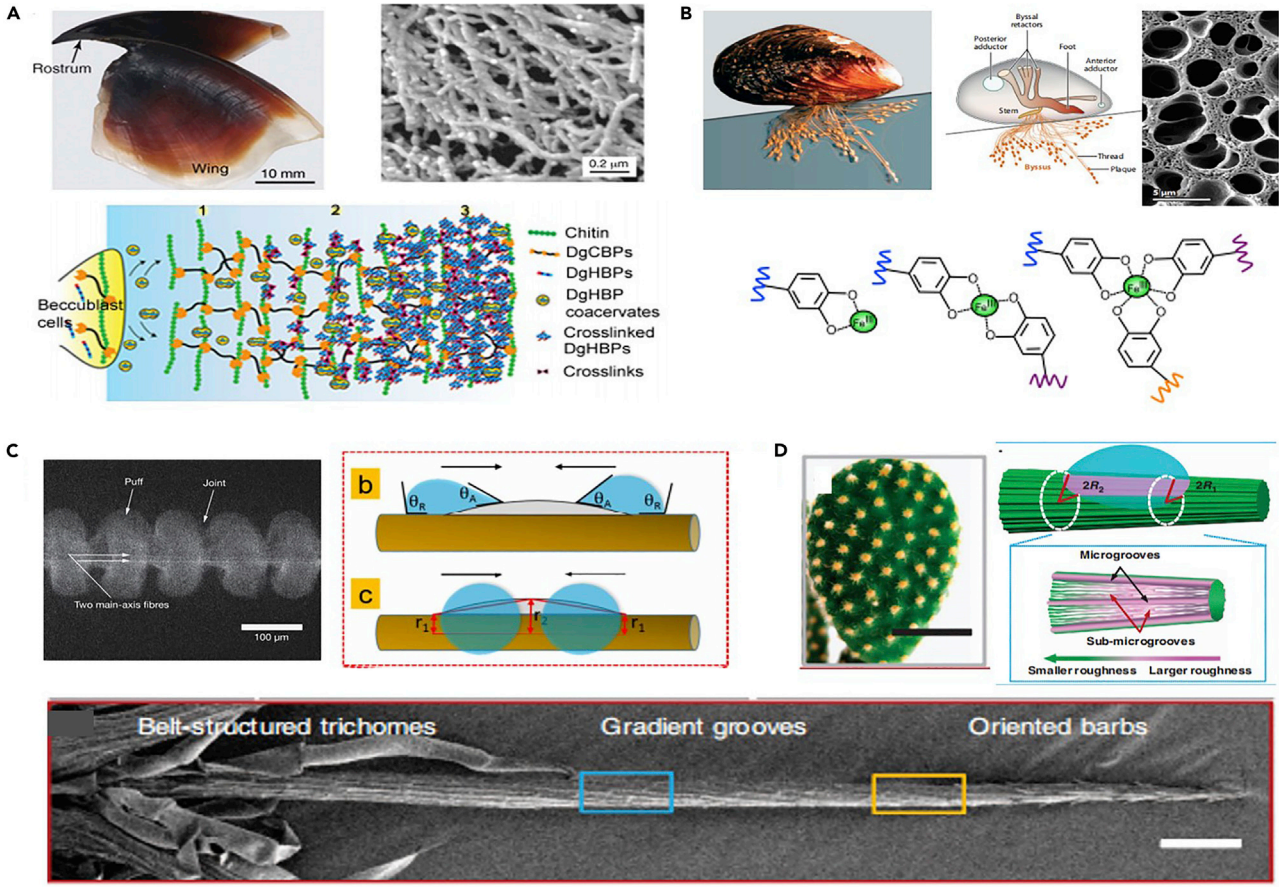

Figure 2. Several Representative Organisms of W-gradient

(A) The SEM images of squid beaks and the schematic of the content of histidine-rich proteins decreases from the tip to the base (Fox et al., 2013; Miserez et al., 2008; Tan et al., 2015).

(B) The mussel's picture and the SEM image of mussel's byssal plaques and the diameter of pores present a gradient state of plaques. The schematic diagram of Fe^{3+} ions regulating interactions between positively charged proteins as well as reveals the important role of Fe^{3+} in mussel thread (Waite, 2017; Lee et al., 2011).

(C) The SEM images and the schematic diagram of the Laplace pressure gradient during the water collection process of spider silk (Wang et al., 2016b; Zheng et al., 2010).

(D) Cactus and the SEM image of a single spine. Driving force diagram of cactus generated by Laplace pressure gradient and the surface-free energy gradient. Due to the Laplace pressure is relatively small, the water drop on the cone spine should toward the base side with a larger radius (R2) (Ju et al., 2012).

organisms is caused by their structure, the display of their functional properties needs to appear in the presence of liquid. In these organisms there is a variety in the formation of their structures as discussed in detail below.

Spiders can be praised as one of the best "manufacturing engineers." Their spider silk has excellent mechanical properties such as high strength, elasticity, and torsional superelastic behavior (Liu et al., 2017a; Muiznieks and Keeley, 2016), which does a magical job of efficiently collecting water from air. Zhang et al. reviewed the natural factors that affect the physical properties of spider silk, such as drawing speed, environmental conditions, and nutrient intake (Zhang and Tso, 2016). According to scientific research the micro- and nanoscale structures, as well as the sequences of its constituent proteins of spider silk, play important roles in the excellent chemical and physical properties of spider silk (Xu et al., 2014; Madurga et al., 2015; Holland et al., 2006; Porter and Vollrath, 2007). Jiang and coworkers show that the water-collecting ability of spider silk is the result of a unique fibrous structure that forms after wetting (Zheng et al., 2010). These structural features lead to a surface energy gradient between the spindle-knots and the joints as well as differences in Laplace pressure, both factors of which act together to achieve continuous condensation and directional collection of water drops around spindle-knots (Figure 2C) (Wang et al., 2016b;

Zheng et al., 2010; Xing et al., 2019). There are many applications inspired by the characteristics of spider silk, such as smart flexible electronics (Liao et al., 2020), water collectors (Deng et al., 2017; Huang et al., 2018) etc.. Recently, Feng et al. produced a high-efficiency water harvesting system inspired by spider silk and butterfly wings, which is achieved by integrating a tapered surface with a physical tapered structure and chemical wetting gradient. The system is made by anodizing methods introduced by nano-needles of copper hydroxide. Synergism of Laplace pressure and wetting gradient play essential roles in the water collection process and the continuous, directional, and long-range transport of fog droplets (Feng et al., 2020). Hou et al., inspired by spider silk and cactus, fabricated a multilevel-structure bioinspired fiber with multigradients. The fiber can achieve self-propelling control of droplets in a low temperature and high humidity environment, whereas the multigradients provide multiple driving forces to overcome resistance and can be controlled via temperature (Hou et al., 2020). These bionic designs through spider silk and other creatures all provide important guidance in related fields such as liquid directional transportation due to their unique gradient structures. Cacti, water striders, and pitcher plants are associated with Laplace pressure. Laplace pressure plays an important role in guiding the design of biomimetic devices that collect water. There are related introductions below. A cactus can collect water from fog with high efficiencies, which allow them to live in an arid environment. Ju et al. confirm the core reason of this phenomenon is the unique structure of the cactus (Figure 2D) (Ju et al., 2012), where the spines and the barbs with aligned gradient grooves and cooperation between the spines and the trichomes (Ju et al., 2012). Cacti form a cytoplasmic concentration gradient inversely correlated to the nuclear translocation gradient of its dorsal side (Bergmann et al., 1996). Some studies have shown that the phosphorylation of a cactus causes it to degenerate and release its dorsal side, forming a dorsal gradient from its ventral to dorsal nuclei. Signal dependent phosphorylation was also proposed to guide the spatial regulation of cactus protein proteolysis (Reach et al., 1996; Drier et al., 2000). Bhushan and co-workers proposed design guidelines that collected water droplets driven by the Laplace pressure gradient and gravity and fabricate a water collection tower inspired by cacti. They also explore bioinspired triangular patterns with various wettability for the transport of condensed water and came to the conclusion that the hydrophilic triangle pattern surrounded by superhydrophobic regions are most effective in self-transportation (Gurera and Bhushan, 2019; Song and Bhushan, 2019). Researchers demonstrate that a water strider can glide freely across the water because of the special hierarchical structure of its legs and wax coating. The legs are covered with a large amount of directional micro bristles and fine nanoscale grooves, which are more important in inducing water resistance. The SEM images show a gradient structure of a small region of water strider's leg. When compared with the vertical legs, the legs parallel to the water surface can support up to ten times the force before immersion (Gao and Jiang, 2004; Hurchalla, 2018; Hurchalla and Drelich, 2019). The cross-section model of a water strider standing on the water surface shows that the radius and contact angle of water strider's legs are the main forces supporting the water strider. This provides an inspiration for the design of related small aquatic robots (Figure 3A) (Watson et al., 2010; Zhang et al., 2011). Pitcher plants are one of the "carnivores" of the plant world that has attracted attention for preying on flies and ants. Such plants are naturally endowed with a gradient energy distribution and Laplace pressure on its surface. Related studies have shown that the slippery inner surface grown with hierarchical micro-thorn structures lead to reduced friction, which may be the fundamental mechanism for prey capture and retention (Gan et al., 2018). A pitcher plant has the function of directional transportation of droplets. Wang and co-workers proved that the existence of the asymmetric arch-shaped microcavity with its gradient wedge corners and sharp edges, as well as its structural gradient in the first layer of microgrooves of the peristome are the main reasons for the directional transportation in pitcher plants (Li et al., 2018). Yao and co-worker studied the smoothness and robustness of Lubricant-Impregnated Surfaces (LISs) of pitcher plants under different microtextured topologies. They found that the LISs' slippery properties were closely related to the states of the oil-layer on the interface, which were changed after rinsed. They concluded that the proper microstructure can enhance the anti-slip performance of the material and prolong its service life (Zhang and Yao, 2019). Zhang et al. found that the slippery zone of the pitcher plant had an anisotropic morphology of lunate structure (63 um in length and 15 um in width) and 2–3 um in a thick dense wax layer. Due to its special structure the slippery zone presents anisotropic wettability. The biomimetic slippery surface of pitcher, a plant's slippery zone, is also fabricated by a simply replica modeling method and is of significance to the bionic research on the surface of the pitcher plant (lower left) (Zhang et al., 2015). Chen et al. found the continuous, directional water transport occurs on the surface of the ''peristome,'' which can enhance the capillary rise in the transport directions and prevent the backflow in the reverse direction (Chen et al., 2016). Jiang and coworkers deeply researched the relationship between liquid diffusion distance and wettability by surface gradient properties of pitcher plants. The results showed that the unidirectional liquid spreading is

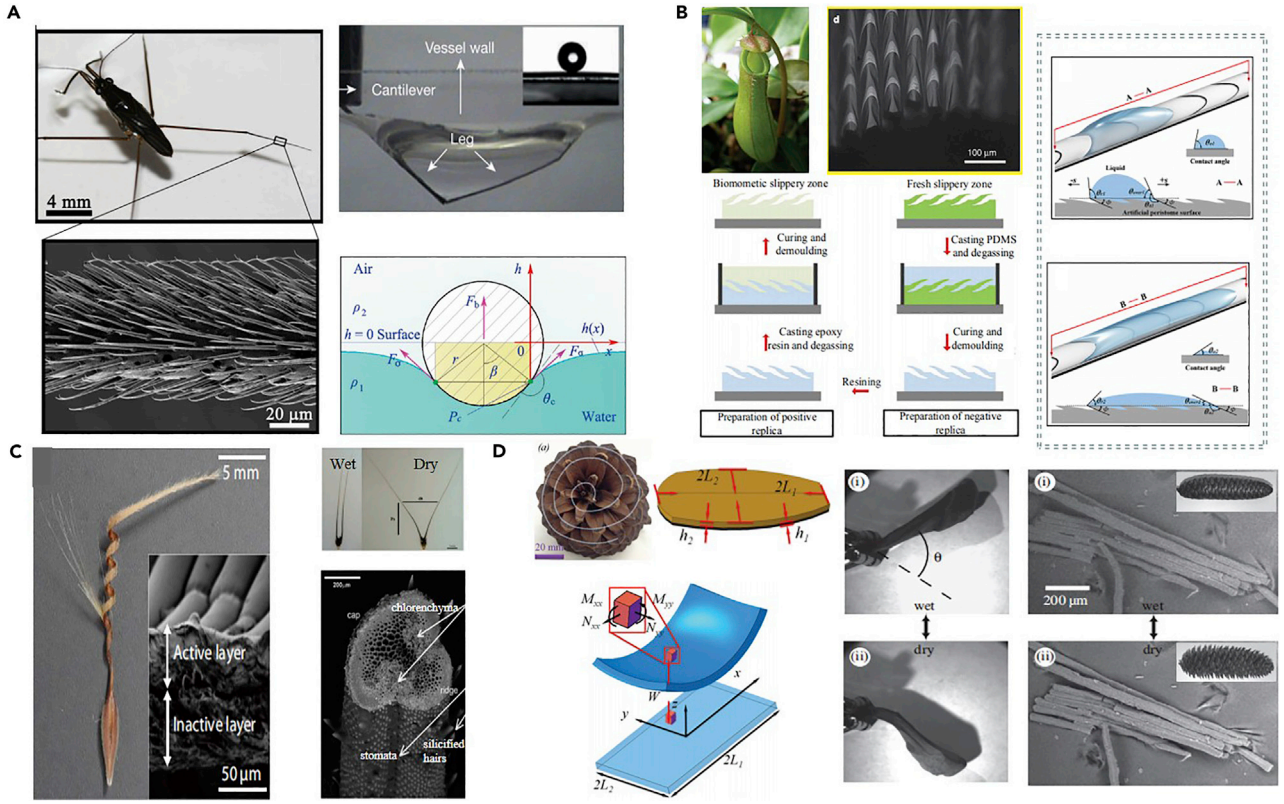

Figure 3. Several Representative Organisms of W-gradient

(A) A picture of a water strider resting on water and the SEM image of a small region of its leg. The microstructure of the water strider's legs produces a Laplace pressure difference and can stay on the water for a long time. A schematic model of the water strider floating on water and the cross-section model of the air water interface of a *Partially Submerged* leg (Zhang et al., 2011; Watson et al., 2010).

(B) A pitcher plant and the SEM images of the surface. The Laplace pressure formed by the surface structure is the main reason for the water collection. The modeling for biomimetic slippery surface of *Nepenthes alata's* slippery zone and the schematic diagram liquid diffusion in the negative direction (−s) and positive direction (+s) (Chen et al., 2016; Yong et al., 2017; Zhang et al., 2015, 2017).

(C) A hygroscopically responsive bilayer structures and the SEM images of wheat awns. A picture of wheat awn under wet and dry conditions and an SEM image in the back scattering mode of a section through wheat awn (Shin et al., 2018).

(D) The geometry model of pine cone and the deformation diagram. The state of pine cone under wet and dry conditions and their SEM images (Reyssat and Mahadevan, 2009; Lin et al., 2016).

determined by spreading in negative directions (−s) and positive direction (+s). In the negative direction, the tendency of the liquid to diffuse is blocked by the sharp edges of microcavity, i.e. pinning effect. In the positive direction the liquid spreading can be described as the liquid exceeding the sharp edge and overflowing around the second-order ridge allowing the liquid to fill the microcavity along the wedge. The research of this mechanism has a guiding significance for the field of controllable microfluidics (the right) (Figure 3B) (Zhang et al., 2015, 2017; Chen et al., 2016; Yong et al., 2017). Guo and co-workers designed a fog collector that integrated conical copper needles with a gradient wettability and rough hydrophilic slippery surfaces inspired by cacti and pitcher plants. Due to the synergy between the Laplace pressure difference from the conical needle, wettability force, and released surface energy in drop coalescence, the whole system realizes an enhanced fog harvesting and higher fog collection rate (Zhou et al., 2020). In addition, Jiao et al. designed a large area of a lubricated slippery surface to achieve buoyancy-driven bubble self-transport and gas capture by femtosecond laser processing inspired by pitcher plants. Once decorated, the lubricated slippery surface on a large area on the gas catcher is used to capture underwater bubbles. The device keeps working with an air output of 3.4 L min^{-1} and obtains a capture efficiency of up to 90% (Jiao et al., 2019). These bionic designs provide inspiration for related fields and effectively realize energy collection and are environmental friendly. The abovementioned organisms all have a common characteristic, their own gradient microstructure, and the Laplace pressure. As a result, these organisms have certain biological characteristics such as a water collection function in a wet environment.

There are also two kinds of organisms, wheat awns and pinecones, that have the abilities of changing with the environmental humidity due to their specific structures. The hygroscopically responsive bilayer structures of wheat awn enables it to realize functional adaptations to various environment stimuli (the left) (Shin et al., 2018). Researchers discovered that the arrangement of cellulose fibrils is well along the long axis of the cap but randomly at the ridge (Figure 3C) (Shin et al., 2018). The asymmetry and gradient distribution in this arrangement causes bending of awns with changes in humidity. They also identified a region that contains fibrils aligned in all directions at the base of the awn. This region is the active art that contracts as it dries and pulls the awn to a bent position. And expanding in length with humidity would push the awns together and contracting with drying would pull the awns apart, thereby pushing the seeds into the soil for dissemination. This phenomenon is explained by the fact that water molecules absorbed by the matrix may cause large microscopic distortions by expanding vertically through adjacent layers. There are tiny gaps between the fibrous layers to facilitate the exchange and transport of water through the cell wall, thus increasing the sensitivity of the drive unit to the regulation of moisture changes (Elbaum et al., 2007, 2008; Jung et al., 2014). Jung et al. revealed that the self-burial of the seed was a sophisticated outcome of the helically coiled configuration of the awn (Jung et al., 2014). Recently, Lin et al. developed an artificial system with hierarchical structures by using a 3D printing technology. These structures are used for fog drop capture and fast transportation inspired by wheat awns. The collection efficiency of bioinspired system is up to 5.90g/cm^{-2}·h, which is higher than individual ones and other bionic systems (Xiao et al., 2020). As for pine cones, the non-uniform arrangement of cellulose microfibrils lead to a reversible deformation: open in dry and close in wet (Reyssat and Mahadevan, 2009). The scale consists of two regions with different structural organizations: a fibrous sclerenchyma region and a porous sclerenchyma region composed of cellulose that absorbs water easily. The structure of the porous region also graded from its interface with more robust fibrous region to the external surface with the highest porosity. The length of the fiber components remains constant, and the porous components shirks when dry and swells when hydrated, which causes the local strain to increase monotonically as the distance from the fiber layer increases. The two-layer scale structure of pine cone can be regarded as a 3D structure that provides an idea for the construction of the bionic model of a pine cone (Figure 3D) (Reyssat and Mahadevan, 2009; Lin et al., 2016; Dawson et al., 1997; Hellum, 1982). Lin et al. revealed that the pine cone's opening and closing mechanism was due to the self-bending action of its scales. They found that at critical humidity levels the longitudinal and transverse principal curvature bifurcated according to the thickness and shape of the scale. These findings help to understand the shape transformation of double or multilayer natural structures and provide insights into the design of convertibles/materials with great application potential (Lin et al., 2016).

In summary, the gradient phenomenon caused by the structure of organisms plays an important role in the function of water collection and responding to humidity. Because the realization of these biological functional characteristics requires the existence of liquid or water vapor, these organisms are grouped into the chapter of W-gradient.

In this chapter, we reviewed in detail the gradient phenomenon in dozens of organisms and divided them into D-gradient and W-gradient according to whether liquid or high humidity environments are needed for the realization of organisms' characteristics. In the detailed introduction above, we know that the gradient phenomenon plays an important role in the development of biological functions. The discovery of these gradient phenomena provides inspiration for researchers in this field. However, the gradient phenomena of these organisms are somewhat abstract to understand. In the following chapter, we simplify them to models for the convenience of the readers' understanding.

SIMPLIFIED MODELS OF GRADIENT PHENOMENON

In this chapter, we simplified the common gradient phenomenon in nature into six models: composite gradient, mud-brick gradient, pore structure gradient, gradient microstructure, gradient assembly, and soft gradient materials. The modeling of complex problems can help us better understand the essence of the phenomenon.

Model 1 in Figure 4A is built based on the gradient distribution of elements in the same matrix. In other words, this model usually refers to a gradient distribution of an element in the same matrix. Taking a single gecko seta as an example, the β-keratin had a gradient distribution along the length of single gecko seta and plays a key role in enhancing the Young's modulus of the seta. Thus, the single gecko seta showed a

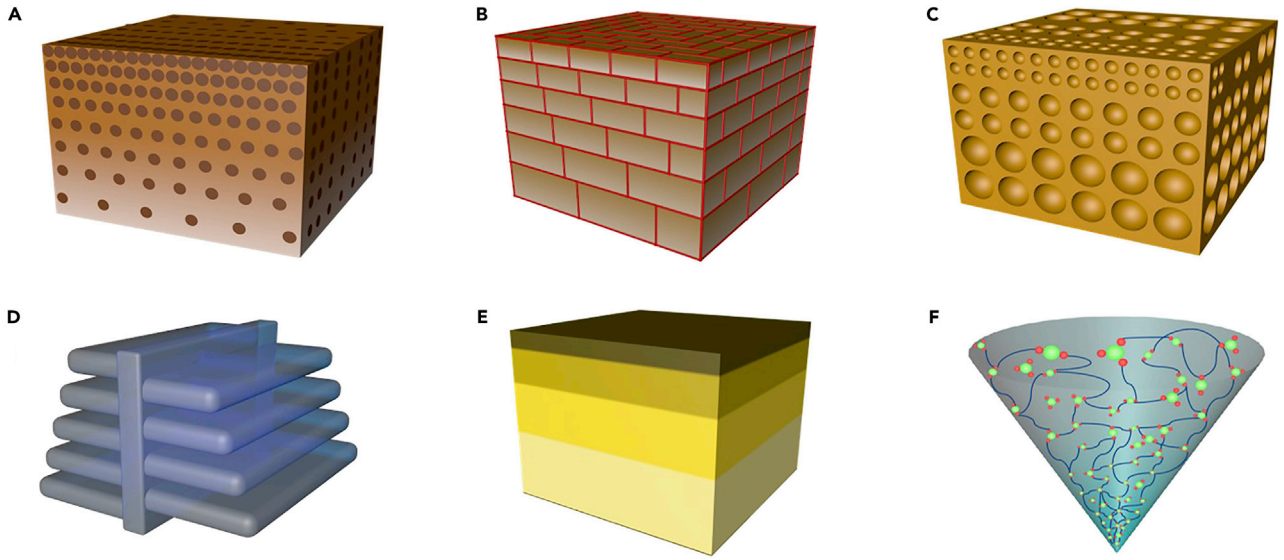

Figure 4. The Models of Gradient Phenomenon Inspired from Organisms

(A) Composite in organisms in a gradient state. The addition of composites in a gradient state to material can improve its durability. The main representatives are the gecko and ladybird.

(B) Gradient state of brick and mortar structure. This structure can improve the mechanical properties of the design materials and enhance the toughness and strength. The typical organism is a shell.

(C) The pore structure inside the organisms' present gradient. The gradient distribution of pore structure provides the impetus for the growth of organisms, such as bamboo and mussels.

(D) The gradient microstructure with a Christmas tree shape. This is a structural model for butterflies' wings, which are reflective and hydrophobic.

(E) Hierarchical gradient structure. The different density of each layer can make the structure have deformation characteristics under certain circumstances, such as wheat awns.

(F) Two or more ions in organism present a gradient. Through the REDOX reaction between different ions, the designed material has specific functions like self-healing ability.

gradient Young's modulus distribution along the length of the seta body with a range from 95 MPa at the top to 1725 MPa at the bottom, a difference of 20 times higher (Dong et al., 2020). Similar phenomena was also observed in ladybirds and squid beaks (Miserez et al., 2008; Peisker et al., 2013). Figure 4B is the model 2 for turning the local arrangement of constituents to enhance the performances even without alteration of chemistry. Shells, for example, are anisotropic with a hierarchical nature and exhibit distinctly anisotropic mechanical behaviors. The crossed lamellar structure of shells in the inner and middle layers and a fibrous/blocky and porous structure are composed of nanoscaled particulates (~100 nm diameter) in the outer layer. The layers of a shell are 95% calcium carbonate, with the remaining 5% organic matter. The highly ordered brick-and-mortar microstructure of the shell gives it both excellent strength and toughness. All of these have important inspiration and contribution to design new bio-inspired synthetic materials (Jiao et al., 2015, 2016; Yang et al., 2011). Yu and coworkers reported a novel biomimetic strategy named assembly-and-mineralization for the first time. Through mesoscopic "assembly and mineralization," in order to simulate the growth mode and control process of the pearl layer in mollusks, they mineralized the prefabricated layered organic framework and successfully prepared millimeter-thick blocks of shell layer structure. The chemical composition and multistage-ordered structure of the artificial material are similar to that of the natural shell layer (Mao et al., 2016). Model 3 in Figure 4C represents the fibrous region or porous region gradient of the organisms. Examples of this model with functionally gradient structures are pine cones, bamboo, and mussels. The difference between the pine cones and bamboo is that pine cones are porous forms with constant fiber length, whereas bamboo is a fiber-reinforced cellular material. Because of the gradient structure of Figure 3C, they have the properties of deformation according to the humidity of the environment and high flexural rigidity. Wheat awns and pine cones have a similar variation with ambient humidity, with the difference being that the gradient of wheat awn is caused by the uneven distribution of cellulose fibrils. The plaque of a mussel exhibits the gradient distribution of pores, and the diameters of these pores also show a gradient state, which has been mentioned above in detail. Model 4 represents the gradient structure formed due to its own structure. The wing of butterfly under the scanning electron microscope is a typical representation (Figure 4D) (Biró and Vigneron, 2011). The wings of the

butterflies are colorless. Because of the gradient of the microstructure of the butterfly, it will be in the light under the irradiation of a profusion of colors. Model 5 in Figure 4E represents a component model derived from mussel protective coating, mainly mfp-1 (~10 mol%), which plays the key role in enhancing the toughness and self-healing performance of the mussel thread. The inside part is mainly fibers that are soft but could deliver energy. Therefore, the mussel threads can undergo 10 levels waves and storms on the ocean (Holten-Andersen et al., 2007). Similar composite structure can also be observed in teeth (Weaver et al., 2010; Wang et al., 2013; Yang et al., 2013), crayfish (Bentov et al., 2012) etc.. Model 6 in Figure 4F represents two different chemical elements that appear as a gradient in one organism. The typical example explained in the previous part is the Fe^{2+} and Fe^{3+} gradient distribution across the cuticle thickness of mussel thread, where there is more Fe^{2+} and little Fe^{3+} inside the inner cuticle. During the lateral expansion the outer cuticle content of Fe^{2+} decreased, whereas the content of Fe^{3+} increased. All of these support the hypothesis that the cuticle is a functionally graded material with high stiffness, extensibility, and self-healing ability (Xu et al., 2019). Another model, similar to squid beaks, contains no mineralized structures, only protein with some crosslinking modifications and chitin (Miserez et al., 2008; Linder, 2015).

PROCESS DESIGN AND FUNCTION CLASSIFICATION

The gradient structures/surfaces of these organisms have provided the outstanding performance far beyond traditional materials. To further understand their performance, we have separated the discussion into bioadhesion, surface patterns, locomotion, seed dispersal, predator-prey, and other points of view.

Gradient Bioadhesion

The gradient phenomenon that exists in bioadhesive organisms (e.g. geckos, mussels, ladybirds) are related to the chemical compositions or constituents, which to some extent determine the reversible adhesion and duration of the bioadhesive organisms.

Outstanding bioadhesive organisms, such as the ladybird and gecko, all have a gradient composite protein distribution along their bristles and seta. Mussels have a gradient linear distribution of Fe^{2+} and Fe^{3+} ions across the cuticle thickness of mussel byssal threads. The gradient distribution of chemical compositions along the bristles, seta, and thread of organisms are a key factor that affect the adhesive performance of the organisms. Here we further summarize the material selectivity and fabrication methods of making bioadhesive organisms. The linear distribution of resilin protein in ladybird bristles results in the gradient distribution of Young's modulus. Inspired by this, Geikowsky et al. fabricated titled, mushroom-like, stiff fibers to make a biomimetic functional surface with an elastic modulus gradient. The results show that the soft joint fibers achieved 22 KPa in shear and a pull-off stress of 110 KPa in the gripping direction. The data in the direction of release are two times and ten times higher, respectively. It was concluded that adding a flexible joint, which was more flexible than the stalk of the fiber, between the tip and the stalk improved both shear and pull-off stresses (Geikowsky et al., 2018; Peisker et al., 2013). Gong et al. performed finite element modeling on the viscoelastic contact of composite micropillars with gradient distribution characteristics, and the results showed that the soft top layer of the composite pillar had a critical thickness. It also suggested that the thickness of the soft top layer should not be less than the critical value. The viscoelasticity of soft materials helps them to better adapt to rough surfaces. This research helped to understand the viscoelastic contact problem of composite micropillars and guide the optimal design of biomimetic composite micropillars to achieve bioinspired bioadhesives (Gong et al., 2019).

Geckos and ladybirds have a similar principle. The property of a gecko's β-keratin gradient distribution indirectly affects their outstanding reversible adhesion, stiffness, and self-cleaning properties (Zhou et al., 2013; Boesel et al., 2010). The "contact-splitting principle" reported by Gao et al. (Varenberg et al., 2006) has been considered as the principle for fabricating long standing and anti-fatigue properties. They further reported the fibrillar ends were not sensitive to defects when the size of the fibril was less than some critical length scale (provide number) determined through theoretical analysis (Gao et al., 2003). Varenberg et al. demonstrated that the adhesion force hardly increased with the number of contact elements, whereas the total contact area was constant (Varenberg et al., 2011).

The mechanical properties of the design-inspired gecko surface mainly depended on two aspects, the structure and the materials (Zhou et al., 2013). The hierarchical structure of geckos' feet, which include the toe pads, setal arrays, and spatulae, allows the gecko to generate strong adhesion and friction to climb on various surfaces (Figure 5A) (Yu et al., 2011). The following shapes are commonly used in current designs

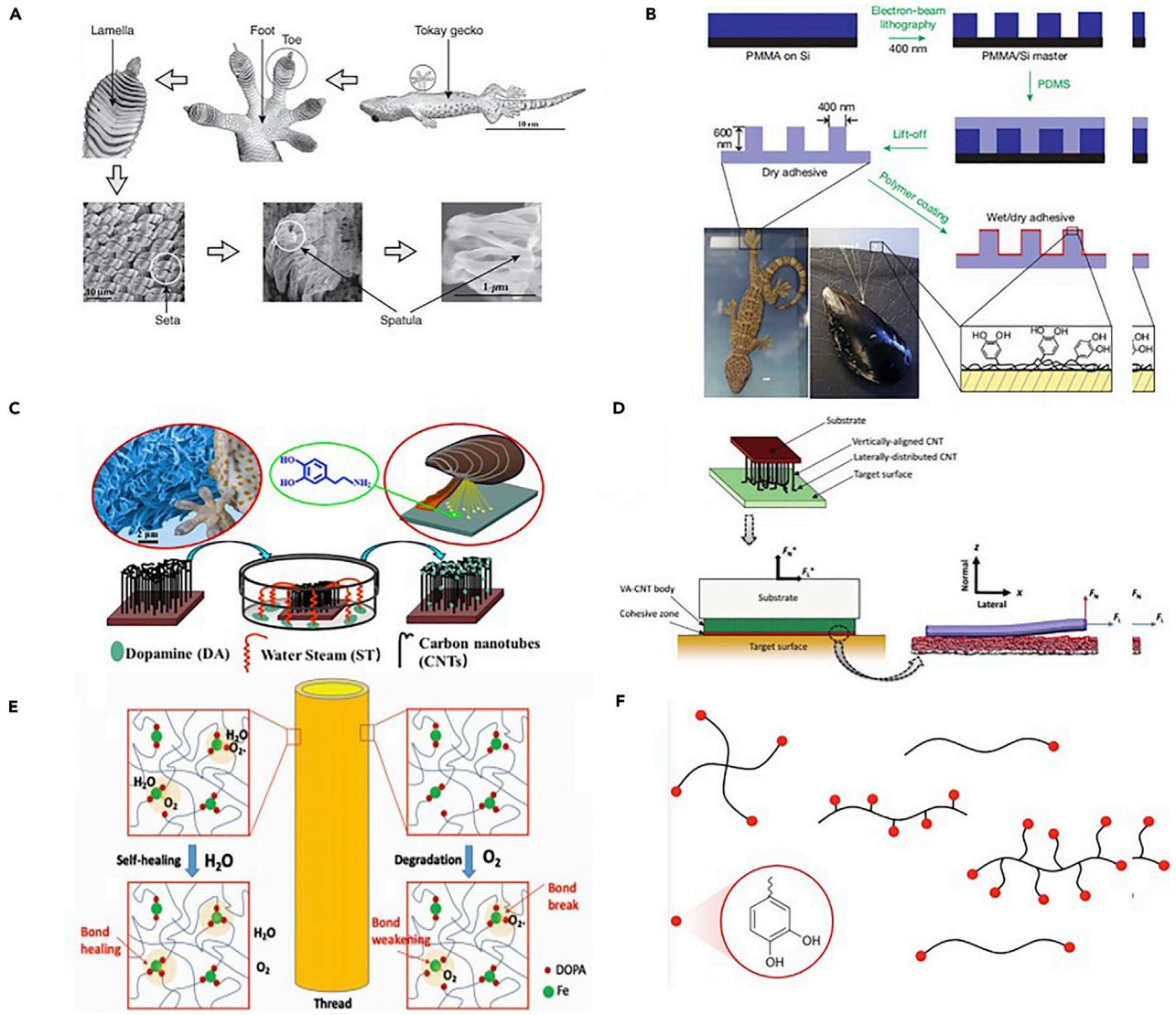

Figure 5. The Hierarchical Structure of Nature Animals

(A) Hierarchical structures of a Tokay gecko, including optical images of a Tokay gecko, its foot, and its toe; SEM images of a setal array, spatula pads, and a magnified view of a spatula pad (Yu et al., 2011).

(B) Rational, design, and fabrication of a wet/dry hybrid nano adhesive (Lee et al., 2007).

(C) Schematic diagram of carbon nanotube modifications with polydopamine (Li et al., 2019).

(D) Schematics of vertical aligned CNT arrays with laterally distributed CNT segments adhering on a target surface; FEA model for simulating the macroscopic adhesive behaviors of vertical aligned CNT arrays and a snapshot of a lateral CNT being peeled from substrate in molecular dynamics (Hu et al., 2012).

(E) Schematic diagram of the self-healing principle of a mussel thread (Xu et al., 2019).

(F) Schematic diagram of a polymer system of a mussel adhesive protein simulation (Lee et al., 2002; Brubaker et al., 2010).

for the pillars: simple fiber arrays, fiber ends with different geometries (such as mushroom shaped micro-fibers, fiber arrays with asymmetric spatulas, and fiber arrays with concaved pillar ends), titled fiber arrays, hierarchical fiber arrays, and fiber arrays combined with a lamellar structure (del Campo and Greiner, 2007; Del Campo et al., 2007b; del Campo et al., 2007a; Haefliger and Boisen, 2006; Sameoto and Menon, 2009). As for the materials classification, polymer materials such as polyimide (Yoon et al., 2009), PVS (Gorb et al., 2007), PDMS (Dong et al., 2019; Greiner et al., 2007; Menon et al., 2004), poly (methyl methacrylate) (PMMA) (Yu et al., 2011), polystyrene (PS) (Kustandi et al., 2007), polyethylene (Lee and Fearing, 2008), and polyurethane (Kim et al., 2007; Jin et al., 2012) have been reported to be suitable for making gecko inspired

functional surfaces. These materials are generally characterized by a low Young's modulus. Based on the "contact and splitting model" these materials can generate strong and reversible adhesion. This can be attributed to the polar group's contribution in enhancing the adhesive. Besides these functional surfaces, which are bionic for gecko adhesion alone, some studies have incorporated the bionic principle of a mussel's strong underwater adhesion into the gecko adhesion's surface design (Figures 5B and 5C) (Lee et al., 2007; Li et al., 2019). The fabricated pillars with a mussel-adhesion-protein-mimetic polymer can improve the reversible wet adhesion property under water. This chemical coating method seems to be effective in enhancing the adhesion of the functional surface, which is worthy of reference in the further functional surface design. To increase the functionality of the prepared bioadhesive system, thermal and electrical materials are selected to expand the applications of this system's multiwalled carbon nanotubes (MWCNT) with stable electrical and thermal properties having attracted increased attention (Figure 5D) (Yurdumakan et al., 2005; Hu et al., 2012; Qu and Dai, 2007; Wirth et al., 2008). Chen et al. presented an unprecedented photo-detachable mechanism of making gecko-inspired smart surfaces, which used carbon dot (CD) and PDMS (Chen et al., 2019a). To fabricate gradient-distributed gecko-inspired surfaces, Wang et al. used state-of-the-art technologies to fabricate bioinspired functional gradient interfaces/surfaces. This was achieved by using spatial distribution of nanocomposites (FGNCs) with a controllable stiff-to-soft or soft-to-stiff transition within region as narrow as 10 microns. The manufactured gradient surface has stronger mechanical properties that can be used in numerous surface/interface fields (Wang et al., 2017c). Dong et al. successfully input Fe_3O_4 nanoparticles inside PDMS and tuned the magnetic field at the outside surfaces. Results indicated the fatigue life has been increased, and the shear adhesion force of the fabricated surface in 300 repeated tests for the gradient PDMS-based pillar arrays can still be restored to more than 90% of the original. These have solidly supported the hypothesis that gradient surfaces can dramatically enhance the fatigue life and reversible adhesion performances of the biomimic gecko-inspired surfaces (Dong et al., 2020).

Mussel threads can withstand storms and winds in the ocean. To adapt to the turbulent environment, they have evolved to have a special toughness, self-healing ability, high elastic modulus, and high extensibility (Lim et al., 2016; Lee et al., 2006; Holten-Andersen et al., 2007). Some related researches of mussels have shown that the cuticle of a mussel's byssal thread mainly contains the catecholic amino acid 3,4-dihydroxyphenylalanine (Dopa) and iron, which forms a cross-linked iron catecholic structure. When regarding the self-healing ability of mussels, the relevant results indicate that mussel threads are distributed linearly by two chemical components: Fe^{2+} and Fe^{3+}. The self-healing ability of a mussel is realized by the mutual conversion between Fe^{2+} and Fe^{3+} contained in mussel filaments shown in Figure 5E. The discovery of the self-healing mechanism of mussels provides a design idea for future bionic relative self-healing of mussels. Politi et al. found that the cuticle of mussels showed a 2-fold decrease in the hardness after removing metals from it (Politi et al., 2012). For all the components iron is the key to its mechanical and self-healing properties. In addition, crosslinking also plays an important role in metal coordination to form different structures, the environmental impact, and the protection of their own materials. Some researchers have developed methods that mimic the mussel's function to enhance its properties and metal coordination (Qu and Dai, 2007; Filippidi et al., 2017; Kang et al., 2016; Kirschner and Brennan, 2012). Inspired by the natural adhesive protein distribution in the mussel, a series of researches have been carried out to functionalized linear or branched polymers by using a variety of chemical methods. Among them, the linear and branched polymer families based on the commonly used polyethylene glycol (PEG) are taken as an example, in which each polymer chain contains Dopa as the terminal group (Figure 5F) (Brubaker et al., 2010; Lee et al., 2002). There are also materials that are protein- and polypeptide-based that mimic a mussel with adhesive properties. At first, researchers tried to mimic a mussel with Dopa peptides synthesized by chemical methods of solid or liquid peptides (Yamamoto, 1987; Yamamoto et al., 1992; Yamamoto and Ohkawa, 1993; Tatehata et al., 2000). Subsequently, Dopa and lysine polypeptide copolymers are obtained by the ring-opening polymerization of N-carboxylic anhydride monomer (Yu and Deming, 1998; Yu et al., 1999; Yin et al., 2009). In addition, DNA technologies also have been employed to create adhesive proteins (Maugh et al., 1988; Filpula et al., 1990; Strausberg et al., 1989). In the past two decades, hydrogels have made great progress in the field of biomimetic mussels. At the beginning researchers attempted to use hydrogels for bionic mussels, but the hardness of the hydrogel ($E < 50$mpa) was far less than cuticle of a mussel (1 GPa) (Holten-Andersen et al., 2009; Yan et al., 2017; Lee et al., 2007; Gebbie et al., 2017). In subsequent research, the hydrogel had developed self-adhesiveness (Xie et al., 2020) and additional properties including conductivity (Shao et al., 2018), toughness (Han et al., 2017), self-healing (Chen et al., 2018b), antibacterial (Gan et al., 2019), and a tolerance to an extreme environment (Han et al., 2018; Xie et al., 2020).

In summary, Dopa, Dopa peptides, or their catechol mimics are used to prepare biomimetic protein-inspired polymers for simulating the adhesion property of mussels. Among these original polymer materials, catechols can enhance the adhesion of wet surfaces. The adhesive properties of catechols may be important for anchoring polymers, biomolecules, and other compounds to solid surfaces. These carefully designed polymer compositions and the structure of their coatings can produce adhesives or anti-adhesive coatings in our daily lives. However, biomimetic materials related to the self-healing abilities of mussels need to be further studied.

Body Shapes

In the bionic world, there are organisms with gradient characteristics of body shape, such as squid beaks and butterflies. Instead of seashells and chiton teeth having a mineralized inorganic component, the squid beak is entirely organic with the hardest and stiffest wholly organic materials known and has attracted the attention of many researchers. This gradient phenomenon occurs from the spatially controlled crosslinking of chitin nanofibers with a protein matrix aided by catecholamines (Waite and Broomell, 2012). The forming mechanism of composite materials and the selected materials play important roles in the process of bionic squid beaks.

Tan et al. proposed a mechanism, a layer-by-layer polyelectrolyte deposition for forming biocomposite materials. The metastable protein phase model of the composite copolyester was prepared from polyaspartic acid (polyAsp), polyl-histidine (polyHis), and can be used for the bionics of squid beaks (Figure 6A) (Tan et al., 2013). Zhang et al. carried out chemical synthesis of the bionic squid beak through a simple one step process, which is initiated by $NaIO_4$-induced $_L$-dopa oxidation (Figure 6B). They introduced a spatially controlled crosslinking (supplemented by catecholamines) water-treated chitin deacetylation composite. Chitin was also used as a bridging material for mechanical mismatches (Zhang et al., 2016). Miserez et al. reported L-3,4-dihydroxyphenylalanine (dopa)-histidine (dopa-His) as an important covalent crosslink, which provides a mechanical strengthening to the material of the beak. The only other component of a squid beak besides protein is chitin. It is relatively simple as a material; it is a linear N-acetylglucosamine homopolymer that forms fibrils much in the same way as cellulose (Miserez et al., 2008). Rowan et al. had developed a film where the degree of crosslinking was controlled along the length, while the film had the gradient character of water-enhanced mechanical properties. They applied tunicate cellulose nanocrystals as the nanofiller that were functionalized with allyl moieties. In order to crosslink the CNC nanofiller, they used photoinduced thiol-ene chemistry (Figure 6C) (Fox et al., 2013). These researches provided the guidance to the formation of biomaterials of hard organic materials in the software.

In addition to the bionics of biology, there are also bionic combinations of two kinds of organisms. For example, inspired by mussel thread coating and squid beak interfacial chemistry, Zvarec et al. prepared inorganic/organic (γ-Fe_2O_3/catechol) interfaces (Figure 6D). The interfaces produced stability and strengthen as well as improved stability at high temperature, physiological pH, and acid/base conditions, which can be potentially used in engineering areas (Zvarec et al., 2013). Such research ideas also provide some new design schemes for researchers and scientists.

As for the butterfly, the ridge structure surface polarity gradient pattern is like the "Christmas tree" shape. Han et al. used a combination of sol-gel and subsequent selective etching. The fabrication process of bionic butterfly's wings is shown in Figure 6E. They synthesized an inverse SiO_2 copy of the light-trapping structure in butterfly wing scales (Figure 6F). Even though the synthesis of materials and structures were different from the actual butterfly wings, this work could open up possibilities for an extensive study into mimicking novel bio-inspired functional materials (Han et al., 2013). The bionics of butterfly wings can be applied to photonic security tags, self-cleaning surfaces, gas separators, protective clothing, sensors, space exploration, space equipment, etc. (Potyrailo et al., 2013; Han et al., 2013).

Locomotion

This section mainly introduces examples of the bionics of locomotion. Locomotion means that organisms with a special function, due to the presence of gradient properties, exhibit motion characteristics when they perform their function. Specific content is mainly reviewed in accordance with the spindle-knots of spider silk and cactus gradient surface shape for water collection, transportation, or even energy harvesting, based on the pitcher plant's superhydrophobic surface bionic smart surface. The structure of pine cones and wheat awns are bionic according to their function of changing with the environmental humidity.

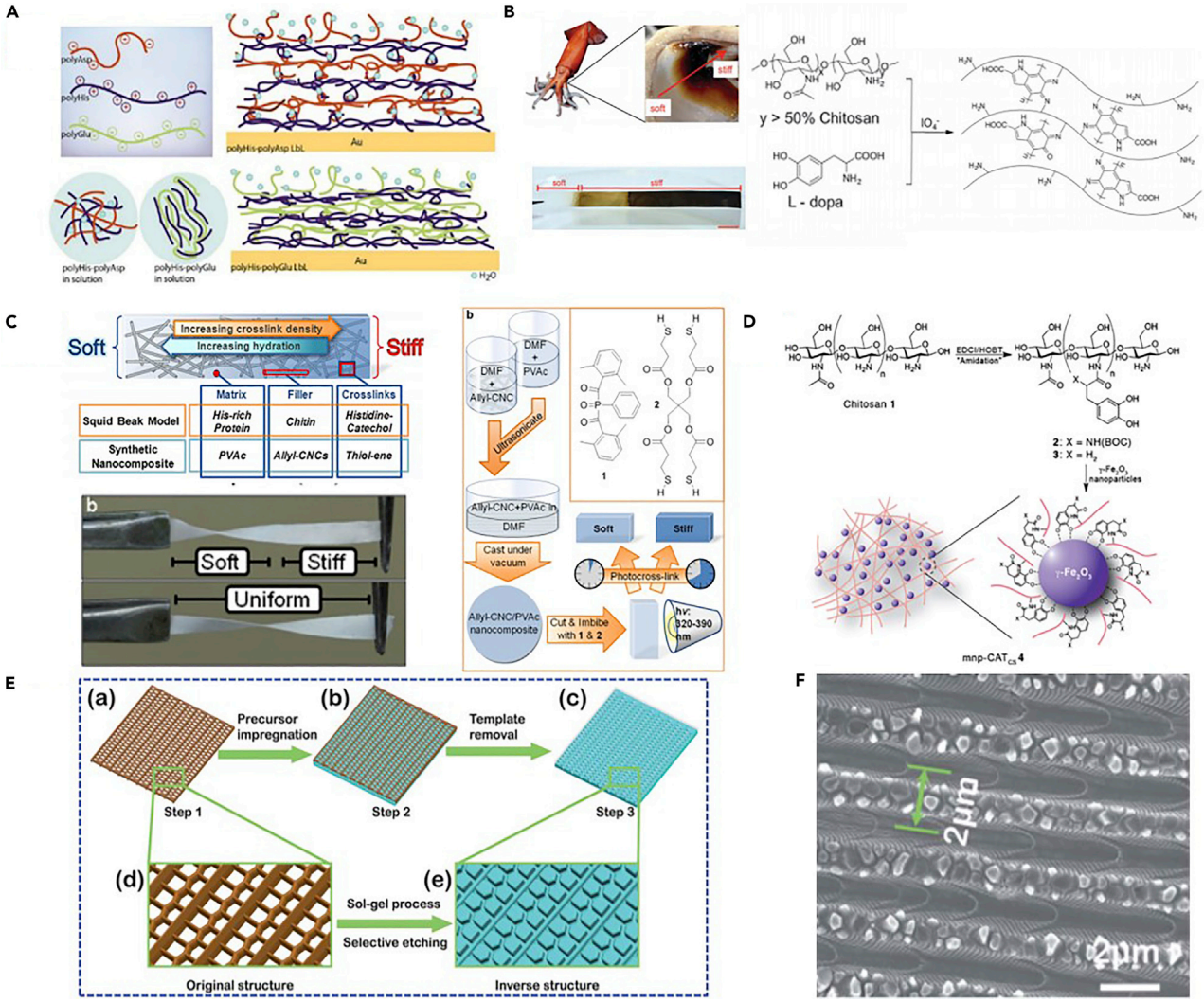

Figure 6. Examples of Fabrication Artificial Gradient Structure Materials

(A) Schematic representation of individual polyelectrolytes in solution, poly-His−polyAsp and poly-His−polyGlu complexes in solution, polyHis−polyAsp LbL and polyHis−polyGlu Layer-by-Layer (Tan et al., 2013).

(B and C) (B) The picture of a Humboldt squid Dosidicus gigas and the optical image of the fabricated ChitoDX film (the left). The brief reaction scheme where L-dopa is oxidized and covalently cross-links with chitosan (the right) (Zhang et al., 2016). (C) The schematic of water-enhanced mechanical gradient nanocomposite and the film casting and photo-cross-linking process (Fox et al., 2013).

(D) Synthetic strategy of chitosan derived bioinspired organic/inorganic composites (Zvarec et al., 2013).

(E) Schematic diagram of fabrication process of bionic butterfly wings.

(F) The SEM image of SiO_2 inverse replica to bionic butterfly wings (Han et al., 2013).

At first, we introduce the methods and synthetic materials of bionic spider silk and cacti. Unlike other materials, spider silk is not the result of a cell growth process. The inspiration for spider silk is used as a template for designing and producing functional biomaterials. In previous studies, researchers used recombinant DNA technology to synthesize genes. Genes are inserted into yeast and bacteria to make them produce silk protein copies (Eisoldt et al., 2011; Riekel and Vollrath, 2001; Omenetto and Kaplan, 2010; Sahni et al., 2010; Li et al., 2010). Andersson et al. extracted spidroin from one liter of a bacterial shake-flask culture to spin a kilometer of the toughest synthetic spider silk fiber ever made (Andersson et al., 2017). To mimic the micro-structure of spider silks' ability to collect water, some researchers are trying new methods. Dhinojwala et al. reported fabricating functional microthreads by the dip-coating method using poly (dimethylsiloxane) solution, which mimicked the spider silk with a good bonding property. The method controlled well the morphology and structure of the functional spindle-knots by varying the

capillary number. The dip-coating method of functional fiber provided a good guarantee for its wide application (Sahni et al., 2012). Jiang et al. developed a novel dip-coating method to open a wider perspective for the design of bioinspired materials. After calcining, they created smooth spiral cracks on the coated core-shell's spindle joints, which was of great significance to the fracture technology and fracture mechanism of materials (Wang et al., 2012). Chen et al. made the bionic fiber with long distance transmission capacity by dipping it at an inclined Angle. The fibers were inspired by biology with gradient spindle-knots (BFGs). The multilayer synergy of water droplets coalesced and released energy along the gradient spindle joint, coupled with the capillary adhesion and the continuous Laplace pressure difference, and enabled the rapid directional motion of water droplets over long distances on BFGS (Chen et al., 2013). In addition to above methods, Jiang and co-workers proposed the method of combining coaxial electrospinning and electrospraying to fabricate the fibers of bionic spider silk in response to the environmental humidity. The materials chosen are a low viscosity outer fluid that can be sprayed and a high viscosity inner fluid that can be spun (Tian et al., 2011). At the same time, they also proposed using the fluid-coating method to make bionic fibers with a directional water collection (Bai et al., 2011). Wu et al. designed a new type of graphene microfiber material inspired by spider silk with a microstructure of spinning knots by using microfluid emulsification and spinning synergy technology. The microfibers have hydrophobic surface chemical properties and can absorb oil in the water-oil mixing environment. Due to the difference in the surface energy curvature gradient and Laplace pressure, the collected oil tend to form droplets that move from joint to joint between spindles (Figure 7A) (Wu et al., 2018b). In summary, in order to achieve the water collection ability by mimicking the micro-/nanostructure features of spider silk, there are four methods to fabricate spindle knots that have been reported: the dip-coating method (Hou et al., 2012), the coaxial electrospinning method (Tian et al., 2011; Yuan and Zhang, 2012), the fluid-coating method (Shen et al., 2002; Seveno et al., 2004; Oda et al., 2008), and the microfluid method (Figure 7B) (Kang et al., 2010, 2011; Shin et al., 2007; Dufour et al., 2013). Although these methods are suitable for making bionic silk with multigradients, these methods also have limitations. For example, it is difficult to obtain a very long length of fiber by using the dip-coating method, and it is hard to use the coaxial electrospinning method to get a single bioinspired fiber since the surface energy difference should be considered. There is also a way to develop the fabrication methods of bioinspired spider silks to design multifunctional materials. Hou et al. immersed a carbon fiber in the resin solution (epoxy E−44 and diethylenetriamine are mixed in the ratio of 10:1) and fabricated them by a dip-coating method. As a result, they got a variety of hump fibers with less homogeneity and gradient pores, as well as microstructures. The viscosity of the solution will increase with an increase of reaction time, so the different reaction times will lead to different morphologies of the biological fiber. At the same time, the relative humidity will also affect the pore structure. Therefore, these external factors should be strictly controlled in the production process (Feng et al., 2013a). Feng et al. synthesized a biomimetic fiber made of Azo polymer whose roughness and curvature gradient were like a spider silk's spindle-knots. This bionic fiber has a good light control effect on water accumulation. Under the irradiation of visible and UV light, the synergistic effects of photosensitive wettability, roughness, and curvature all influence the biological fiber to effectively adjust the water droplets to separate from or converge toward the spindle joint. This work provides a new gradient surface design scheme, which has a great prospect in the application of water collecting equipment (Feng et al., 2013b). Wang et al. mimicked spider silk in designing a superhydrophobic surface. They made the surface to prepare on the surface of cotton fabric to control the superhydrophobic surface roughness and energy. Subsequently, TiO_2 nano-sol spraying on the surface of the super-hydrophobic fiber resulted in light-induced superhydrophilic bumps with a unique raised structure because of the interfacial tension. These raised TiO_2 bumps induced wettability gradients and shape gradients simultaneously to accelerate water coalescence and water collection (Wang et al., 2016b). Wu et al. produced the hydrogel inspired by the spider silk model, which was primarily formed by host-guest interactions with cucurbit[8]uril (CB[8]). This is a supercontractile fiber (SCF) that can shrink to 50% of its original length at a high humidity, and water absorption ability can reach 300%. At the same time, SCF exhibits adjustable mechanical properties, such as long-term failure strain and a reversible damping capacity by changing the humidity (Figure 7C) (Wu et al., 2018a).

Inspired by the fog harvesting property of cacti, Heng et al. developed an artificial water harvesting system. The structure consisted of a large ZnO wire and a set of small ZnO wires that branch off from the large wire. These wires tend to increase in diameter from tip to root. As a result, the tip of each wire condenses a drop of water, driven by a capillary force caused by a diameter gradient (Figure 7D) (Heng et al., 2014). Cao et al. fabricated a novel cactus-inspired continuous fog collector with a high efficiency, which can collect, transport, and store fog water automatically and continuously. They used PDMS and MPs to produce a cactus

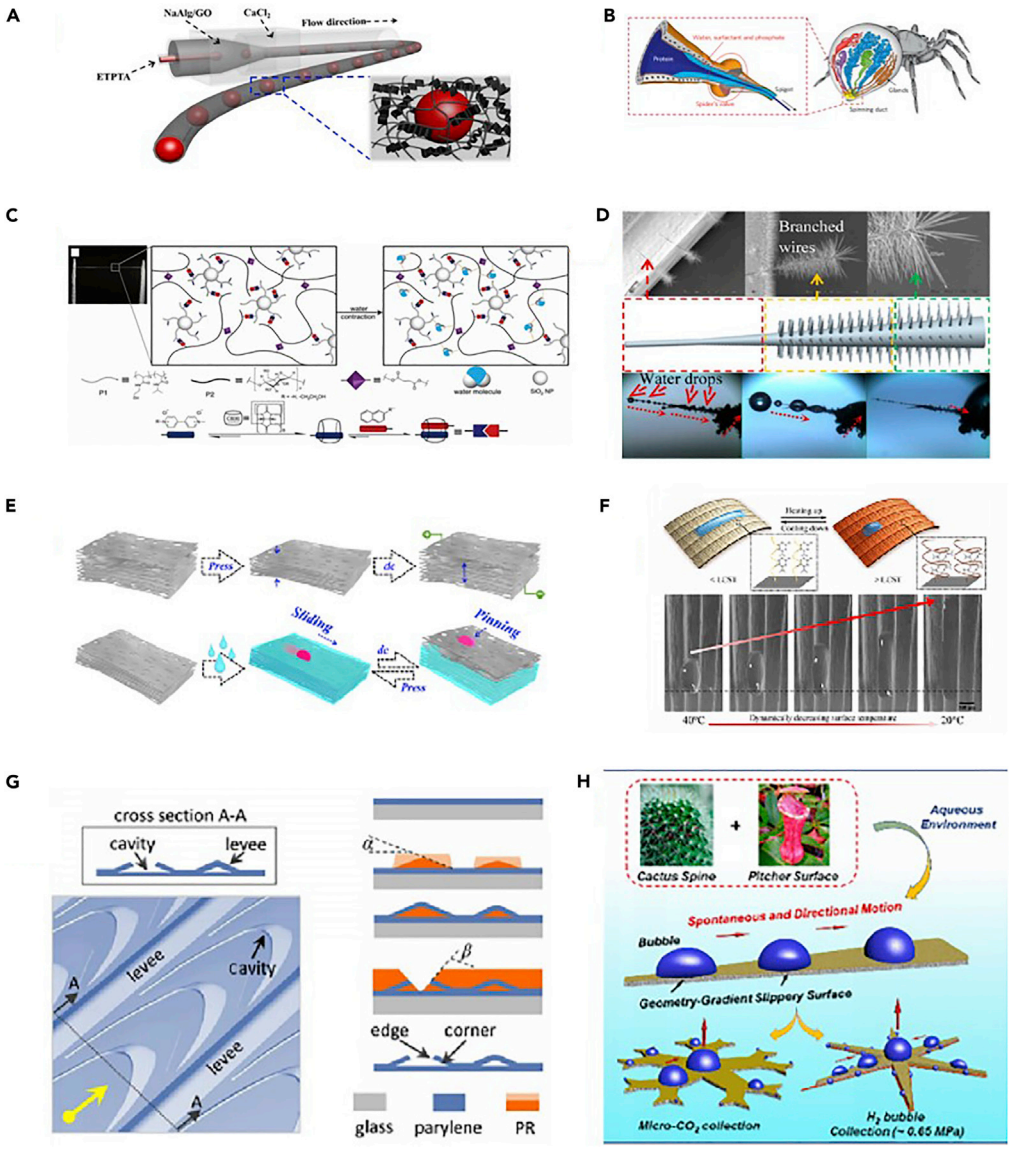

Figure 7. Examples of Artificial Structures with Gradient Properties can Exhibit Motion Characteristics when Performing Their Function

(A) Schematic illustration of capillary microfluidic system for generating the microfibers containing droplets (Wu et al., 2018b).

(B) Anatomy of the silk-spinning system of spiders (Kang et al., 2011).

(C) Photograph of the supercontractile fiber and schematic illustration of SCF undergoing supercontraction at high humidity (Wu et al., 2018a).

(D) Synthesized branched wire structures (Heng et al., 2014).

(E) Schematic diagram of an electrothermal and shape-memory graphene sponge with specific wettability (Wang et al., 2017a).

(F) Schematic showing reversible unidirectional water spreading on the smart artificial peristome (Zhang et al., 2017).

(G) Design and fabrication of the biomimetic film (Tang et al., 2018).

(H) The present strategy of utilizing the geometry-gradient's slippery surface to directionally transport gas bubbles in an aqueous environment (Zhang et al., 2018).

spine-like conical micro-tip arrays through a modified magnetic particle-assisted molding (MPAM) method under an external magnetic field. By adjusting the weight ratio between PDMS and MPs, the structure of the micro tip can be controlled. It was found that the optimal condition was achieved when the weight ratio of PDMS to MPs was 2:1. The work is promising in areas with a shortage of drinking water (Cao et al., 2014).

The following is a bionic smart surface based on the pitcher plant, which has hydrophobic properties. We can take the smart surface as a two-dimensional structure. Wang et al. presented a novel slippery film with tunable wettability based on a shape-memory graphene sponge, which is inspired by the pitcher plant. In order to lock-in inert lubricants and construct slippery surfaces to repel different liquids, they coated the surface of the porous graphene sponge with a shape memory polymer. The super elasticity, high strength, and good conductivity of the graphene sponge enabled the graphene/polymer composite film to have a rapidly recoverable shape memory performance. The shape memory graphene films they made are endowed with controllable smooth properties and functions. They are suitable for a variety of applications, such as liquid handling for microplates (Figure 7E) (Wang et al., 2017a). Inspired by the wax regeneration ability of plant leaves and the slippery surfaces of the *Nepenthes* pitcher plants, Wang et al. developed a new cross-species bionic wet fluid injection porous surface (x-slip) that can repair itself under thermal stimulation, even after extensive physical and chemical damage. These thermally self-healing pantophobia coatings can be applied to metals, plastics, glass, and ceramics in a variety of shapes and exhibit excellent repulsion of water and organic liquids (Wang et al., 2016a). Young et al. inspired by the pitcher plant used femtosecond laser technology to successfully create a slippery liquid infused porous surface (SLIPS). Using the one-step femtosecond laser direct writing technology, a three-dimensional porous network microstructure can be generated directly on the polyamide-6 (PA6) substrate. The porous layer and the substrate layer are an inherent material, and the porous layer of this method comprises of foreign materials against the substrate. The results show that the resulting SLIPS has a good liquid-repellent ability. Even if the SLIPS suffer serious physical damage, the surface can repair itself quickly, without any additional treatment, and gain a slippery ability again. The SLIPS surface development is expected to help in the fields of self-cleaning antifouling biomedical equipment and fuel transportation with panophobia materials (Yong et al., 2017).

At the same time, the pitcher plant is biomimetic due to its structure and materials that can be used as a response to stimuli. Zhang et al. prepared intelligent artificial microtubule pitcher plants by grafting the thermal response PAIPAAM on the artificial PDMS microtubules with completely natural structural characteristics. The wettability of PNIPAAM-grafted PDMS had a significant response to the temperature, leading to a successful dynamic control of unidirectional water spreading by regulating the surface temperature. Moreover, by exploring the liquid expansion with different contact angle (CA) attributes, they found that the expansion of the liquid in the stoma-like structure mainly depended on the wettability of the surface. This work provides new insights into the design of materials with a unidirectional liquid diffusion capacity from the perspectives of structural and stimulus responsive materials and provides new strategies for the control of liquid diffusion (Figure 7F) (Yong et al., 2017; Zhang et al., 2017). Tang et al. demonstrated a bionic microstructure inspired by *Nepenthes alata*. It enables high-speed and long-distance unidirectional water spreading on a flexible film. Through the commonly used fine processing equipment, it is convenient to process fine structures with polypropylene or other materials. The unidirectional water spreading is researched by studying the lubrication of the precursor. Biomimetic microstructures are attractive for physical and chemical research, biomedical engineering, and applications of microfluidic devices (Figure 7G) (Tang et al., 2018).

In addition, in order to achieve a multifunction, the pitcher plant's structures play an important role. Manabe et al. investigated bionic moth-eye, lotus leaf, and pitcher plant biological structures, through a layer by layer self-assembly production method, using CHINFs and SiO_2 material to produce anti-reflection film. The highest transmittance of the anti-reflection film is 96.7%, and the lowest refractive index is 1.20. After improving the hydrophobic performance, the ultra-hydrophobic transparent film with the highest light transmittance (97.5%), anti-reflection performance, the lowest refractive index, and the reflectance were obtained, as well as the contact angle with water of 152°. Through experiments, they proved that the use of low reflectance film, as the bottom layer lubricant, improved the light transmittance of the liquid injected surface. In addition, the three biomimetic structures showed that the film injected with a lubricating oil can prevent frost formation by keeping the fog from sliding and resisting thermal changes. The combination of the three biomimetic methods helped to improve various materials and opens up a new way to produce highly functional materials (Manabe et al., 2014). Zhang et al. fabricated asymmetric smooth surfaces with a snowflake and star structure through CO_2 laser cutting, superhydrophobic modification, fluorination, and other processes. The surface can resist pressure (0.65 MPa) and deliver bubbles, that mimic the cactus spine with a shape-gradient morphology and the pitcher plant with a liner lubricated (Figure 7H) (Zhang et al., 2018).

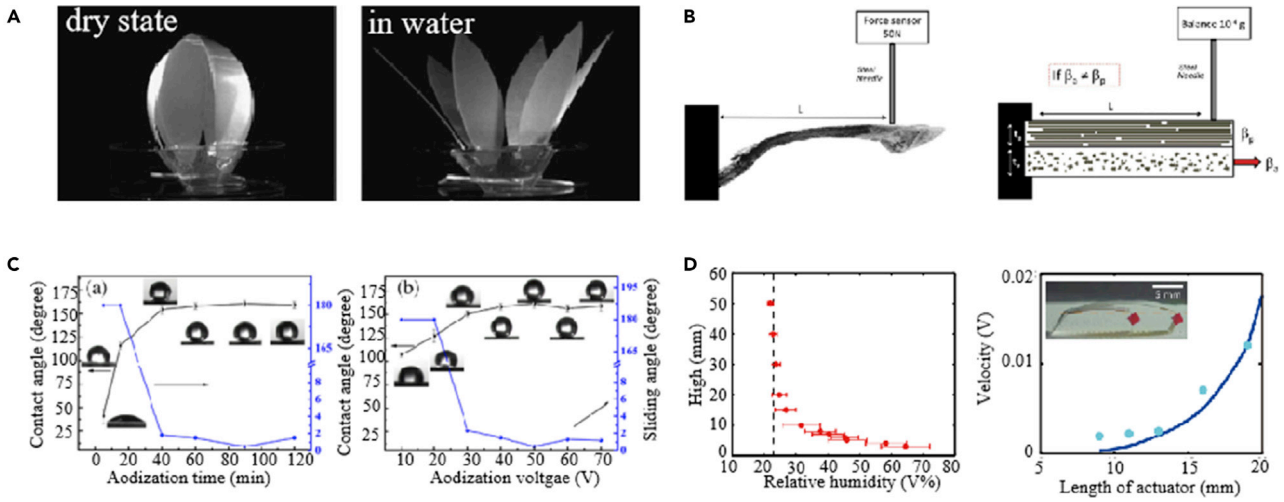

Figure 8. Examples of Bionic Smart Surface Inspired from Pitcher Plant

(A) A flower made of paper-plastic double petals by mimicking the pine cones. It closes in the dry air and opens in the water (Reyssat and Mahadevan, 2009).

(B) Diagrams about principle of the blocking force measurement on a pine cone and a bicomposite analogue. The force produced due to the difference in the coefficient of active and passive layers (Le Duigou and Castro, 2016).

(C) The variation of contact angles and sliding angles of the surface of bionic pine cone for different anodization times (Li et al., 2016).

(D) Spatial distribution robots of a bionic pine cone in relative humidity and velocity images of humidity robots of different lengths (Shin et al., 2018).

The abovementioned organisms are concerned with water collection and transportation. Next, we will introduce a pine cone and wheat awn with gradient properties that change with environmental humidity. With regard to pine cones, Reyssat et al. created an active bionic bilayer with controllable properties, constructed of a natural tiling made of epoxy resin bonded to a flat polymer strip (Figure 8A) (Reyssat and Mahadevan, 2009). The size of the model was about 5 cm in length with a width of 5 mm and a thickness of 0.3 mm. The active material used was the cellulose paper that expanded if it was softened in the wet environment and contracted if it was hardened in the dry environment. This simple model mimicked the properties of pine cones (Reyssat and Mahadevan, 2009). Duigou et al. created a water-reactive biocomposite analogue with two layers, each embedded in the same polymer matrix by flax fibers. The principles of the blocking force of pine cones and bionic composites are shown in Figure 8B (Le Duigou and Castro, 2016). In order to simulate the sclerenchyma fibers and sclerenchyma tissues of pine cones, the directions of each layer of the hemp fibers were set to 0° and 90°, respectively. The materials have good shapeability and can make full use of the by-products with low economic value (Le Duigou and Castro, 2016). Li et al. fabricated a superhydrophobic surface via an economical, simple, and highly effective anodization process with a low surface energy modifying by mimicking a pinecone. Adjusting anodization parameters including the anodization time and voltage was helpful to control the microstructures and the wettability of the bionic surfaces (Figure 8C) (Li et al., 2016). The results showed that the superhydrophobic surface prepared by this method had good long-term stability, mechanical robustness, self-cleaning ability, and corrosion resistance (Li et al., 2016). As mentioned above, wheat awns, like pine cones, also have the function of changing with the environmental humidity. Inspired by wheat and grass, Shin et al. invented a bilayer actuator that varied in bending speed and magnitude in response to changes in ambient humidity. By attaching legs with an asymmetric friction coefficient, the oscillatory motion of the actuator changes periodically with humidity and is modified to the direction of the motion (Figure 8D) (Shin et al., 2018). In addition to temporal variations in humidity, the spatial humidity gradient that naturally exists on wet surfaces has been shown to power wet robots without any human intervention. The tiny robots are lightweight and flexible, requiring no human input, and can be used in a wide range of medical, military and industrial applications (Shin et al., 2018).

As mentioned above, in general this part summarizes the functional classification formed by a gradient phenomenon in nature and some design principles that should be followed related to bionics from a chemical perspective and physical perspective. From the chemical point of view, the ladybird, gecko, and mussel with their linear distribution of chemical elements and the squid beak with its network distribution of chemical elements are described. From the physical point of view, the structural and functional characteristics of organisms with a gradient phenomenon are classified. Among them, the structural characteristics are divided into four categories: arrangement, distribution, dimension, and

orientation, whereas the functional characteristics are described in terms of the classification of biological functions.

BIOINSPIRED APPLICATIONS FROM GRADIENT ORGANISMS

Medical

The fabrication of functional gradient materials processes unique complex architecture, which can maintain, respond, and change shape when they are subjected to its surrounding environment's changes such as outside stimuli, including pH, temperatures, and ion strength. Earlier researches have demonstrated that some inorganic gradient devices and organic functional materials have a medical application in blood and tissue engineering (Le Duigou and Castro, 2016; Di Luca et al., 2015; Karabanova et al., 2012; Major et al., 2007; Shi et al., 2019). Because of its outstanding stimuli-response and fast response capabilities, the functional gradient materials' applications in biomedical applications have been reviewed and include scaffolding (Liu et al., 2009; Singh et al., 2010; Wang et al., 2019), hydrogel (Wei et al., 2017; Jo et al., 2019; Khorshidi and Karkhaneh, 2018), bioimaging (Ng et al., 2017; Zhao et al., 2019a; Moreno and Smedby, 2015), biocompatibility (Li et al., 2017; O'Connor et al., 2000; Donnelly et al., 2012), and therapeutic agent delivery system (Li et al., 2014; Duan et al., 2016). Finally, the challenges for fabrication of these materials and future perspective are also summarized.

The stem cell differentiation and cell transformation can be affected by the gradient cross-linkers of hydrogels, as shown in Figures 9A and 9B. More elongation of the encapsulated cells was observed in the high cross-linker section of the hydrogel. The average ratio of the encapsulated cells increased with the increase of the cross-linker content. Therefore, this kind of hydrogel can be used for tissue regeneration. It offers an insight in designing scaffolds in tissue engineering field.

The gradient stiffness of a hydrogel can further be used in cell recruitment and medicine delivery. The cells and drugs encapsulated in the 3D gradient stiffness of a hydrogel platform could recruit more cells and better realize drug gradient releases than conventional hydrogels. Thus, it can be used as a promising approach to create diffusion gradients of cells or drugs, aid the design of therapeutic biomaterials, and promote the research on biomechanics.

The gradient structure can also be fabricated via 4D printing technology. Song et al. (Song et al., 2020) reported a biomimetic, non-uniform, dual stimuli, self-morphing gradient, 4D printing structure. This can configure continuously smooth gradients of volume fraction of the active material in bilayer structures. The shape-shifting results can be predicted by the established mathematical model and computational simulations. It could produce different changes in the shape in response to humidity and different temperatures simply by printing the graded water-responsive elastomer materials onto a heat-shrinkable shape memory polymer (Figure 9C). This gives it a promising application in the biomedical field. Similar gradient functional hydrogels were also reported by Gao et al. (Gao et al., 2018) for efficient repair of osteochondral, which had robust tensile strength (up to 0.41 MPa), large stretchability (up to 860%), and high compressive strength (up to 8.4 MPa).

The accurately and efficiently targeted delivery of therapeutic/diagnostic agents into tumor areas in a controllable fashion is still a very big challenge. Here Duan et al. (Duan et al., 2016) reported a novel cancer targeting magnetic microbubble system for accurate diagnostic of a tumor (Figure 9D). As shown in the previous figure, because of the RGD-L-TRAIL protein on the MMBs surface, the microbubbles were able to actively target the tumor angiogenesis. The size of the micro-scaled bubbles around the tumor was helpful for real-time US imaging and for the MRI to define the tumor margin. The microbubbles, *in situ*, around the tumor were broken after the US imaging was completed. As a result, nanoscale SPIOs with RGD-L-TRAIL molecules were able to pass through the blood vessel and enter the tumor's tissue with the cooperative effect of both of the tumor passive enhanced permeability and retention effect and integrin $\alpha_v\beta_3$-receptor-mediated endocytosis induced by RGD-L-TRAIL ligand. In this step, the MRI can be used to image tumor tissues. During this process, the RGD-L-TRAIL and SPIOs were accumulated in the tumor's tissues and cells. As a result, the tumor apoptosis, induced by TRAIL molecules, can also be detected. In addition, since SPIOs remain in the tumor tissue, an MRI can be used to assess tumor' progression and treatment outcomes, whereas no other contrast agents are injected again. It could be developed as a molecularly targeted multimodality imaging delivery system with the addition of chemotherapeutic cargos to improve cancer diagnosis and therapy.

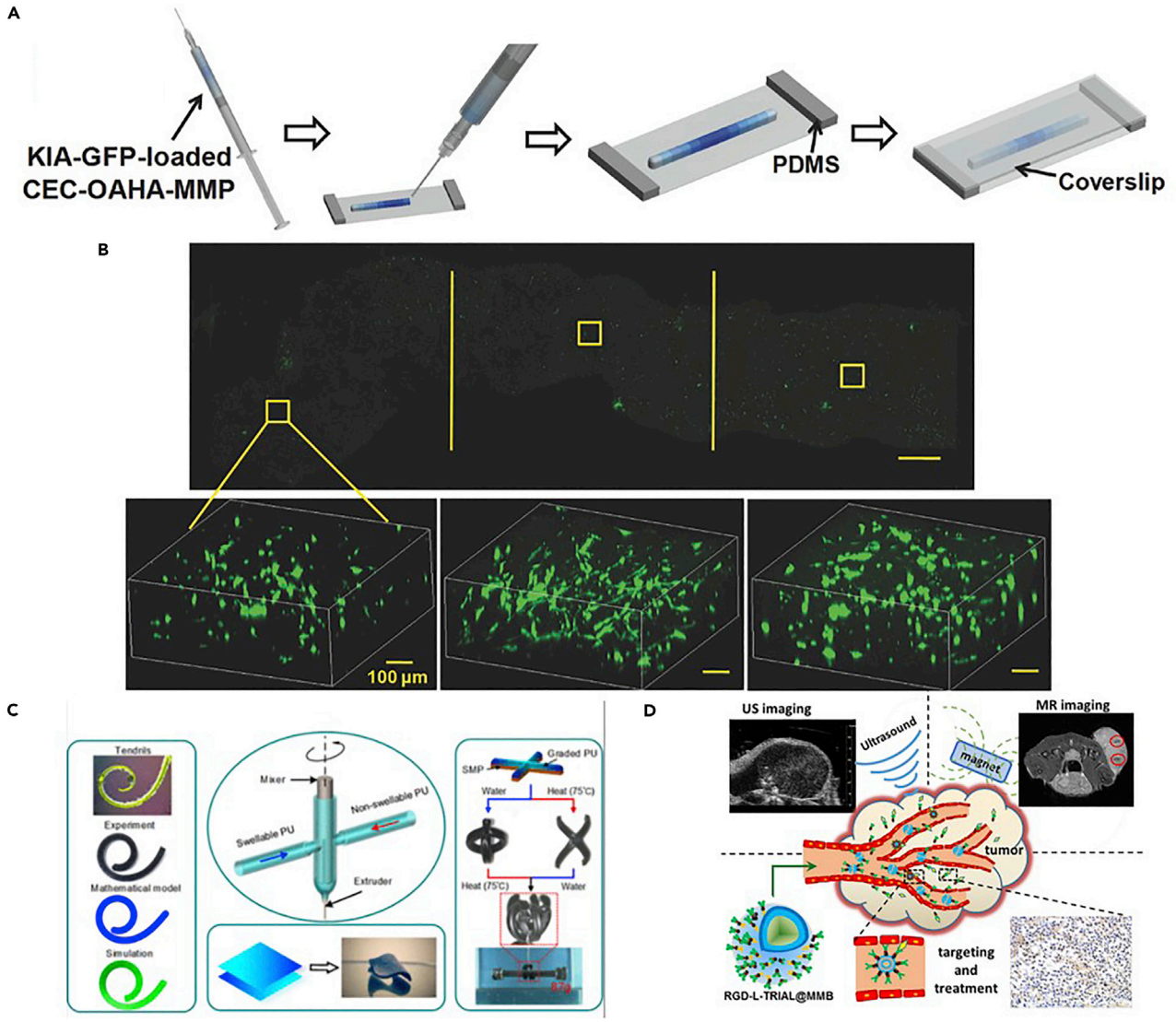

Figure 9. Tissue Engineering and Regenerative Medicine

(A) Preparation of gradient hydrogel constructs for microscopic observation (Wei et al., 2017).

(B) Confocal images of the entire view of encapsulated KIA-GFP cells (Wei et al., 2017).

(C) The fabrication of gradient structure for shape and water and heat transportation (Song et al., 2020).

(D) The multigradient targeting microbubble system for tumor diagnostics and therapy (Duan et al., 2016).

Besides structure variations, we can further stimuli the gradient with pH, humidity, or magnetic force field to manipulate the surface proteins and cells to help understand the basic science in biomedical applications. One good example was reported by Li et al. (Li et al., 2014) in using an external-field-induced gradient wetting technology to control liquid transport from movement on the surface to penetrate into the surface, particularly for liquid motion on, patterned wetting into, and permeation through films on super wetting surfaces with external field cooperation (e.g., light, electric fields, magnetic fields, temperature, pH, gas, solvent, and their combinations). Because of the cooperative effect of the interface and the external field, the gradient wetting and dewetting on the surface achieved a dynamic balance. It can be tuned to achieve a good direction, confined range, and selectivity of liquid wetting. The liquid transport on the surface was categorized into three levels. The first level was about the directional liquid motion moving on the film. The second level was the partial wetting of the film for liquid patterning. The third level was the permeation into the film for selective separation. This technology opened a new window in the field of liquid separation and the biomedical field.

Energy

The gradient design of functional materials can achieve effects of high efficiency and energy savings, all of which create a convenience for the comfortable life of a human being. The relative studies have showed that the functional gradient materials can efficiently achieve water collection and transportation (Ju et al., 2013; Wang et al., 2011; Zhu et al., 2016a), as well as inspired by the bionic gradient property, devices for energy collection, and energy reuse of related gradient structures can be designed, such as sensors (Bührig-Polaczek et al., 2016; Tan et al., 2016; Osotsi et al., 2020; Zhao et al., 2019). These gradient functional materials play an important role in the field of long-distance transportation and energy reuse, as well as gives important inspiration to researchers in related fields (Sun et al., 2019b).

By designing the material part of the devices into a gradient distribution state, the multifunctions can be realized, such as micro controls, collection, and transportation.

Wang and co-workers found that a drop exhibits asymmetric bouncing dynamics with a distinct spreading and retraction along two perpendicular directions when they hit the *Echeveria* leaves. This biological phenomenon indicates that on anisotropic surfaces, the asymmetric distribution of momentum and mass allows the preferred liquid to be pumped at the edge of the drop (Liu et al., 2015). The effect of the gradient on the anisotropic surface, due to the different degree of the density, has laid a foundation for follow-up research. Deng and co-workers created a rewritable surface charge density gradient using easily manipulatable droplet printing on a superhydrophobic surface, simulating droplet propulsion under environmental conditions without requiring additional energy input (Sun et al., 2019a). Recently, Xu et al. used a polytetrafluoroethylene (PTFE) film structure on an indium tin oxide (ITO) substrate and an aluminum electrode to produce a droplet-based electricity generator with a high instantaneous power density. The charge density on the solid surface of the device can be greatly increased by the repeated impact of droplets or ion implants when compared with conventional generators. At the same time, the structure design of the FET transistor was adopted in this work to form an interfacial effect, which can make the large generated amount of charge be transferred quickly. In practice, the device can light up to one hundred commercial light-emitting diode (LED) bulbs with a drop of water. These droplets were 100.0 μL each and were released from a height of 15.0 cm. To sum up this part, the device had a great potential to be applied in the energy field and other fields in the future (Xu et al., 2020). Wang and co-workers were inspired by the gradient structure of bamboo culms to fabricate ceramic nanowires/polymer composites with gradient-layered $BaTiO_3$NWs/p(VDF-HFP). The content of ceramic fibers is increased gradually from the upper to bottom layers (Figure 10A). The design of this gradient structure plays an important role in preventing the breakdown, so that even in the presence of many high-dielectric permittivity fillers, the gradient-layered polymer nanocomposite can have a significantly enhanced breakdown strength. The designed composite material exhibits an energy density of 17.6 J/cm^3 and a high charge-discharge efficiency of 71.2% (Figure 10B), which are significantly better than traditional single-layer films (Wang et al., 2020). With regard to the application of bionic gradient in sensors, Peng and co-workers designed a free-standing compressible carbon nanotube array (CCNA) with a gradual crosslinking structure, which was inspired from the gradient structures of squid beaks (Figure 10C). CCNA shows highly reversible compressibility of up to 100,000 cycles and has high electrical conductivity. The design of the gradient structure is conducive to energy storage. An all-solid-state compression-sensing supercapacitor (CSS) is designed on the basis of CCNA, showing that it has a high capacitance (as high as 93.2 mF cm^{-2}) (Figure 10D) and can maintain the original 94% after 3,000 continuous compression cycles under 60% strain. As sensors, these CSSs have a broad application in the fields of electronic skin equipment and biological electronic equipment (Figure 10E) (Zhao et al., 2019).

Environmental

The environment, especially the planet earth, plays an essential and inseparable role in human life. Taking inspiration from living organisms and biological materials helps to achieve better biocompatibility and environmental compatibility, e.g., improve fabrication/construction efficiency, save energy, reduce emissions of toxic chemicals, and increase degradability of wastes. In previous studies, in the fields of architecture and those closely related to the environment, some researchers developed high-strength and fire-resistant building materials with gradient stratification properties inspired by shells and nacres (Tian et al., 2013; Walther et al., 2010; Wan et al., 2015), whereas others took inspiration from mussel to design materials that reduce the effect of seismic impedance. Some researchers develop devices with gradient

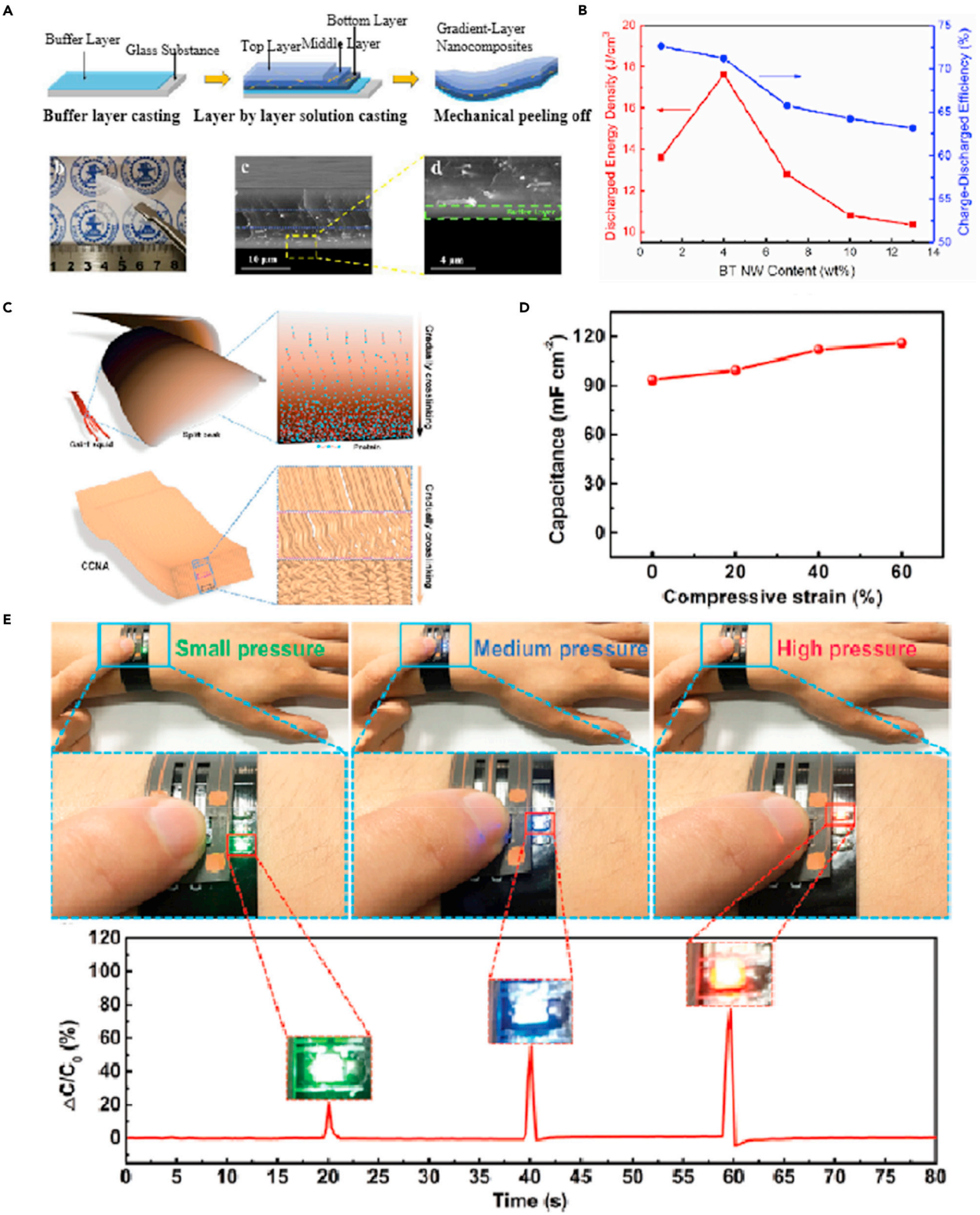
A
Buffer Layer
Glass Substance
Bottom Layer
Top Layer
Middle Layer
Gradient-Layer Nanocomposites
Buffer layer casting
Layer by layer solution casting
Mechanical peeling off
B
Discharged Energy Density (J/cm³)
Charge-Discharged Efficiency (%)
BT NW Content (wt%)
C
CCNA
D
Capacitance (mF cm⁻²)
Compressive strain (%)
E
Small pressure
Medium pressure
High pressure
ΔC/C₀ (%)
Time (s)

Figure 10. Examples of Devices with Gradient Structure and Multifunctions in Energy Field

(A) The schematic illustration of the preparation, optical image, cross-section SEM image, and magnified SEM image of the gradient-layered $BaTiO_3$NWs/p(VDF-HFP) nanocomposities.

(B) The relationship between the discharge energy density, charge-discharge efficiency of the gradient layer $BaTiO_3$NWs/p(VDFHFP) nanocomposite, and the $BaTiO_3$ content in the intermediate layer.

(C) Schematic diagram of the gradient crosslinked structure of a squid beak and the biomimetic free-standing and highly CCNA with gradually crosslinking structure.

(D) The specific capacitances under increasing compressive strains of CCNA.

(E) The application of CCS prepared based on CCNA as a sensor. Apply a small pressure of 30 KPa on the flexible integrated watchband to light up the green LED, apply a medium pressure of 55 KPa to light up the blue LED, and apply a high pressure of 80 KPa to light up the red LED. And the relative capacitance response obtained from CSS during compression.

structures and apply them to practical industrial applications. Inspired by the gradient characteristics of organisms, the device designed is both efficient and environmentally friendly.

For example, Huang and co-workers prepared an enzymatic membrane bioreactor by using the gradient microporous hollow-fiber polysulfone membranes as the immobilized enzyme carrier (Figure 11A). The bioreactor has the characteristics of high throughput, high mass transfer, and high catalytic separation efficiency (Zhu et al., 2016b). In a follow-up study, they prepared a biomimetic interface with perfect radial gradient holes to construct an efficient and stable EMBR (Figure 11B). This method is based on the integration of phospholipid with a polysulfone hollow fiber membrane (RGM-PSF). Because RGM-PSF has a special gradient distribution of porous structures, the enzyme molecules can be evenly distributed on the three-dimensional skeleton of the membrane. In addition, the phospholipid layer supported by the membrane (via physical adsorption) is used for the immobilization of the enzyme, which provides sufficient links for the leaching of the enzyme, while accommodating as many enzyme molecules as possible to maintain high biological activity. The results of energy-dispersive X-ray and circular dichroism spectroscopy show that when compared with the unmodified membrane, the enzyme activity of the modified membrane is increased by 42% and the catalytic efficiency is increased by 78% (Guo et al., 2018). Inspired by cacti, Xue and co-workers prepared a completely inorganic hierarchical structure made up of a Co and Ni double hydroxide (Co-Ni-OH) via a simple one-step *in situ* method. The biomimetic cactus-like Co-Ni-OH_4-coated stainless steel mesh combines a unique layered structure with a powerful water-locking function, which can separate high-throughput (>37,227 L m^{-2} h^{-1}). This oil/water mixture shows high separation ability. It has an excellent oil rejection rate (>99.95%) and an excellent recoverability of over 20 cycles with a stable flow rate at 37,000 L m^{-2} h^{-1} (Zhu et al., 2020).

New materials designed inspired by nacre have potential applications for architectural engineering (Gerhard et al., 2017). Zhao et al. proposed a modified bidirectional freezing method followed by uniaxial pressing and a chemical reduction to prepare a graphene/poly (vinyl alcohol) composite film. This strategy is inspired by the "brick-and-mortar" structures of nacre. They also introduced both asperities and bridges to the lamellar layers to mimic the interfacial architectural interactions. The composite film exhibits strong, tough, and highly stretchable properties (Zhao et al., 2017). Similar research has also fabricated a high-performance BP-OHx/NFC composite film inspired by nacre (Qiu et al., 2020). Chen and co-workers produced an environmentally friendly water collection device inspired by cacti. The novelty is that the nanoscale hydrophobic coating is sputtered on the surface of the 3D-printed spines to accelerate the water growth rate (Li et al., 2020). Yu and co-workers prepared biomimetic nacreous bulk nanocomposites by using a multiscale soft-rigid dual-network interfacial design strategy combined with a scalable bottom-up fabrication method (Figure 11C). The new nanocomposite exhibits good mechanical stability under high humidity and high thermal stability (Figure 11D) (Chen et al., 2019b). In addition, Yu and co-workers produced hierarchical helical nanocomposite macrofibers (emulating bacterial cellulose nanofibers), which exhibit strong toughness and high strength (Figure 11E). Through a wet-spinning process, the new nanocomposite material had a tensile strength of 420 MPa, about 2.2 times that of the sodium alginate macrofiber. Then, by combining multiple wet twisting processes, a macroscopic artificial fiber material with similar structural characteristics of biological fibers were obtained. Its tensile strength continued to increase by 25%, whereas the fracture elongation and toughness increased by nearly 50% and 100%, respectively (Yu et al., 2020). Zhang et al. proposed an idea that allyl functionalized cellulose nanocrystal (CNC)/polymer nanocomposites allows formation of films by photo-induced thiol-ene crosslinking. This design drew inspiration from the mechanical gradient characteristics of squid beaks. The thickness of the produced film can be controlled by UV treatment, and the results show that the film exhibit enhanced mechanical properties

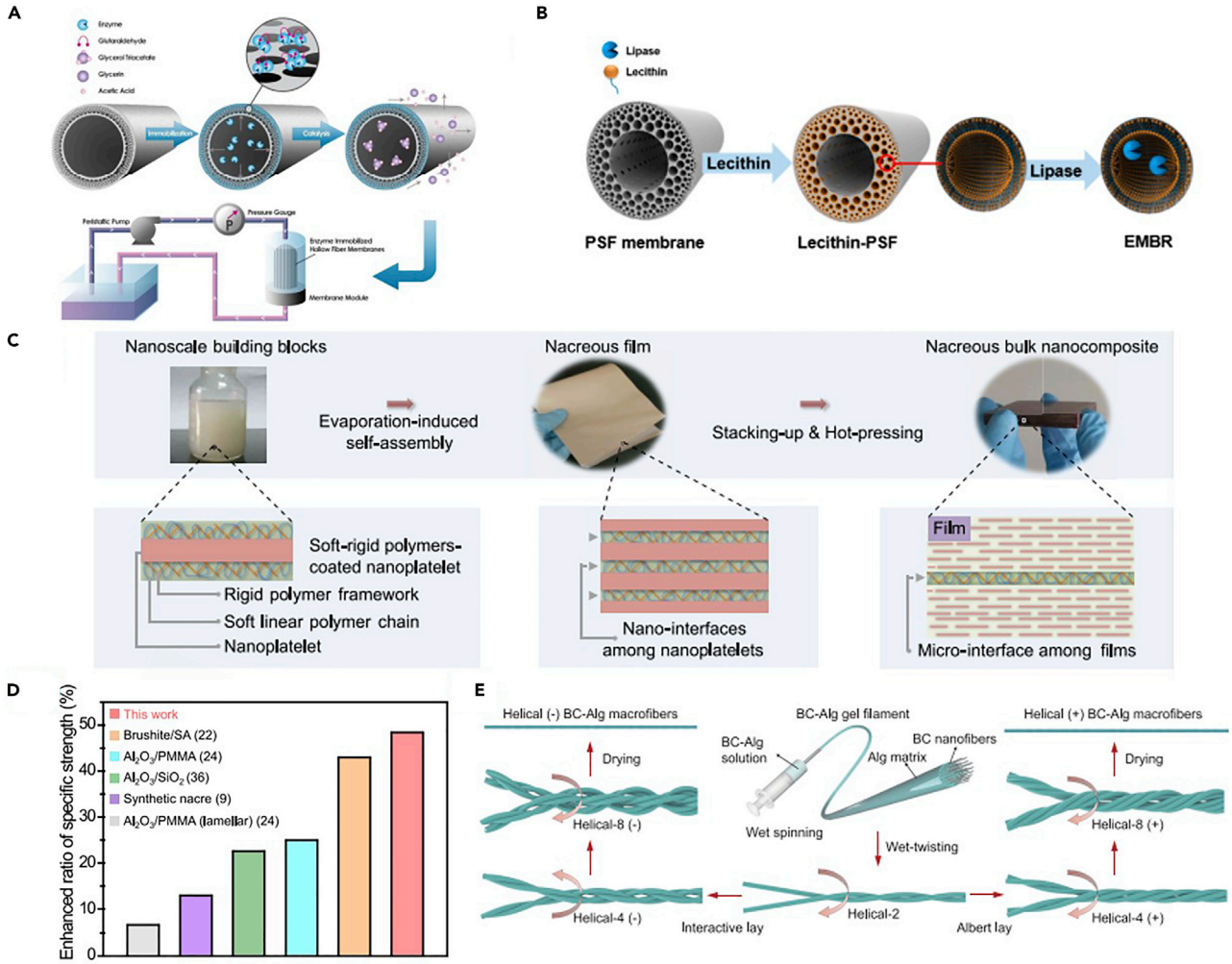

Figure 11. Examples of Devices with Gradient Structure in Environmental Applications

(A) Schematic diagram of enzyme immobilization and catalytic process and dead-end filtration equipment.

(B) Schematic diagram of lecithin modification and enzyme immobilization on the membrane.

(C) The overall schematic diagram of the bottom-up fabrication strategy of nacreous nanocomposite and the schematic diagram of each part of the finished interface.

(D) The enhanced ratio of specific strength of the prepared nacreous bulk nanocomposite.

(E) A process diagram of bioinspired hierarchical helical nanocomposite macrofibers are made by combining a facile wet-spinning process with a subsequent multiple wet-twisting procedure.

when it is heated above its glass transition temperature during the UV irradiation. The film thickness is also an important factor influencing the degree of crosslinking (Zhang et al., 2019). These bioinspired structural design strategies lay the foundation for the design and preparation of other complex structural materials in renewable architecture and related fields.

Robot

The influence of gradient structure in organisms or the gradient phenomenon in nature on organisms have essential inspirations for designing robots. In a previous study, researchers developed robots subjected to the gradient structure of wheat awns and pine cones with the change of the environmental humidity. This kind of robot supplies its own energy by recycling the surrounding energy, which has the advantage of not consuming extra energy (Lee et al., 2013). By analyzing the mechanical response of the designed robot with artificial intelligence, the behavior of the robot can be controlled and conceptualized (Shin et al., 2018). In addition, there are soft robots with energy recovery characteristics designed by the biological utilization of the energy

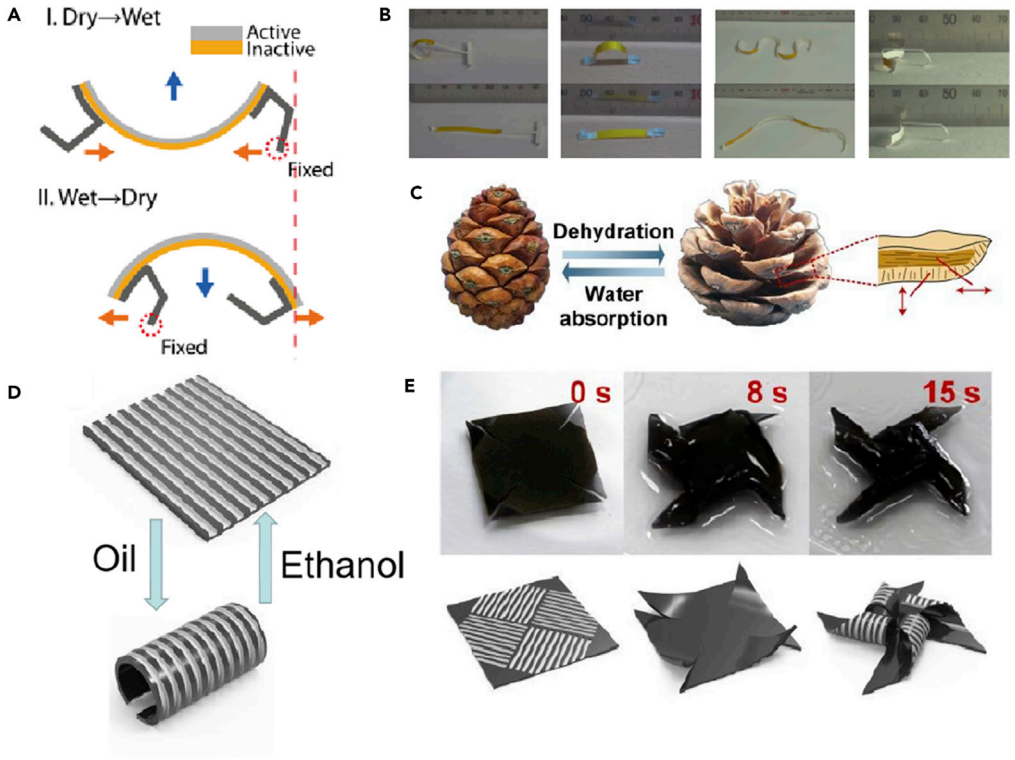

Figure 12. Examples of Gradient Structure in Robot Fields

(A) Schematic diagram of a wheat-awns-inspired robot. The principle in the picture shows the ratcheting of two legs attached to a bilayer actuator.

(B) Schematic diagram of the designed robot driven by environmental humidity.

(C) The schematic of the reversible moisture-responsive movements and the cross-section region of the pine cone.

(D) The schematic diagram of the actuator with the oriented microchannels by laser etching and the schematic diagram of the actuator under the oil response.

(E) Schematic diagram of the prepared artificial quadrilateral windmill driven in response to oil.

gradient in nature. This bionic robot, made according to the characteristics of natural biological gradient, opens up people's cognition in the field of robotics and makes scientific research more innovative.

Kim and co-workers designed a hygrobot with a self-locomotive ratcheted actuator driven by the ambient humidity. They used a film of neatly arranged nanofibers produced by directional electrospinning and can swell and shrink quickly in the vertical direction in response to changes in humidity. The schematic diagram of the robot sensing environmental humidity movement is shown in Figure 12A. The designed robot can sterilize a trail on an agar plate without any artificial energy (Figure 12B) (Shin et al., 2018). Liu and co-workers fabricated an actuator inspired by moisture-responsive pine cones (Figure 12C) that consist of a smooth hydrophobic surface and a superhydrophobic surface with aligned microchannels through simple method. The material used is a mixture of PDMS and graphene, and the method used is a simple laser etch. The actuator can deform into different desirable shapes and return to its original shape when being acted upon by oil and ethanol molecules (Figure 12D). The one-dimensional folding, deformation, rolling, twisting, curling, and object-inspired architecture can be programmed by changing the direction of the patterned microchannel. The schematic diagram of the designed real-time actuation for the artificial quadrangular windmills is shown in Figure 12E.

In recent research, popular 3D printing technology is incorporated into bionic design. Ren et al. fabricated a soft actuator that is inspired by the structural gradient of wheat awns through modified 3D printing techniques. The prepared bionic actuator realizes local response and continuously varying shape memory properties (Ren et al., 2019). There are more advanced 4D printing technology combined with bionic robot. Antoine and co-workers proposed a novel 4D printed multi-stimuli-responsive material, inspired by pine cones. These 4D printed

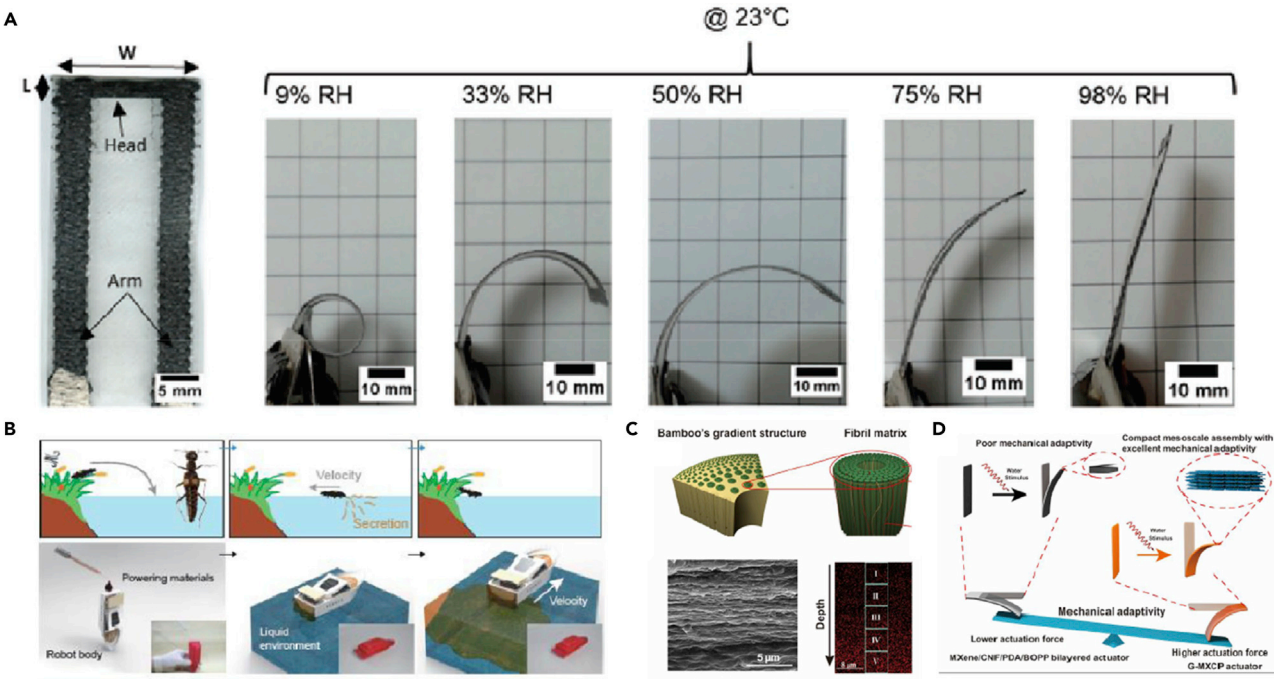

Figure 13. Examples of a Fully Soft with Gradient Structure which can be Trigger by Environmental Humidity or Electroheating

(A) Schematic diagram of the changes of the actuator under a different relative environmental humidity of 23°C.

(B) The schematic diagram of surface gradient energy in biological recovery and the movement of a soft robot on the surface inspired by the beetles.

(C) The gradient structure of bamboo and the distribution of internal fibers, as well as the SEM image of MXenes of the bionic bamboo structure.

(D) Moisture-absorbing actuator model diagram of the G-MXCP actuator and MXene/CNF/PDA/BOPP double-layer actuators with different mechanical adaptability.

materials have a microstructure and are based on conductive carbon-reinforced materials combined with moisture-sensitive polymers. The functional materials produced can be triggered by environmental humidity and electroheating. At the same time, when compared with other materials that respond to humidity with the same effect, the actuator speed is increased by 10 times. The schematic diagram of the change of the actuator under different relative humidity conditions at 23°C is shown in Figure 13A (Le Duigou et al., 2019). The researches highlight that these actuators have a wide range of applications in the field of soft robots.

There is also the application of biomimetic robots in saving energy according to the design of biological gradient structures. Ding and co-workers, inspired by the natural phenomenon of beetles that can pick up a kinetic energy from the induced surface energy gradient of water and return to their familiar habitat, produced a fully soft robot based on the induced energy gradient and developed corresponding manufacturing and maneuver strategies (Figure 13B). The soft robot can reach a speed of 5.5 body lengths per second, seven times faster than previously reported. On this basis, they demonstrated a soft robot swarm, which can approach the target simultaneously to assure a hit with high accuracy. The design of the soft robot with a bio-inspired surface energy gradient provides a new idea for a soft robot to recycle energy (Lyu et al., 2019). The application of new material MXene based in actuator. Zhang and co-workers presented a hierarchical gradient structure of a soft actuator inspired by bamboo. They assembled two-dimensional MXenes on the micro-nano scale and one-dimensional cellulose nanofibers with strong hydrogen bonds on the molecular scale to form a gradient (Figure 13C). The prepared actuator has a tensile strength of up to 237.1 MPa, a Young's modulus of 8.5 GPa and excellent toughness (10.9 MJ/m^3). This bio-inspired assembled gradient material has strong robustness and can achieve strong mechanical properties even after bending 100,000 times (Figure 13D). This research provides ideas for preparing robust robots (Cao et al., 2020).

CONCLUSIONS AND PERSPECTIVES

In order to adapt the complex living environment, living organisms have gradually evolved and flourished by enhancing their functions. There are some organisms that enhance their functions through gradient

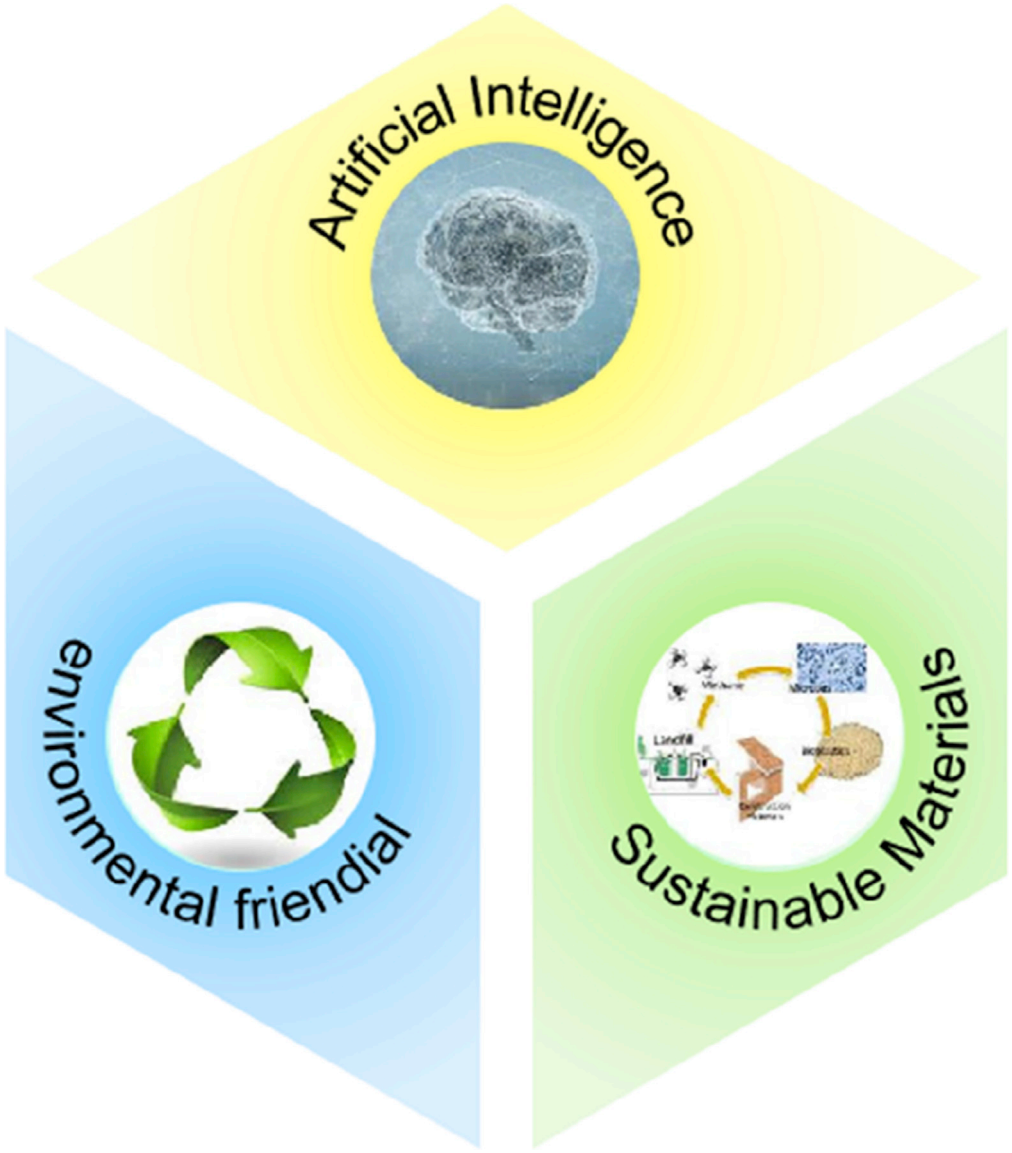

Figure 14. Applications Prospect of Bionic Gradient in the Future, such as Artificially Intelligent, Environmental Friendly, Sustainable Materials

phenomena, such as the ion gradient phenomenon of mussel enhances the self-healing and the brick-mud structure of shell enhances the mechanical strength, both caused by chemical factors and physical characteristics. Herein, we review the gradient phenomena in nature and divide them into two types: D-gradient and W-gradient. Then, we simplified these gradient phenomena into six simple models to help readers understand the essence of a gradient phenomenon. Furthermore, the biological functionalization caused by gradient phenomena is classified from the chemical and physical perspectives. The bionics-inspired applications of the gradients in the fields of medicine, energy, environmental, and robotics are also summarized. The potential bionic applications of the gradient phenomenon are shown in Figure 14, such as artificial intelligence and environmentally friendly sustainable materials. The gradient characteristics of wheat awns and pine cones give researchers the design of bionic surfaces that respond to humidity. A similar gradient phenomenon in biology can inspire researchers to design more artificially intelligent surfaces. Another example highlighted is that in order for organisms to save energy, they have evolved their gradient structures, and this has provided designers with ideas for making bionic surfaces. The prepared bionic surface reduces the waste of energy due to their reasonable structural design, which is beneficial to form an

environmentally friendly state. Regarding sustainable materials, the gradient distribution of protein of gecko seta and ladybird beetle that lead to the Young's modulus present the gradient phenomenon, which makes the seta or beetle resistant to external fatigue. This also provides inspiration for bionics and designing similarly functional gradient materials that give the materials sustainable performance.

Although some progress has been made in the field of bionic gradients, there are still some challenges. First, any organism with a gradient is a very complex structure at the nano- to near-macro scales, and scientists still need to further explore their cognition. Only by better understanding the nature behind the phenomenon can a more ideal biomimetic material or structure be made. Secondly, the experimental techniques and materials used to simulate the specific function of certain organisms need to be further improved. As described before, each creature is complex, and it is difficult to restore to a high degree the properties of the original creature. Therefore, the development of a wide range of new materials is the way to improve the bionic effect. Finally, nearly all the devices made by bionics are not intelligent, which makes the research results to the practical application still a fantasy. To solve this problem, we can combine computer science and artificial intelligence technology into bionics. Computer programming can be developed to control the synthesis of biomimetic materials and the design of biological structures in a fast, precise, and accurate manner and then combined with artificial intelligence technology to make the designed devices suitable for the required environment while achieving intelligence. As described in the five sections above, the functional gradient in materials have a wide application in the fields of medicine, energy, environmental science, and robotics. We believe that these materials will have significant influence on the development of artificial intelligence. The bionic property of the functional gradient in materials ensures that they can respond kindly to external stimuli. This is a prerequisite for the application of artificial intelligence in skin response, neural system control, and the behavior conduction. The in-depth study of gradients plays an important role in promoting the progress of bionics. A better understanding of the nature of gradients, the development of new materials, and the combination of artificial intelligence and bionics will make the field of bionics have a broader future.

ACKNOWLEDGMENTS

We thank National Nature Science Foundation of China (No. 51875577), Tribology Science Fund of State Key Laboratory of Tribology (No. SKLTKF16A06), and U.S. National Science Foundation (No. 2004251) for the support.

We declare no conflict of interest in this paper.

REFERENCES

Akinbade, Y., Harries, K.A., Flower, C.V., Nettleship, I., Papadopoulos, C., and Platt, S. (2019). Through-culm wall mechanical behaviour of bamboo. Construct. Build. Mater. *216*, 485–495.

Andersson, M., Jia, Q., Abella, A., Lee, X.-Y., Landreh, M., Purhonen, P., Hebert, H., Tenje, M., Robinson, C.V., and Meng, Q. (2017). Biomimetic spinning of artificial spider silk from a chimeric minispidroin. Nat. Chem. Biol. *13*, 262–264.

Arzt, E. (2006). Biological and artificial attachment devices: lessons for materials scientists from flies and geckos. Mater. Sci. Eng. C *26*, 1245–1250.

Autumn, K., Liang, Y.A., Hsieh, S.T., Zesch, W., Chan, W.P., Kenny, T.W., Fearing, R., and Full, R.J. (2000). Adhesive force of a single gecko foot-hair. Nature *405*, 681–685.

Autumn, K., Sitti, M., Liang, Y.A., Peattie, A.M., Hansen, W.R., Sponberg, S., Kenny, T.W., Fearing, R., Israelachvili, J.N., and Full, R.J. (2002). Evidence for van der Waals adhesion in gecko setae. Proc. Natl. Acad. Sci. U S A *99*, 12252–12256.

Bai, H., Sun, R., Ju, J., Yao, X., Zheng, Y., and Jiang, L. (2011). Large-scale fabrication of bioinspired fibers for directional water collection. Small *7*, 3429–3433.

Ballen, C., Healey, M., Wilson, M., Tobler, M., Wapstra, E., and Olsson, M. (2012). Net superoxide levels: steeper increase with activity in cooler female and hotter male lizards. J. Exp. Biol. *215*, 731–735.

Barnes, W.J.P., Goodwyn, P.J.P., Nokhbatolfoghahai, M., and Gorb, S.N. (2011). Elastic modulus of tree frog adhesive toe pads. J. Comp. Physiol. A *197*, 969.

Bauer, U., and Federle, W. (2009). The insect-trapping rim of Nepenthes pitchers: surface structure and function. Plant Signal. Behav. *4*, 1019–1023.

Bentov, S., Zaslansky, P., Al-Sawalmih, A., Masic, A., Fratzl, P., Sagi, A., Berman, A., and Aichmayer, B. (2012). Enamel-like apatite crown covering amorphous mineral in a crayfish mandible. Nat. Commun. *3*, 839.

Bergmann, A., Stein, D., Geisler, R., Hagenmaier, S., Schmid, B., Fernandez, N., Schnell, B., and Nüsslein-Volhard, C. (1996). A gradient of cytoplasmic Cactus degradation establishes the nuclear localization gradient of the dorsal morphogen in Drosophila. Mech. Dev. *60*, 109–123.

Bian, X., Yuan, F., Zhu, Y., and Wu, X. (2017). Gradient structure produces superior dynamic shear properties. Mater. Res. Lett. *5*, 501–507.

Biró, L.P., and Vigneron, J.P. (2011). Photonic nanoarchitectures in butterflies and beetles: valuable sources for bioinspiration. Laser Photon. Rev. *5*, 27–51.

Boesel, L.F., Greiner, C., Arzt, E., and Del Campo, A. (2010). Gecko-inspired surfaces: a path to strong and reversible dry adhesives. Adv. Mater. *22*, 2125–2137.

Brubaker, C.E., Kissler, H., Wang, L.-J., Kaufman, D.B., and Messersmith, P.B. (2010). Biological performance of mussel-inspired adhesive in extrahepatic islet transplantation. Biomaterials *31*, 420–427.

Bührig-Polaczek, A., Fleck, C., Speck, T., Schüler, P., Fischer, S., Caliaro, M., and Thielen, M. (2016). Biomimetic cellular metals—using hierarchical

structuring for energy absorption. Bioinspir. Biomim. *11*, 045002.

Cao, M., Ju, J., Li, K., Dou, S., Liu, K., and Jiang, L. (2014). Facile and large-scale fabrication of a cactus-inspired continuous fog collector. Adv. Funct. Mater. *24*, 3235–3240.

Cao, J., Zhou, Z., Song, Q., Chen, K., Su, G., Zhou, T., Zheng, Z., Lu, C., and Zhang, X. (2020). Ultrarobust Ti3C2Tx MXene-based soft actuators via bamboo-inspired mesoscale Assembly of hybrid nanostructures. ACS Nano *14*, 7055–7065.

Ceylan, H., Urel, M., Erkal, T.S., Tekinay, A.B., Dana, A., and Guler, M.O. (2013). Mussel inspired dynamic cross-linking of self-healing peptide nanofiber network. Adv. Funct. Mater. *23*, 2081–2090.

Chand, N., Jain, D., and Nigrawal, A. (2006). Investigations on gradient ac conductivity characteristics of bamboo (Dendrocalamus strictus). Bull. Mater. Sci. *29*, 193–196.

Chen, W., and Guo, Z. (2019). Hierarchical fibers for water collection inspired by spider silk. Nanoscale *11*, 15448–15463.

Chen, Y., and Zheng, Y. (2014). Bioinspired micro-/nanostructure fibers with a water collecting property. Nanoscale *6*, 7703–7714.

Chen, Y.-H., Li, M.-H., Zhang, Y., He, L.-L., Yamada, Y., Fitzmaurice, A., Shen, Y., Zhang, H., Tong, L., and Yang, J. (2004). Structural basis of the α 1–β subunit interaction of voltage-gated Ca 2+ channels. Nature *429*, 675–680.

Chen, P.-Y., Mckittrick, J., and Meyers, M.A. (2012). Biological materials: functional adaptations and bioinspired designs. Prog. Mater. Sci. *57*, 1492–1704.

Chen, Y., Wang, L., Xue, Y., Jiang, L., and Zheng, Y. (2013). Bioinspired tilt-angle fabricated structure gradient fibers: micro-drops fast transport in a long-distance. Sci. Rep. *3*, 2927.

Chen, H., Zhang, P., Zhang, L., Liu, H., Jiang, Y., Zhang, D., Han, Z., and Jiang, L. (2016). Continuous directional water transport on the peristome surface of Nepenthes alata. Nature *532*, 85–89.

Chen, G., Luo, H., Wu, S., Guan, J., Luo, J., and ZhaO, T. (2018a). Flexural deformation and fracture behaviors of bamboo with gradient hierarchical fibrous structure and water content. Compos. Sci. Technol. *157*, 126–133.

Chen, Y., Diaz-Dussan, D., Wu, D., Wang, W., Peng, Y.-Y., Asha, A.B., Hall, D.G., Ishihara, K., and Narain, R. (2018b). Bioinspired self-healing hydrogel based on benzoxaborole-catechol dynamic covalent chemistry for 3D cell encapsulation. ACS Macro Lett. *7*, 904–908.

Chen, P., Li, X., Ma, J., Zhang, R., Qin, F., Wang, J., Hu, T.S., Zhang, Y., and Xu, Q. (2019a). Bioinspired photodetachable dry self-cleaning surface. Langmuir *35*, 6379–6386.

Chen, S.-M., Gao, H.-L., Sun, X.-H., Ma, Z.-Y., Ma, T., Xia, J., Zhu, Y.-B., Zhao, R., Yao, H.-B., Wu, H.-A., and Yu, S.-H. (2019b). Superior biomimetic nacreous bulk nanocomposites by a multiscale soft-rigid dual-network interfacial design strategy. Matter *1*, 412–427.

Cherel, Y., Bustamante, P., and Richard, P. (2019). Amino acid δ13C and δ15N from sclerotized beaks: a new tool to investigate the foraging ecology of cephalopods, including giant and colossal squids. Mar. Ecol. Prog. Ser. *624*, 89–102.

Cui, J., Qin, Z., Masic, A., and Buehler, M.J. (2020). Multiscale structural insights of load bearing bamboo: a computational modeling approach. J. Mech. Behav. Biomed. Mater. *107*, 103743.

Dawson, C., Vincent, J.F., and RoccA, A.-M. (1997). How pine cones open. Nature *390*, 668.

Del Campo, A., and Greiner, C. (2007). SU-8: a photoresist for high-aspect-ratio and 3D submicron lithography. J. Micromech. Microeng. *17*, R81.

Del Campo, A., Greiner, C., Álvarez, I., and Arzt, E. (2007a). Patterned surfaces with pillars with controlled 3D tip geometry mimicking bioattachment devices. Adv. Mater. *19*, 1973–1977.

Del Campo, A., Greiner, C., and Arzt, E. (2007b). Contact shape controls adhesion of bioinspired fibrillar surfaces. Langmuir *23*, 10235–10243.

Deng, S., Shang, W., Feng, S., Zhu, S., Xing, Y., Li, D., Hou, Y., and Zheng, Y. (2017). Controlled droplet transport to target on a high adhesion surface with multi-gradients. Sci. Rep. *7*, 45687.

Derocher, K.A., Smeets, P.J., Goodge, B.H., Zachman, M.J., Balachandran, P.V., Stegbauer, L., Cohen, M.J., Gordon, L.M., Rondinelli, J.M., and Kourkoutis, L.F. (2020). Chemical gradients in human enamel crystallites. Nature *583*, 66–71.

Di Luca, A., Van Blitterswijk, C., and Moroni, L. (2015). The osteochondral interface as a gradient tissue: from development to the fabrication of gradient scaffolds for regenerative medicine. Birth Defects Res. C Embryo Today *105*, 34–52.

Dong, X., Zhao, H., Wang, Z., Ouzounian, M., Hu, T.S., Guo, Y., Zhang, L., and Xu, Q. (2019). Gecko-inspired composite micro-pillars with both robust adhesion and enhanced dry self-cleaning property. Chin. Chem. Lett. *30*, 2333–2337.

Dong, X., Zhang, R., Tian, Y., Ramos, M.A., Hu, T.S., Wang, Z., Zhao, H., Zhang, L., Wan, Y., Xia, Z., and Xu, Q. (2020). Functionally graded gecko setae and the biomimics with robust adhesion and durability. ACS Appl. Polym. Mater. *2*, 2658–2666.

Donnelly, R.F., Singh, T.R.R., Garland, M.J., Migalska, K., Majithiya, R., Mccrudden, C.M., Kole, P.L., Mahmood, T.M.T., Mccarthy, H.O., and Woolfson, A.D. (2012). Hydrogel-forming microneedle arrays for enhanced transdermal drug delivery. Adv. Funct. Mater. *22*, 4879–4890.

Drier, E.A., Govind, S., and Steward, R. (2000). Cactus-independent regulation of Dorsal nuclear import by the ventral signal. Curr. Biol. *10*, 23–26.

Duan, L., Yang, F., He, W., Song, L., Qiu, F., Xu, N., Xu, L., Zhang, Y., Hua, Z., and Gu, N. (2016). A multi-gradient targeting drug delivery system based on RGD-I-TRAIL-labeled magnetic microbubbles for cancer theranostics. Adv. Funct. Mater. *26*, 8313–8324.

Dufour, R., Dibao-Dina, A., Harnois, M., Tao, X., Dufour, C., Boukherroub, R., Senez, V., and Thomy, V. (2013). Electrowetting on functional fibers. Soft Matter *9*, 492–497.

Eisoldt, L., Smith, A., and Scheibel, T. (2011). Decoding the secrets of spider silk. Mater. Today *14*, 80–86.

Elbaum, R., Zaltzman, L., Burgert, I., and Fratzl, P. (2007). The role of wheat awns in the seed dispersal unit. Science *316*, 884–886.

Elbaum, R., Gorb, S., and Fratzl, P. (2008). Structures in the cell wall that enable hygroscopic movement of wheat awns. J. Struct. Biol. *164*, 101–107.

Federle, W., Barnes, W., Baumgartner, W., Drechsler, P., and Smith, J. (2006). Wet but not slippery: boundary friction in tree frog adhesive toe pads. J. R. Soc. Interface *3*, 689–697.

Feng, L., Li, S., Li, Y., Li, H., Zhang, L., Zhai, J., Song, Y., Liu, B., Jiang, L., and Zhu, D. (2002). Super-hydrophobic surfaces: from natural to artificial. Adv. Mater. *14*, 1857–1860.

Feng, S., Hou, Y., Chen, Y., Xue, Y., Zheng, Y., and Jiang, L. (2013a). Water-assisted fabrication of porous bead-on-string fibers. J. Mater. Chem. A *1*, 8363–8366.

Feng, S., Hou, Y., Xue, Y., Gao, L., Jiang, L., and Zheng, Y. (2013b). Photo-controlled water gathering on bio-inspired fibers. Soft Matter *9*, 9294–9297.

Feng, S., Wang, Q., Xing, Y., Hou, Y., and Zheng, Y. (2020). Continuous directional water transport on integrating tapered surfaces. Adv. Mater. Interfaces *7*, 2000081.

Filippidi, E., Cristiani, T.R., Eisenbach, C.D., Waite, J.H., Israelachvili, J.N., Ahn, B.K., and Valentine, M.T. (2017). Toughening elastomers using mussel-inspired iron-catechol complexes. Science *358*, 502–505.

Filpula, D.R., Lee, S.M., Link, R.P., Strausberg, S.L., and Strausberg, R.L. (1990). Structural and functional repetition in a marine mussel adhesive protein. Biotechnol. Prog. *6*, 171–177.

Fox, J.D., Capadona, J.R., Marasco, P.D., and Rowan, S.J. (2013). Bioinspired water-enhanced mechanical gradient nanocomposite films that mimic the architecture and properties of the squid beak. J. Am. Chem. Soc. *135*, 5167–5174.

Gan, Y., Chen, H., Ran, T., Zhang, P., and Zhang, D. (2018). The prey capture mechanism of micro structure on the Sarracenia Judith Hindle inner surface. J. Bionic Eng. *15*, 34–41.

Gan, D., Xu, T., Xing, W., Ge, X., Fang, L., Wang, K., Ren, F., and Lu, X. (2019). Mussel-inspired contact-active antibacterial hydrogel with high cell affinity, toughness, and recoverability. Adv. Funct. Mater. *29*, 1805964.

Gao, X., and Jiang, L. (2004). Water-repellent legs of water striders. Nature *432*, 36.

Gao, H., Ji, B., Jäger, I.L., Arzt, E., and Fratzl, P. (2003). Materials become insensitive to flaws at nanoscale: lessons from nature. Proc. Natl. Acad. Sci. U S A *100*, 5597–5600.

Gao, F., Xu, Z., Liang, Q., Liu, B., Li, H., Wu, Y., Zhang, Y., Lin, Z., Wu, M., Ruan, C., and Liu, W.

(2018). Direct 3D printing of high strength biohybrid gradient hydrogel scaffolds for efficient repair of osteochondral defect. Adv. Funct. Mater. *28*, 1706644.

Gebbie, M.A., Wei, W., Schrader, A.M., Cristiani, T.R., Dobbs, H.A., Idso, M., Chmelka, B.F., Waite, J.H., and Israelachvili, J.N. (2017). Tuning underwater adhesion with cation–π interactions. Nat. Chem. *9*, 473–479.

Geikowsky, E., Gorumlu, S., and Aksak, B. (2018). The effect of flexible joint-like elements on the adhesive performance of nature-inspired bent mushroom-like fibers. Beilstein J. Nanotechnol. *9*, 2893–2905.

Gerhard, E.M., Wang, W., Li, C., Guo, J., Ozbolat, I.T., Rahn, K.M., Armstrong, A.D., Xia, J., Qian, G., and Yang, J. (2017). Design strategies and applications of nacre-based biomaterials. Acta Biomater. *54*, 21–34.

Gong, L., Pan, D., and Wang, X. (2019). Finite element modeling of the viscoelastic contact for a composite micropillar. Mech. Adv. Mater. Struct. 1–13, https://doi.org/10.1080/15376494.2019.1578011.

Gorb, S.N., and Filippov, A.E. (2014). Fibrillar adhesion with no clusterisation: functional significance of material gradient along adhesive setae of insects. Beilstein J. Nanotechnol. *5*, 837–845.

Gorb, S., Varenberg, M., Peressadko, A., and Tuma, J. (2007). Biomimetic mushroom-shaped fibrillar adhesive microstructure. J. R. Soc. Interface *4*, 271–275.

Gorb, E.V., Lemke, W., and Gorb, S.N. (2019). Porous substrate affects a subsequent attachment ability of the beetle Harmonia axyridis (Coleoptera, Coccinellidae). J. R. Soc. Interface *16*, 20180696.

Greiner, C., Del Campo, A., and Arzt, E. (2007). Adhesion of bioinspired micropatterned surfaces: effects of pillar radius, aspect ratio, and preload. Langmuir *23*, 3495–3502.

Guo, L., and Tang, G. (2015). Experimental study on directional motion of a single droplet on cactus spines. Int. J. Heat Mass Transfer *84*, 198–202.

Guo, Y., Zhu, X., Fang, F., Hong, X., Wu, H., Chen, D., and Huang, X. (2018). Immobilization of enzymes on a phospholipid bionically modified polysulfone gradient-pore membrane for the enhanced performance of enzymatic membrane bioreactors. Molecules *23*, 144.

Gurera, D., and Bhushan, B. (2019). Optimization of bioinspired conical surfaces for water collection from fog. J. Colloid Interface Sci. *551*, 26–38.

Habibi, M.K., and Lu, Y. (2014). Crack propagation in bamboo's hierarchical cellular structure. Sci. Rep. *4*, 1–7.

Habibi, M.K., Samaei, A.T., Gheshlaghi, B., Lu, J., and Lu, Y. (2015). Asymmetric flexural behavior from bamboo's functionally graded hierarchical structure: underlying mechanisms. Acta Biomater. *16*, 178–186.

Haefliger, D., and Boisen, A. (2006). Three-dimensional microfabrication in negative resist using printed masks. J. Micromech. Microeng. *16*, 951.

Han, Z., Niu, S., Yang, M., Zhang, J., Yin, W., and Ren, L. (2013). An ingenious replica templated from the light trapping structure in butterfly wing scales. Nanoscale *5*, 8500–8506.

Han, Z., Mu, Z., Li, B., Niu, S., Zhang, J., and Ren, L. (2016). A high-transmission, multiple antireflective surface inspired from bilayer 3D ultrafine hierarchical structures in butterfly wing scales. Small *12*, 713–720.

Han, L., Yan, L., Wang, K., Fang, L., Zhang, H., Tang, Y., Ding, Y., Weng, L.-T., Xu, J., Weng, J., et al. (2017). Tough, self-healable and tissue-adhesive hydrogel with tunable multifunctionality. NPG Asia Mater. *9*, e372.

Han, L., Liu, K., Wang, M., Wang, K., Fang, L., Chen, H., Zhou, J., and Lu, X. (2018). Mussel-inspired adhesive and conductive hydrogel with long-lasting moisture and extreme temperature tolerance. Adv. Funct. Mater. *28*, 1704195.

Hanna, G., Jon, W., and Barnes, W.J. (1991). Adhesion and detachment of the toe pads of tree frogs. J. Exp. Biol. *155*, 103–125.

Harrington, M.J., Masic, A., Holten-Andersen, N., Waite, J.H., and Fratzl, P. (2010). Iron-clad fibers: a metal-based biological strategy for hard flexible coatings. Science *328*, 216–220.

Heepe, L., Höft, S., Michels, J., and Gorb, S.N. (2018). Material gradients in fibrillar insect attachment systems: the role of joint-like elements. Soft Matter *14*, 7026–7033.

Hellum, A. (1982). Cone moisture and relative humidity effects on seed release from lodgepole pine cones from Alberta. Can. J. For. Res. *12*, 102–105.

Heng, X., Xiang, M., Lu, Z., and Luo, C. (2014). Branched ZnO wire structures for water collection inspired by cacti. ACS Appl. Mater. Interfaces *6*, 8032–8041.

Heymann, D., Mohanram, H., Kumar, A., Verma, C.S., Lescar, J., and Miserez, A. (2020). Structure of a consensus chitin-binding domain revealed by solution NMR. bioRxiv, 2020.01.08.899344. https://www.researchgate.net/deref/http%3A%2F%2Fdx.doi.org%2F10.1101%2F2020.01.08.899344.

Holland, C., Terry, A., Porter, D., and Vollrath, F. (2006). Comparing the rheology of native spider and silkworm spinning dope. Nat. Mater. *5*, 870–874.

Holten-Andersen, N., Fantner, G.E., Hohlbauch, S., Waite, J.H., and Zok, F.W. (2007). Protective coatings on extensible biofibres. Nat. Mater. *6*, 669–672.

Holten-Andersen, N., Zhao, H., and Waite, J.H. (2009). Stiff coatings on compliant biofibers: the cuticle of Mytilus californianus byssal threads. Biochemistry *48*, 2752–2759.

Hou, Y., Chen, Y., Xue, Y., Wang, L., Zheng, Y., and Jiang, L. (2012). Stronger water hanging ability and higher water collection efficiency of bioinspired fiber with multi-gradient and multi-scale spindle knots. Soft Matter *8*, 11236–11239.

Hou, Y., Xing, Y., Feng, S., Gao, C., Zhou, H., and Zheng, Y. (2020). Droplet self-propelling control on bioinspired fiber in low temperature and high humidity environment. Adv. Mater. Interfaces *7*, 1901183.

Hu, S., Xia, Z., and Gao, X. (2012). Strong adhesion and friction coupling in hierarchical carbon nanotube arrays for dry adhesive applications. ACS Appl. Mater. Interfaces *4*, 1972–1980.

Huang, Z.-X., Liu, X., Wu, J., Wong, S.-C., and Qu, J.-P. (2018). Electrospinning water harvesters inspired by spider silk and beetle. Mater. Lett. *211*, 28–31.

Hurchalla, G. (2018). Effect of Hierarchical Structure and Orientation on Water-Repellent Legs of Water-Walking Insects (Michigan Tech).

Hurchalla, G., and Drelich, J.W. (2019). Water repellency of hierarchically structured legs of water-walking striders and fire ants. Surf. Innov. *7*, 184–193.

Iwata, M., and Otaki, J.M. (2016). Spatial patterns of correlated scale size and scale color in relation to color pattern elements in butterfly wings. J. Insect Physiol. *85*, 32–45.

Jiang, L., Zhao, Y., and Zhai, J. (2004). A lotus-leaf-like superhydrophobic surface: a porous microsphere/nanofiber composite film prepared by electrohydrodynamics. Angew. Chem. Int. Ed. *43*, 4338–4341.

Jiao, D., Liu, Z., Zhang, Z., and Zhang, Z. (2015). Intrinsic hierarchical structural imperfections in a natural ceramic of bivalve shell with distinctly graded properties. Sci. Rep. *5*, 12418.

Jiao, D., Liu, Z., Qu, R.T., and Zhang, Z.F. (2016). Anisotropic mechanical behaviors and their structural dependences of crossed-lamellar structure in a bivalve shell. Mater. Sci. Eng. C *59*, 828–837.

Jiao, Y., Lv, X., Zhang, Y., Li, C., Li, J., Wu, H., Xiao, Y., Wu, S., Hu, Y., and Wu, D. (2019). Pitcher plant-bioinspired bubble slippery surface fabricated by femtosecond laser for buoyancy-driven bubble self-transport and efficient gas capture. Nanoscale *11*, 1370–1378.

Jin, K., Tian, Y., Erickson, J.S., Puthoff, J., Autumn, K., and Pesika, N.S. (2012). Design and fabrication of gecko-inspired adhesives. Langmuir *28*, 5737–5742.

Jo, H., Yoon, M., Gajendiran, M., and Kim, K. (2019). Recent strategies in fabrication of gradient hydrogels for tissue engineering applications. Macromol. Biosci. *20*, e1900300.

Ju, J., Bai, H., Zheng, Y., Zhao, T., Fang, R., and Jiang, L. (2012). A multi-structural and multi-functional integrated fog collection system in cactus. Nat. Commun. *3*, 1–6.

Ju, J., Xiao, K., Yao, X., Bai, H., and Jiang, L. (2013). Bioinspired conical copper wire with gradient wettability for continuous and efficient fog collection. Adv. Mater. *25*, 5937–5942.

Jung, W., Kim, W., and Kim, H.-Y. (2014). Self-burial mechanics of hygroscopically responsive awns. Integr. Comp. Biol. *54*, 1034–1042.

Kang, E., Shin, S.-J., Lee, K.H., and Lee, S.-H. (2010). Novel PDMS cylindrical channels that generate coaxial flow, and application to fabrication of microfibers and particles. Lab Chip *10*, 1856–1861.

Kang, E., Jeong, G.S., Choi, Y.Y., Lee, K.H., Khademhosseini, A., and Lee, S.-H. (2011). Digitally tunable physicochemical coding of material composition and topography in continuous microfibres. Nat. Mater. *10*, 877–883.

Kang, T., Banquy, X., Heo, J., Lim, C., Lynd, N.A., Lundberg, P., Oh, D.X., Lee, H.-K., Hong, Y.-K., and Hwang, D.S. (2016). Mussel-inspired anchoring of polymer loops that provide superior surface lubrication and antifouling properties. ACS Nano *10*, 930–937.

Karabanova, L.V., Mikhalovsky, S.V., and Lloyd, A.W. (2012). Gradient semi-interpenetrating polymer networks based on polyurethane and poly (2-hydroxyethyl methacrylate) for biomedical applications. J. Mater. Chem. *22*, 7919–7928.

Karthick, B., and Maheshwari, R. (2008). Lotus-inspired nanotechnology applications. Resonance *13*, 1141–1145.

Khorshidi, S., and Karkhaneh, A. (2018). A review on gradient hydrogel/fiber scaffolds for osteochondral regeneration. J. Tissue Eng. Regen. Med. *12*, e1974–e1990.

Kim, K., Kim, H., Ho Park, S., and Joon Lee, S. (2017). Hydraulic strategy of cactus trichome for absorption and storage of water under arid environment. Front. Plant Sci. *8*, 1777.

Kim, S., Sitti, M., Hui, C.Y., Long, R., and Jagota, A. (2007). Effect of backing layer thickness on adhesion of single-level elastomer fiber arrays. Appl. Phys. Lett. *91*, 161905.

Kirschner, C.M., and Brennan, A.B. (2012). Bio-inspired antifouling strategies. Annu. Rev. Mater. Res. *42*, 211–229.

Kustandi, T.S., Samper, V.D., Yi, D.K., Ng, W.S., Neuzil, P., and Sun, W. (2007). Self-assembled nanoparticles based fabrication of gecko foot-hair-inspired polymer nanofibers. Adv. Funct. Mater. *17*, 2211–2218.

Lappin Scott, H.M., and Costerton, J.W. (1989). Bacterial biofilms and surface fouling. Biofouling *1*, 323–342.

Le Duigou, A., and Castro, M. (2016). Evaluation of force generation mechanisms in natural, passive hydraulic actuators. Sci. Rep. *6*, 18105.

Le Duigou, A., Chabaud, G., Scarpa, F., and Castro, M. (2019). Bioinspired electro-thermo-hygro reversible shape-changing materials by 4D printing. Adv. Funct. Mater. *29*, 1903280.

Lee, J., and Fearing, R.S. (2008). Contact self-cleaning of synthetic gecko adhesive from polymer microfibers. Langmuir *24*, 10587–10591.

Lee, B.P., Dalsin, J.L., and Messersmith, P.B. (2002). Synthesis and gelation of DOPA-modified poly (ethylene glycol) hydrogels. Biomacromolecules *3*, 1038–1047.

Lee, H., Scherer, N.F., and Messersmith, P.B. (2006). Single-molecule mechanics of mussel adhesion. Proc. Natl. Acad. Sci. U S A *103*, 12999–13003.

Lee, H., Lee, B.P., and Messersmith, P.B. (2007). A reversible wet/dry adhesive inspired by mussels and geckos. Nature *448*, 338–341.

Lee, B.P., Messersmith, P.B., Israelachvili, J.N., and Waite, J.H. (2011). Mussel-inspired adhesives and coatings. Annu. Rev. Mater. Res. *41*, 99–132.

Lee, S.-W., Prosser, J.H., Purohit, P.K., and Lee, D. (2013). Bioinspired hygromorphic actuator exhibiting controlled locomotion. ACS Macro Lett. *2*, 960–965.

Li, X., Tian, J., and Shen, W. (2010). Thread as a versatile material for low-cost microfluidic diagnostics. ACS Appl. Mater. Interfaces *2*, 1–6.

Li, Z., Yin, S., Cheng, L., Yang, K., Li, Y., and Liu, Z. (2014). Magnetic targeting enhanced theranostic strategy based on multimodal imaging for selective ablation of cancer. Adv. Funct. Mater. *24*, 2312–2321.

Li, S.-Y., Li, Y., Wang, J., Nan, Y.-G., Ma, B.-H., Liu, Z.-L., and Gu, J.-X. (2016). Fabrication of pinecone-like structure superhydrophobic surface on titanium substrate and its self-cleaning property. Chem. Eng. J. *290*, 82–90.

Li, Y., He, L., Zhang, X., Zhang, N., and Tian, D. (2017). External-field-induced gradient wetting for controllable liquid transport: from movement on the surface to penetration into the surface. Adv. Mater. *29*, 1703802.

Li, J., Zheng, H., Yang, Z., and Wang, Z. (2018). Breakdown in the directional transport of droplets on the peristome of pitcher plants. Commun. Phys. *1*, 1–7.

Li, W., Li, Y., Sheng, M., Cui, S., Wang, Z., Zhang, X., Yang, C., Yu, Z., Zhang, Y., Tian, S., et al. (2019). Enhanced adhesion of carbon nanotubes by dopamine modification. Langmuir *35*, 4527–4533.

Li, X., Yang, Y., Liu, L., Chen, Y., Chu, M., Sun, H., Shan, W., and Chen, Y. (2020). 3D-Printed cactus-inspired spine structures for highly efficient water collection. Adv. Mater. Interfaces *7*, 1901752.

Liao, J., Yang, M., Zhang, W., Zeng, D., Ning, C., and Yuan, H. (2020). Spider silk-inspired universal strategy: directional patching of one-dimensional nanomaterial-based flexible transparent electrodes for smart flexible electronics. Chem. Eng. J. *389*, 123663.

Lim, C., Huang, J., Kim, S., Lee, H., Zeng, H., and Hwang, D.S. (2016). Nanomechanics of poly (catecholamine) coatings in aqueous solutions. Angew. Chem. Int. Ed. *55*, 3342–3346.

Lin, A.G., Ding, X.F., Xie, Z.D., and Sun, B.Y. (2009). Mechanical properties of the natural heterogeneous composites. Mater. Sci. Forum *628-629*, 657–662.

Lin, S., Xie, Y.M., Li, Q., Huang, X., and Zhou, S. (2016). On the shape transformation of cone scales. Soft Matter *12*, 9797–9802.

Linder, M.B. (2015). Biomaterials: recipe for squid beak. Nat. Chem. Biol. *11*, 455.

Liu, L., Xiong, Z., Yan, Y., Zhang, R., Wang, X., and Jin, L. (2009). Multinozzle low-temperature deposition system for construction of gradient tissue engineering scaffolds. J. Biomed. Mater. Res. B Appl. Biomater. *88*, 254–263.

Liu, M., Zheng, Y., Zhai, J., and Jiang, L. (2010). Bioinspired super-antiwetting interfaces with special liquid– solid adhesion. Acc. Chem. Res. *43*, 368–377.

Liu, Y., Andrew, M., Li, J., Yeomans, J.M., and Wang, Z. (2015). Symmetry breaking in drop bouncing on curved surfaces. Nat. Commun. *6*, 1–8.

Liu, D., He, Y., Hu, P., and Ding, H. (2017a). Characterizing torsional properties of microwires using an automated torsion balance. Exp. Mech. *57*, 297–311.

Liu, Z., Meyers, M.A., Zhang, Z., and Ritchie, R.O. (2017b). Functional gradients and heterogeneities in biological materials: design principles, functions, and bioinspired applications. Prog. Mater. Sci. *88*, 467–498.

Long, L., Wang, Z., and Chen, K. (2015). Analysis of the hollow structure with functionally gradient materials of moso bamboo. J. Wood Sci. *61*, 569–577.

Low, I.M., Che, Z.Y., and Latella, B.A. (2006a). Mapping the structure, composition and mechanical properties of bamboo. J. Mater. Res. *21*, 1969–1976.

Low, I.M., Che, Z.Y., Latella, B.A., and Sim, K.S. (2006b). Mechanical and fracture properties of bamboo. Key Eng. Mater. *312*, 15–20.

Lu, T., Peng, W., Zhu, S., and Zhang, D. (2016). Bio-inspired fabrication of stimuli-responsive photonic crystals with hierarchical structures and their applications. Nanotechnology *27*, 122001.

Lu, J., Pan, Y., Zhong, Q., and Liu, B. (2019). Guided cellular orientation concurrently with cell density gradient on butterfly wings. RSC Adv. *9*, 25875–25879.

Lyu, L.X., Li, F., Wu, K., Deng, P., Jeong, S.H., Wu, Z., and Ding, H. (2019). Bio-inspired untethered fully soft robots in liquid actuated by induced energy gradients. Natl. Sci. Rev. *6*, 970–981.

Maderson, P.F.A. (1964). Keratinized epidermal derivatives as an aid to climbing in gekkonid lizards. Nature *203*, 780–781.

Madurga, R., Blackledge, T.A., Perea, B., Plaza, G., Riekel, C., Burghammer, M., Elices, M., Guinea, G., and Pérez-Rigueiro, J. (2015). Persistence and variation in microstructural design during the evolution of spider silk. Sci. Rep. *5*, 1–11.

Magazù, S., Migliardo, F., and Ramirez-Cuesta, A. (2005). Inelastic neutron scattering study on bioprotectant systems. J. R. Soc. Interface *2*, 527–532.

Major, B., Major, R., Bruckert, F., Lackner, J., Ebner, R., Kustosz, R., and Lacki, P. (2007). New gradient coatings on TiN and TiCN basis for

biomedical application to blood contact. Adv. Mater. Sci. *7*, 63–70.

Manabe, K., Nishizawa, S., Kyung, K.-H., and Shiratori, S. (2014). Optical phenomena and antifrosting property on biomimetics slippery fluid-infused antireflective films via layer-by-layer comparison with superhydrophobic and antireflective films. ACS Appl. Mater. Interfaces *6*, 13985–13993.

Mao, L.-B., Gao, H.-L., Yao, H.-B., Liu, L., Cölfen, H., Liu, G., Chen, S.-M., Li, S.-K., Yan, Y.-X., and Liu, Y.-Y. (2016). Synthetic nacre by predesigned matrix-directed mineralization. Science *354*, 107–110.

Márk, G.I., Kertész, K., Piszter, G., Bálint, Z., and Biró, L.P. (2019). Modeling the reflectance changes induced by vapor condensation in Lycaenid butterfly wing scales colored by photonic nanoarchitectures. Nanomaterials *9*, 759.

Maugh, K., Anderson, D., Strausberg, R., Strausberg, S., Mccandliss, R., Wei, T., and Filpula, D. (1988). Recombinant Bioadhesive Proteins of Marine Animals and Their Use in Adhesive Compositions (Genex Corp), p. 124.

Mejdoubi, A., Andraud, C., Berthier, S., Lafait, J., Boulenguez, J., and Richalot, E. (2013). Finite element modeling of the radiative properties of Morpho butterfly wing scales. Phys. Rev. E *87*, 022705.

Menon, C., Murphy, M., and Sitti, M. (2004). Gecko inspired surface climbing robots. In IEEE International Conference on Robotics and Biomimetics, 2004 (IEEE), pp. 431–436.

Meyers, M.A., Mckittrick, J., and Chen, P.-Y. (2013). Structural biological materials: critical mechanics-materials connections. Science *339*, 773–779.

Miserez, A., Li, Y., Waite, J.H., and Zok, F. (2007). Jumbo squid beaks: inspiration for design of robust organic composites. Acta Biomater. *3*, 139–149.

Miserez, A., Schneberk, T., Sun, C., Zok, F.W., and Waite, J.H. (2008). The transition from stiff to compliant materials in squid beaks. Science *319*, 1816–1819.

Miserez, A., Rubin, D., and Waite, J.H. (2010). Cross-linking chemistry of squid beak. J. Biol. Chem. *285*, 38115–38124.

Monteiro, A., French, V., Smit, G., Brakefield, P.M., and Metz, J.A. (2001). Butterfly eyespot patterns: evidence for specification by a morphogen diffusion gradient. Acta Biotheor. *49*, 77–88.

Moreno, R., and Smedby, Ö. (2015). Gradient-based enhancement of tubular structures in medical images. Med. Image Anal. *26*, 19–29.

Muiznieks, L.D., and Keeley, F.W. (2016). Phase separation and mechanical properties of an elastomeric biomaterial from spider wrapping silk and elastin block copolymers. Biopolymers *105*, 693–703.

Murphy, M.P., Aksak, B., and Sitti, M. (2009). Gecko-inspired directional and controllable adhesion. Small *5*, 170–175.

Naleway, S.E., Porter, M.M., Mckittrick, J., and Meyers, M.A. (2015). Structural design elements in biological materials: application to bioinspiration. Adv. Mater. *27*, 5455–5476.

Ng, J.L., Collins, C.E., and Tate, M.L.K. (2017). Engineering mechanical gradients in next generation biomaterials–lessons learned from medical textile design. Acta Biomater. *56*, 14–24.

Nishimoto, S., and Bhushan, B. (2013). Bioinspired self-cleaning surfaces with superhydrophobicity, superoleophobicity, and superhydrophilicity. RSC Adv. *3*, 671–690.

O'connor, S.M., Deanglis, A.P., Gehrke, S.H., and Retzinger, G.S. (2000). Adsorption of plasma proteins on to poly (ethylene oxide)/poly (propylene oxide) triblock copolymer films: a focus on fibrinogen. Biotechnol. Appl. Biochem. *31*, 185–196.

Oda, M., Suga, S., Yoshii, H., and Furuta, T. (2008). Multilayer coating by drawing a thin plastic fiber through a polymer solution. Asia Pac. J. Chem. Eng. *3*, 63–69.

Omenetto, F.G., and Kaplan, D.L. (2010). New opportunities for an ancient material. Science *329*, 528–531.

Osotsi, M.I., Zhang, W., Zada, I., Gu, J., Liu, Q., and Zhang, D. (2020). Butterfly wing architectures inspire sensor and energy applications. Natl. Sci. Rev.nwaa107 https://doi.org/10.1093/nsr/nwaa107.

Otaki, J.M. (2011a). Artificially induced changes of butterfly wing colour patterns: dynamic signal interactions in eyespot development. Sci. Rep. *1*, 111.

Otaki, J.M. (2011b). Color-pattern analysis of eyespots in butterfly wings: a critical examination of morphogen gradient models. Zoolog. Sci. *28*, 403–413.

Palombini, F.L., Kindlein, W., Jr., De Oliveira, B.F., and De Araujo Mariath, J.E. (2016). Bionics and design: 3D microstructural characterization and numerical analysis of bamboo based on X-ray microtomography. Mater. Char. *120*, 357–368.

Peisker, H., Michels, J., and Gorb, S.N. (2013). Evidence for a material gradient in the adhesive tarsal setae of the ladybird beetle Coccinella septempunctata. Nat. Commun. *4*, 1–7.

Petersen, D.S., Kreuter, N., Heepe, L., Büsse, S., Wellbrock, A.H.J., Witte, K., and Gorb, S.N. (2018). Holding tight to feathers – structural specializations and attachment properties of the avian ectoparasite Crataerina pallida (Diptera, Hippoboscidae). J. Exp. Biol. *221*, jeb179242.

Politi, Y., Priewasser, M., Pippel, E., Zaslansky, P., Hartmann, J., Siegel, S., Li, C., Barth, F.G., and Fratzl, P. (2012). A spider's fang: how to design an injection needle using chitin-based composite material. Adv. Funct. Mater. *22*, 2519–2528.

Poncelet, O., Tallier, G., Mouchet, S.R., Crahay, A., Rasson, J., Kotipalli, R., Deparis, O., and Francis, L.A. (2016). Vapour sensitivity of an ALD hierarchical photonic structure inspired by Morpho. Bioinspir. Biomim. *11*, 036011.

Porter, D., and Vollrath, F. (2007). Nanoscale toughness of spider silk. Nano Today *2*, 6.

Potyrailo, R.A., Starkey, T.A., Vukusic, P., Ghiradella, H., Vasudev, M., Bunning, T., Naik, R.R., Tang, Z., Larsen, M., and Deng, T. (2013). Discovery of the surface polarity gradient on iridescent Morpho butterfly scales reveals a mechanism of their selective vapor response. Proc. Natl. Acad. Sci. U S A *110*, 15567–15572.

Pouya, C., Overvelde, J.T., Kolle, M., Aizenberg, J., Bertoldi, K., Weaver, J.C., and Vukusic, P. (2016). Characterization of a mechanically tunable gyroid photonic crystal inspired by the butterfly parides sesostris. Adv. Opt. Mater. *4*, 99–105.

Qiu, S., Ren, X., Zhou, X., Zhang, T., Song, L., and Hu, Y. (2020). Nacre-inspired black phosphorus/nanofibrillar cellulose composite film with enhanced mechanical properties and superior fire resistance. ACS Appl. Mater. Interfaces *12*, 36639–36651.

Qu, L., and Dai, L. (2007). Gecko-foot-mimetic aligned single-walled carbon nanotube dry adhesives with unique electrical and thermal properties. Adv. Mater. *19*, 3844–3849.

Ray, A.K., Mondal, S., Das, S.K., and Ramachandrarao, P. (2005). Bamboo—a functionally graded composite-correlation between microstructure and mechanical strength. J. Mater. Sci. *40*, 5249–5253.

Reach, M., Galindo, R.L., Towb, P., Allen, J.L., Karin, M., and Wasserman, S.A. (1996). A gradient of cactus protein degradation establishes dorsoventral polarity in the Drosophila embryo. Dev. Biol. *180*, 353–364.

Rebora, M., Michels, J., Salerno, G., Heepe, L., Gorb, E., and Gorb, S. (2018). Tarsal attachment devices of the southern green stink bug Nezara viridula (Heteroptera: pentatomidae). J. Morphol. *279*, 660–672.

Ren, L., Li, B., Song, Z., Liu, Q., Ren, L., and Zhou, X. (2019). 3D printing of structural gradient soft actuators by variation of bioinspired architectures. J. Mater. Sci. *54*, 6542–6551.

Reyssat, E., and Mahadevan, L. (2009). Hygromorphs: from pine cones to biomimetic bilayers. J. R. Soc. Interface *6*, 951–957.

Riekel, C., and Vollrath, F. (2001). Spider silk fibre extrusion: combined wide-and small-angle X-ray microdiffraction experiments. Int. J. Biol. Macromolecules *29*, 203–210.

Ries, J., Schwarze, S., Johnson, C.M., and Neuweiler, H. (2014). Microsecond folding and domain motions of a spider silk protein structural switch. J. Am. Chem. Soc. *136*, 17136–17144.

Rousseau, M., Bourrat, X., Stempflé, P., Brendlé, M., and Lopez, E. (2005). Multi-scale structure of the pinctada mother of pearl: demonstration of a continuous and oriented organic framework in a natural ceramic. Key Eng. Mater. *284-286*, 705–708.

Sahni, V., Blackledge, T.A., and Dhinojwala, A. (2010). Viscoelastic solids explain spider web stickiness. Nat. Commun. *1*, 1–4.

Sahni, V., Labhasetwar, D.V., and Dhinojwala, A. (2012). Spider silk inspired functional microthreads. Langmuir *28*, 2206–2210.

Sameoto, D., and Menon, C. (2009). Direct molding of dry adhesives with anisotropic peel strength using an offset lift-off photoresist mold. J. Micromech. Microeng. *19*, 115026.

Saranathan, V., Osuji, C.O., Mochrie, S.G., Noh, H., Narayanan, S., Sandy, A., Dufresne, E.R., and Prum, R.O. (2010). Structure, function, and self-assembly of single network gyroid (I4132) photonic crystals in butterfly wing scales. Proc. Natl. Acad. Sci. U S A *107*, 11676–11681.

Sekimura, T., Venkataraman, C., and Madzvamuse, A. (2015). A model for selection of eyespots on butterfly wings. PLoS One *10*, e0141434.

Seveno, D., Ogonowski, G., and De Coninck, J. (2004). Liquid coating of moving fiber at the nanoscale. Langmuir *20*, 8385–8390.

Shao, C., Wang, M., Meng, L., Chang, H., Wang, B., Xu, F., Yang, J., and Wan, P. (2018). Mussel-inspired cellulose nanocomposite tough hydrogels with synergistic self-healing, adhesive, and strain-sensitive properties. Chem. Mater. *30*, 3110–3121.

Shen, A.Q., Gleason, B., Mckinley, G.H., and Stone, H.A. (2002). Fiber coating with surfactant solutions. Phys. Fluids *14*, 4055–4068.

Shi, D., Shen, J., Zhang, Z., Shi, C., Chen, M., Gu, Y., and Liu, Y. (2019). Preparation and properties of dopamine-modified alginate/chitosan–hydroxyapatite scaffolds with gradient structure for bone tissue engineering. J. Biomed. Mater. Res. A *107*, 1615–1627.

Shin, S.-J., Park, J.-Y., Lee, J.-Y., Park, H., Park, Y.-D., Lee, K.-B., Whang, C.-M., and Lee, S.-H. (2007). "On the fly" continuous generation of alginate fibers using a microfluidic device. Langmuir *23*, 9104–9108.

Shin, B., Ha, J., Lee, M., Park, K., Park, G.H., Choi, T.H., Cho, K.-J., and Kim, H.-Y. (2018). Hygrobot: a self-locomotive ratcheted actuator powered by environmental humidity. Sci. Robot. *3*, eaar2629.

Silva, E.C.N., Walters, M.C., and Paulino, G.H. (2006). Modeling bamboo as a functionally graded material: lessons for the analysis of affordable materials. J. Mater. Sci. *41*, 6991–7004.

Singh, M., Dormer, N., Salash, J.R., Christian, J.M., Moore, D.S., Berkland, C., and Detamore, M.S. (2010). Three-dimensional macroscopic scaffolds with a gradient in stiffness for functional regeneration of interfacial tissues. J. Biomed. Mater. Res. A *94*, 870–876.

Song, D., and Bhushan, B. (2019). Water condensation and transport on bioinspired triangular patterns with heterogeneous wettability at a low temperature. Philos. Trans. A Math. Phys. Eng. Sci. *377*, 20180335.

Song, J., Fan, C., Ma, H., and Wei, Y. (2015). Hierarchical structure observation and nanoindentation size effect characterization for a limnetic shell. Acta Mech. Sin. *31*, 364–372.

Song, Z., Ren, L., Zhao, C., Liu, H., Yu, Z., Liu, Q., and Ren, L. (2020). Biomimetic nonuniform, dual-stimuli self-morphing enabled by gradient four-dimensional printing. ACS Appl. Mater. Interfaces *12*, 6351–6361.

Stavenga, D., Stowe, S., Siebke, K., Zeil, J., and Arikawa, K. (2004). Butterfly wing colours: scale beads make white pierid wings brighter. Proc. R. Soc. Lond. Ser. B Biol. Sci. *271*, 1577–1584.

Stork, N. (1980). Experimental analysis of adhesion of Chrysolina polita (Chrysomelidae: Coleoptera) on a variety of surfaces. J. Exp. Biol. *88*, 91–108.

Strausberg, R.L., Anderson, D.M., Filpula, D., Finkelman, M., Link, R., Mccandliss, R., Orndorff, S.A., Strausberg, S.L., and Wei, T. (1989). Development of a microbial system for production of mussel adhesive protein. In Adhesives from Renewable Resources, *385*Adhesives from Renewable Resources (American Chemical Society), pp. 453–464.

Sun, Q., Wang, D., Li, Y., Zhang, J., Ye, S., Cui, J., Chen, L., Wang, Z., Butt, H.-J., and Vollmer, D. (2019a). Surface charge printing for programmed droplet transport. Nat. Mater. *18*, 936–941.

Sun, Q., Xu, R., Han, Q., Zhao, K., Mcadams, I., and Xu, W. (2019b). Long distance chemical gradient induced by surface nanocrystallization. Appl. Mater. Today *14*, 137–142.

Suresh, S. (2001). Graded materials for resistance to contact deformation and damage. Science *292*, 2447–2451.

Tamarin, A., Lewis, P., and Askey, J. (1976). The structure and formation of the byssus attachment plaque in Mytilus. J. Morphol. *149*, 199–221.

Tan, T., Rahbar, N., Allameh, S., Kwofie, S., Dissmore, D., Ghavami, K., and Soboyejo, W. (2011). Mechanical properties of functionally graded hierarchical bamboo structures. Acta Biomater. *7*, 3796–3803.

Tan, Y., Yildiz, U.H., Wei, W., Waite, J.H., and Miserez, A. (2013). Layer-by-layer polyelectrolyte deposition: a mechanism for forming biocomposite materials. Biomacromolecules *14*, 1715–1726.

Tan, Y., Hoon, S., Guerette, P.A., Wei, W., Ghadban, A., Hao, C., Miserez, A., and Waite, J.H. (2015). Infiltration of chitin by protein coacervates defines the squid beak mechanical gradient. Nat. Chem. Biol. *11*, 488.

Tan, X., Zhu, Y., Shi, T., Tang, Z., and Liao, G. (2016). Patterned gradient surface for spontaneous droplet transportation and water collection: simulation and experiment. J. Micromech. Microeng. *26*, 115009.

Tan, M., Jiang, X., Ke, H., Wu, W., and Xia, R. (2020). Experimental investigations on the mechanical properties of bamboo fiber and fibril. Fibers Polym. *21*, 1382–1386.

Tang, L., Wang, X., Hong, W., Sun, W., Yang, B., Chen, X., and Liu, J. (2018). Fabrication of a flexible biomimetic film with spontaneously unidirectional water-spreading property. Micro Nano Lett. *13*, 321–325.

Tatehata, H., Mochizuki, A., Kawashima, T., Yamashita, S., and Yamamoto, H. (2000). Model polypeptide of mussel adhesive protein. I. Synthesis and adhesive studies of sequential polypeptides (X-Tyr-Lys) n and (Y-Lys) n. J. Appl. Polym. Sci. *76*, 929–937.

Tian, Y., Pesika, N., Zeng, H., Rosenberg, K., Zhao, B., Mcguiggan, P., Autumn, K., and Israelachvili, J. (2006). Adhesion and friction in gecko toe attachment and detachment. Proc. Natl. Acad. Sci. U S A *103*, 19320–19325.

Tian, X., Bai, H., Zheng, Y., and Jiang, L. (2011). Bio-inspired heterostructured bead-on-string fibers that respond to environmental wetting. Adv. Funct. Mater. *21*, 1398–1402.

Tian, Y., Cao, Y., Wang, Y., Yang, W., and Feng, J. (2013). Realizing ultrahigh modulus and high strength of macroscopic graphene oxide papers through crosslinking of mussel-inspired polymers. Adv. Mater. *25*, 2980–2983.

Tramacere, F., Follador, M., Pugno, N., and Mazzolai, B. (2015). Octopus-like suction cups: from natural to artificial solutions. Bioinspir. Biomim. *10*, 035004.

Varenberg, M., Peressadko, A., Gorb, S., and Arzt, E. (2006). Effect of real contact geometry on adhesion. Appl. Phys. Lett. *89*, 121905.

Varenberg, M., Murarash, B., Kligerman, Y., and Gorb, S.N. (2011). Geometry-controlled adhesion: revisiting the contact splitting hypothesis. Appl. Phys. A *103*, 933–938.

Vickers, N.J. (2017). Animal communication: when i'm calling you, will you answer too? Curr. Biol. *27*, R713–R715.

Voigt, D., Tsipenyuk, A., and Varenberg, M. (2017). How tight are beetle hugs? Attachment in mating leaf beetles. R. Soc. Open Sci. *4*, 171108.

Waite, J.H. (2017). Mussel adhesion - essential footwork. J. Exp. Biol. *220*, 517–530.

Waite, J.H., and Broomell, C.C. (2012). Changing environments and structure–property relationships in marine biomaterials. J. Exp. Biol. *215*, 873–883.

Waite, J.H., Lichtenegger, H.C., Stucky, G.D., and Hansma, P. (2004). Exploring molecular and mechanical gradients in structural bioscaffolds. Biochemistry *43*, 7653–7662.

Walsh, C.T., Garneau-Tsodikova, S., and Gatto, G.J., Jr. (2005). Protein posttranslational modifications: the chemistry of proteome diversifications. Angew. Chem. Int. Ed. *44*, 7342–7372.

Walther, A., Bjurhager, I., Malho, J.M., Ruokolainen, J., Berglund, L., and Ikkala, O. (2010). Supramolecular control of stiffness and strength in lightweight high-performance nacre-mimetic paper with fire-shielding properties. Angew. Chem. Int. Ed. *49*, 6448–6453.

Wan, S., Li, Y., Peng, J., Hu, H., Cheng, Q., and Jiang, L. (2015). Synergistic toughening of graphene oxide–molybdenum disulfide–thermoplastic polyurethane ternary artificial nacre. ACS Nano *9*, 708–714.

Wang, Z. (2018). Slanted functional gradient micropillars for optimal bioinspired dry adhesion. ACS Nano *12*, 1273–1284.

Wang, H., Ding, J., Wang, X., and Lin, T. (2011). Wettability gradient-driven directional water transport across thin fibrous materials. In Proceedings of the 2011 International Symposium on New Frontiers in Fiber Materials Science (American Association of Textile Chemists and Colorists), pp. 140–141.

Wang, L., Ji, X.-Y., Wang, N., Wu, J., Dong, H., Du, J., Zhao, Y., Feng, X.-Q., and Jiang, L. (2012). Biaxial stress controlled three-dimensional helical cracks. NPG Asia Mater. *4*, e14.

Wang, Q., Nemoto, M., Li, D., Weaver, J.C., Weden, B., Stegemeier, J., Bozhilov, K.N., Wood, L.R., Milliron, G.W., and Kim, C.S. (2013). Biomineralization: phase transformations and structural developments in the radular teeth of cryptochiton stelleri (Adv. Funct. Mater. 23/2013). Adv. Funct. Mater. *23*, 2901.

Wang, J., Kato, K., Blois, A.P., and Wong, T.S. (2016a). Bioinspired omniphobic coatings with a thermal self-repair function on industrial materials. ACS Appl. Mater. Interfaces *8*, 8265–8271.

Wang, Y., Wang, X., Lai, C., Hu, H., Kong, Y., Fei, B., and Xin, J.H. (2016b). Biomimetic water-collecting fabric with light-induced superhydrophilic bumps. ACS Appl. Mater. Interfaces *8*, 2950–2960.

Wang, J., Sun, L., Zou, M., Gao, W., Liu, C., Shang, L., Gu, Z., and Zhao, Y. (2017a). Bioinspired shape-memory graphene film with tunable wettability. Sci. Adv. *3*, e1700004.

Wang, Y., Zhang, C., and Chen, W. (2017b). An analytical model to predict material gradient and anisotropy in bamboo. Acta Mech. *228*, 2819–2833.

Wang, Z., Shi, X., Huang, H., Yao, C., Xie, W., Huang, C., Gu, P., Ma, X., Zhang, Z., and Chen, L.-Q. (2017c). Magnetically actuated functional gradient nanocomposites for strong and ultra-durable biomimetic interfaces/surfaces. Mater. Horiz. *4*, 869–877.

Wang, L., Qiu, Y., Lv, H., Si, Y., Liu, L., Zhang, Q., Cao, J., Yu, J., Li, X., and Ding, B. (2019). 3D Superelastic scaffolds constructed from flexible inorganic nanofibers with self-fitting capability and tailorable gradient for bone regeneration. Adv. Funct. Mater. *29*, 1901407.

Wang, Y., Li, Y., Wang, L., Yuan, Q., Chen, J., Niu, Y., Xu, X., Wang, Q., and Wang, H. (2020). Gradient-layered polymer nanocomposites with significantly improved insulation performance for dielectric energy storage. Energy Storage Mater. *24*, 626–634.

Watson, G.S., Cribb, B.W., and Watson, J.A. (2010). Experimental determination of the efficiency of nanostructuring on non-wetting legs of the water strider. Acta Biomater. *6*, 4060–4064.

Weaver, J.C., Wang, Q., Miserez, A., Tantuccio, A., Stromberg, R., Bozhilov, K.N., Maxwell, P., Nay, R., Heier, S.T., and Dimasi, E. (2010). Analysis of an ultra hard magnetic biomineral in chiton radular teeth. Mater. Today *13*, 42–52.

Wegst, U.G. (2011). Bending efficiency through property gradients in bamboo, palm, and wood-based composites. J. Mech. Behav. Biomed. Mater. *4*, 744–755.

Wei, Z., Lewis, D.M., Xu, Y., and Gerecht, S. (2017). Dual cross-linked biofunctional and self-healing networks to generate user-defined modular gradient hydrogel constructs. Adv. Healthc. Mater. *6*, 1700523.

Wei, X., Zhou, H., Chen, F., and Wang, G. (2019). Bending flexibility of moso bamboo (phyllostachys edulis) with functionally graded structure. Materials *12*, 2007.

Weiss, I.M., Kaufmann, S., Mann, K., and Fritz, M. (2000). Purification and characterization of perlucin and perlustrin, two new proteins from the shell of the mollusc Haliotis laevigata. Biochem. Biophys. Res. Commun. *267*, 17–21.

Wirth, C., Hofmann, S., and Robertson, J. (2008). Surface properties of vertically aligned carbon nanotube arrays. Diam. Relat. Mater. *17*, 1518–1524.

Wong, T.-S., Kang, S.H., Tang, S.K., Smythe, E.J., Hatton, B.D., Grinthal, A., and Aizenberg, J. (2011). Bioinspired self-repairing slippery surfaces with pressure-stable omniphobicity. Nature *477*, 443–447.

Wu, X., Jiang, P., Chen, L., Yuan, F., and Zhu, Y.T. (2014). Extraordinary strain hardening by gradient structure. Proc. Natl. Acad. Sci. U S A *111*, 7197–7201.

Wu, Y., Shah, D.U., Wang, B., Liu, J., Ren, X., Ramage, M.H., and Scherman, O.A. (2018a). Biomimetic supramolecular fibers exhibit water-induced supercontraction. Adv. Mater. *30*, 1707169.

Wu, Z., Wang, J., Zhao, Z., Yu, Y., Shang, L., and Zhao, Y. (2018b). Microfluidic generation of bioinspired spindle-knotted graphene microfibers for oil absorption. ChemPhysChem *19*, 1990–1994.

Xiao, L., Li, G., Cai, Y., Cui, Z., Fang, J., Cheng, H., Zhang, Y., Duan, T., Zang, H., and Liu, H. (2020). Programmable 3D printed wheat awn-like system for high-performance fogdrop collection. Chem. Eng. J. *399*, 125139.

Xie, C., Wang, X., He, H., Ding, Y., and Lu, X. (2020). Mussel-inspired hydrogels for self-adhesive bioelectronics. Adv. Funct. Mater. *30*, 1909954.

Xing, Y., Shang, W., Wang, Q., Feng, S., Hou, Y., and Zheng, Y. (2019). Integrative bioinspired surface with wettable patterns and gradient for enhancement of fog collection. ACS Appl. Mater. Interfaces *11*, 10951–10958.

Xu, J., and Zhang, G. (2015). Unique morphology and gradient arrangement of nacre's platelets in green mussel shells. Mater. Sci. Eng. C *52*, 186–193.

Xu, G., Gong, L., Yang, Z., and Liu, X. (2014). What makes spider silk fibers so strong? From molecular-crystallite network to hierarchical network structures. Soft Matter *10*, 2116–2123.

Xu, Q., Xu, M., Lin, C.Y., Zhao, Q., Zhang, R., Dong, X., Zhang, Y., Tian, S., Tian, Y., and Xia, Z. (2019). Metal coordination-mediated functional grading and self-healing in mussel byssus cuticle. Adv. Sci. *6*, 1902043.

Xu, W., Zheng, H., Liu, Y., Zhou, X., Zhang, C., Song, Y., Deng, X., Leung, M., Yang, Z., and Xu, R.X. (2020). A droplet-based electricity generator with high instantaneous power density. Nature *578*, 392–396.

Yamamoto, H. (1987). Adhesive studies of synthetic polypeptides: a model for marine adhesive proteins. J. Adhes. Sci. Technol. *1*, 177–183.

Yamamoto, H., and Ohkawa, K. (1993). Synthesis of adhesive protein from the vitellaria of the liver flukeFasciola hepatica. Amino Acids *5*, 71–75.

Yamamoto, H., Yamauchi, S., and Ohara, S. (1992). Synthesis and adhesive studies of marine adhesive proteins of the Chilean mussel Aulacomya ater. Biomimetics *1*, 219–238.

Yan, B., Huang, J., Han, L., Gong, L., Li, L., Israelachvili, J.N., and Zeng, H. (2017). Duplicating dynamic strain-stiffening behavior and nanomechanics of biological tissues in a synthetic self-healing flexible network hydrogel. ACS Nano *11*, 11074–11081.

Yang, W., Zhang, G., Zhu, X., Li, X., and Meyers, M. (2011). Structure and mechanical properties of Saxidomus purpuratus biological shells. J. Mech. Behav. Biomed. Mater. *4*, 1514–1530.

Yang, W., Chen, I.H., Gludovatz, B., Zimmermann, E.A., Ritchie, R.O., and Meyers, M.A. (2013). Natural flexible dermal armor. Adv. Mater. *25*, 31–48.

Yin, M., Yuan, Y., Liu, C., and Wang, J. (2009). Development of mussel adhesive polypeptide mimics coating for in-situ inducing re-endothelialization of intravascular stent devices. Biomaterials *30*, 2764–2773.

Yin, Z., Hannard, F., and Barthelat, F. (2019). Impact-resistant nacre-like transparent materials. Science *364*, 1260–1263.

Yong, J., Chen, F., Yang, Q., Fang, Y., Huo, J., Zhang, J., and Hou, X. (2017). Nepenthes inspired design of self-repairing omniphobic slippery liquid infused porous surface (SLIPS) by femtosecond laser direct writing. Adv. Mater. Interfaces *4*, 1700552.

Yoon, H., Jeong, H.E., Kim, T.-I., Kang, T.J., Tahk, D., Char, K., and Suh, K.Y. (2009). Adhesion hysteresis of Janus nanopillars fabricated by nanomolding and oblique metal deposition. Nano Today *4*, 385–392.

Yu, M., and Deming, T.J. (1998). Synthetic polypeptide mimics of marine adhesives. Macromolecules *31*, 4739–4745.

Yu, M., Hwang, J., and Deming, T.J. (1999). Role of L-3, 4-dihydroxyphenylalanine in mussel adhesive proteins. J. Am. Chem. Soc. *121*, 5825–5826.

Yu, J., Chary, S., Das, S., Tamelier, J., Pesika, N.S., Turner, K.L., and Israelachvili, J.N. (2011). Gecko-inspired dry adhesive for robotic applications. Adv. Funct. Mater. *21*, 3010–3018.

Yu, S.-H., Wu, H.-A., Liu, C., Wen, S.-M., Meng, Y.-F., Pan, Z., Chen, S.-M., Zhu, Y.-B., Cui, C., Zhao, R., and Gao, H.-L. (2020). Bioinspired hierarchical helical nanocomposite macrofibers

based on bacterial cellulose nanofibers. Natl. Sci. Rev. *7*, 73–83.

Yuan, W., and Zhang, K.-Q. (2012). Structural evolution of electrospun composite fibers from the blend of polyvinyl alcohol and polymer nanoparticles. Langmuir *28*, 15418–15424.

Yurdumakan, B., Raravikar, N.R., Ajayan, P.M., and Dhinojwala, A. (2005). Synthetic gecko foot-hairs from multiwalled carbon nanotubes. Chem. Commun. 3799–3801.

Zeng, H., Hwang, D.S., Israelachvili, J.N., and Waite, J.H. (2010). Strong reversible Fe3+-mediated bridging between dopa-containing protein films in water. Proc. Natl. Acad. Sci. U S A *107*, 12850–12853.

Zhang, S., and Tso, I.-M. (2016). Spider silk: factors affecting mechanical properties and biomimetic applications. In Extracellular Composite Matrices in Arthropods, E. Cohen and B. Moussian, eds. (Springer). https://doi.org/10.1007/978-3-319-40740-1_13.

Zhang, J., and Yao, Z. (2019). Slippery properties and the robustness of lubricant-impregnated surfaces. J. Bionic Eng. *16*, 291–298.

Zhang, X., Zhao, J., Zhu, Q., Chen, N., Zhang, M., and Pan, Q. (2011). Bioinspired aquatic microrobot capable of walking on water surface like a water strider. ACS Appl. Mater. Interfaces *3*, 2630–2636.

Zhang, P., Chen, H., and Zhang, D. (2015). Investigation of the anisotropic morphology-induced effects of the slippery zone in pitchers of Nepenthes alata. J. Bionic Eng. *12*, 79–87.

Zhang, X., Hassanzadeh, P., Miyake, T., Jin, J., and Rolandi, M. (2016). Squid beak inspired water processable chitosan composites with tunable mechanical properties. J. Mater. Chem. B *4*, 2273–2279.

Zhang, P., Chen, H., Li, L., Liu, H., Liu, G., Zhang, L., Zhang, D., and Jiang, L. (2017). Bioinspired smart peristome surface for temperature-controlled unidirectional water spreading. ACS Appl. Mater. Interfaces *9*, 5645–5652.

Zhang, C., Zhang, B., Ma, H., Li, Z., Xiao, X., Zhang, Y., Cui, X., Yu, C., Cao, M., and Jiang, L. (2018). Bioinspired pressure-tolerant asymmetric slippery surface for continuous self-transport of gas bubbles in aqueous environment. ACS Nano *12*, 2048–2055.

Zhang, Y., Edelbrock, A.N., and Rowan, S.J. (2019). Effect of processing conditions on the mechanical properties of bio-inspired mechanical gradient nanocomposites. Eur. Polym. J. *115*, 107–114.

Zhang, T., Duan, C., Wang, A., and Wang, Q. (2020). Dynamic modeling and optimal design of Tube–Diaphragm coupling beam inspired by bamboo. Thin-Walled Structures *155*, 106836.

Zhao, N., Yang, M., Zhao, Q., Gao, W., Xie, T., and Bai, H. (2017). Superstretchable nacre-mimetic graphene/poly (vinyl alcohol) composite film based on interfacial architectural engineering. ACS Nano *11*, 4777–4784.

Zhao, Y., Cao, J., Zhang, Y., and Peng, H. (2019b). Gradually crosslinking carbon nanotube Array in mimicking the beak of giant squid for compression-sensing supercapacitor. Adv. Funct. Mater. *30*, 1902971.

Zhao, C., Wang, Z., Li, H., Wu, X., Qiao, S., and Sun, J. (2019a). A new approach for medical image enhancement based on luminance-level modulation and gradient modulation. Biomed. Signal Process. Control *48*, 189–196.

Zheng, Y., Bai, H., Huang, Z., Tian, X., Nie, F.-Q., Zhao, Y., Zhai, J., and Jiang, L. (2010). Directional water collection on wetted spider silk. Nature *463*, 640–643.

Zhou, M., Pesika, N., Zeng, H., Tian, Y., and Israelachvili, J. (2013). Recent advances in gecko adhesion and friction mechanisms and development of gecko-inspired dry adhesive surfaces. Friction *1*, 114–129.

Zhou, M., Tian, Y., Zeng, H., Pesika, N., and Israelachvili, J. (2015). Clumping criteria of vertical nanofibers on surfaces. Adv. Mater. Interfaces *2*, 1400466.

Zhou, H., Jing, X., and Guo, Z. (2020). Optimal design of a fog collector: unidirectional water transport on a system integrated by conical copper needles with gradient wettability and hydrophilic slippery rough surfaces. Langmuir *36*, 6801–6810.

Zhu, H., Guo, Z., and Liu, W. (2016a). Biomimetic water-collecting materials inspired by nature. Chem. Commun. *52*, 3863–3879.

Zhu, X.-Y., Chen, C., Chen, P.-C., Gao, Q.-L., Fang, F., Li, J., and Huang, X.-J. (2016b). High-performance enzymatic membrane bioreactor based on a radial gradient of pores in a PSF membrane via facile enzyme immobilization. RSC Adv. *6*, 30804–30812.

Zhu, L., Li, H., Yin, Y., Cui, Z., Ma, C., Li, X., and Xue, Q. (2020). One-step synthesis of a robust and anti-oil-fouling biomimetic cactus-like hierarchical architecture for highly efficient oil/water separation. Environ. Sci. Nano *7*, 903–911.

Zvarec, O., Purushotham, S., Masic, A., Ramanujan, R.V., and Miserez, A. (2013). Catechol-functionalized chitosan/iron oxide nanoparticle composite inspired by mussel thread coating and squid beak interfacial chemistry. Langmuir *29*, 10899–10906.